Studies on the interbranchial lymphoid tissue in the gills of Atlantic salmon and common carp

Philosophiae Doctor (PhD) Thesis

Alf Seljenes Dalum

Department of Basic Sciences and Aquatic Medicine

Faculty of Veterinary Medicine and Biosciences

Norwegian University of Life Sciences

Adamstuen 2016

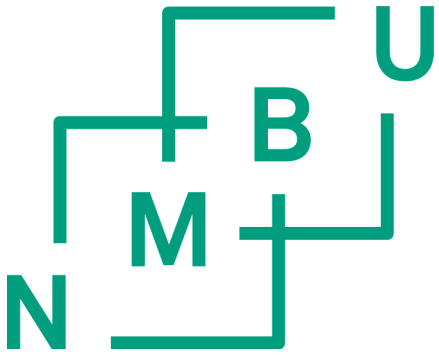

Thesis number 201X:XX

ISSN 1894-6402

ISBN 978-82-575-XXXX-X

CONTENTS

ACKNOWLEDGEMENT

***NMBU*:** It is with deep gratitude I would like to thank Norwegian University of Life Sciences (NMBU) (the former Norwegian School of Veterinary Sciences (NVH)), Department of Basic Sciences and Aquatic Medicine (BasAM), for financing and giving me the opportunity to study the most remarkable organ created; the gills. Particular thanks go to Prof. Mona Aleksandersen and Dr. Ole Taugbøl for supporting me through tough times, and to Julie Jansen and Bendt Rimer for helping me with the administrative part. Thanks to the Norwegian Research Council of Norway (FRIMEDBIO-222207/F20), Torsteds legat, Skretting studentfond and Norsk Biokjemisk Selskap for additional financial support.

***Supervisors*:** In particular I would like to thank Dr. Agnar Kvellestad for a tremendous effort and for not giving up on me, Prof. Charles Press for always being there helping me, and Prof. Erling Koppang for initiating the project.

***Mentors*:**

- Prof. Trygve Poppe; thank you for showing genuine interest in science and for taking me out fishing, aka sampling.
- Prof. David Griffiths; thank you for always helping me with projects, writing and teaching, and for making science fun.

***Evaluation committee**:* Thank you for your valuable time.

***Cell Biology and Immunology Group, Wageningen University & Research*:** Prof. Geert Wiegertjes, Prof. Maria Forlenza, Marleen Scheer, Dr. Jules Petit, Dr. Carmen Embregts, Dr. Eva Dóró, Dr. Annelieke Wentzel, Dr. Sylvia Brugman and the rest of the group; thank you all for giving me a wonderful time in Wageningen, including me in your research activities and showing me what science is about.

Section of Anatomy and Pathology, NMBU: Thanks to all colleagues who have supported me through these years. Particular thanks go to

- Elin Valen for being a true friend and colleague, and for giving me courage to carry on.
- Dr. Guro Løkka for all scientific and practical advices.

- Team at the histology laboratory: Laila Aune, Mari Ådland, Sigbjørn Lunner, Aleksandra Göksu, Soheir Al_Taoyl, Emil Westad and Tore Engen; thank you all for supporting me and keeping me with company, creating a friendly environment to work in.

***Imaging Centre, NMBU*:** Thanks to Lene Hermansen and Hilde Kolstad for excellent technical support.

Indispensable persons:

- Dr. Tonje Høy: Thank you for greatly improving this thesis.
- Anne Cathrine Munthe at NMBU library campus Adamstua: Thank you for all your help and advices.
- Julie Jansen: Apart from all the administrative help, your thoughtfulness and kindness has made my time as a PhD-student much easier.

***Providers of research material*:** Thanks to Frode Laugerud and the Sport Fishermen's Club at Hellefossen, Drammenselva, Norway, Karoline Skaar Amthor and LetSea Helgeland Havbruksstasjon AS, Sandnessjøen, Norway, and Per Gunnar Fjelldal at IMR Matre, Norway, for providing top quality research materials.

Students: It has been a great pleasure and a privilege to teach you through these years. Thank you for all your positive feedback and encouragements.

***Family*:** My mother and Kjell; thank you for always believing in me and always supporting me. Brother, Hanne, father, Ragnhild, Håvard, Arild, Maria; thank you for all your support. Kirsti; I am looking forward to attend your defence for PhD.

Love of my life: Helene and Theodor; without your unconditional love and patience, this thesis would not have been possible. You mean the world to me.

Oslo, October 2016

Alf Seljenes Dalum

ABBREVIATIONS

APC	- antigen presenting cell
CCL	- C-C motif chemokine ligand
CCR7	- C-C chemokine receptor type 7
CD	- cluster of differentiation
DC	- dendritic cell
Dg	- degree days (days times average water-temperature during the day; one day with average water temperature of 10 °C produces 10 degree days).
EGC	- eosinophilic granule cells
FAO	- Food and Agriculture Organization of the United Nations
FOXN1	- forkhead box protein N1
GIALT	- gill-associated lymphoid tissue
HE	- haematoxylin and eosin
HEV	- high endothelial venules
IF	- immunofluorescence
Ig	- immunoglobulin
IHC	- immunohistochemistry
ILT	- interbranchial lymphoid tissue
ISAV	- infectious salmon anaemia virus
MALT	- mucosa-associated lymphoid tissue
M-cell	- microfold cell
MHC	- major histocompatibility complex
NK-cell	- natural killer cell
NKEF	- natural killer cell enhancing factor
PCNA	- proliferating cell nuclear antigen
PSMB11	- proteasome subunit beta 11
qPCR	- quantitative real-time polymerase chain reaction
RAG	- recombination activating gene
TCR	- T-cell receptor
Th	- T helper cell
USD	- United States dollar
ZAP-70	- zeta-chain-associated protein kinase 70

LIST OF PAPERS

Paper I:

Dalum AS, Austbø L, Bjørgen H, Griffiths DJ, Skjødt K, Hordvik I, Hansen T, Fjelldal PG, Press CMcL, Koppang EO (2015): The interbranchial lymphoid tissue of Atlantic salmon (*Salmo salar* L.) extends as a diffuse mucosal lymphoid tissue throughout the trailing edge of the gill filament. *Journal of Morphology* 276:1075-88.

Paper II:

Dalum AS, Griffiths DJ, Valen EC, Amthor KS, Austbø L, Koppang EO, Press CMcL, Kvellestad A (2016): Morphological and functional development of the interbranchial lymphoid tissue (ILT) in Atlantic salmon (*Salmo salar* L.). *Fish & Shellfish Immunology* 58:153-164.

Paper III:

Dalum AS, Kvellestad A, Embregts C, Forlenza M, Griffiths DJ, Petit J, Scheer M, McLean Press CMcL, Koppang EO, Wiegertjes GF (2016): Description of interbranchial lymphoid tissue in the gills of common carp (*Cyprinus carpio* L.): a layered and vascularized lymphoid aggregate. Manuscript.

SUMMARY

As wild-capture fisheries exceed sustainable levels, aquaculture is expected to increase its importance as a source of fish products for a growing world population. Vaccination is a major prophylactic measure in modern aquaculture, but more efficient and more easily administered vaccines are needed. Mucosal delivery of vaccines could fulfil both these requirements, but a better understanding of the organization and function of mucosal lymphoid tissues including the gills, is needed.

The interbranchial lymphoid tissue (ILT) in the gills of Atlantic salmon (*Salmo salar* L.) and rainbow trout (*Oncorhynchus mykiss* Walbaum, 1792) has been described as an intraepithelial aggregation of T-cells residing at the distal end of the interbranchial septum. In this thesis fundamental morphological studies were conducted to increase the knowledge about the Atlantic salmon ILT. It was found that the ILT first becomes discernible after the fish commences exogenous feeding and branchial breathing, that is, after the yolk-sack larva life-stage. From juveniles and onwards, the previously described ILT was shown to extend into the trailing edges of the free filaments, so that the ILT lines the branchial cleft of each gill. A distinction between the previously described ILT as proximal ILT, and the newly described part as distal ILT, was made. The distal ILT constitutes 80 % of the ILT, and it is intimately associated with the secondary vascular system of the gills. Thus, the distal ILT is suggested to be the site of communication between the ILT and the circulatory system, and as such, essential for understanding the function and dynamics of the ILT. However, in the normal-state gills, no major differences in morphology or gene transcription were noted between the two different regions. Discrete regions of proliferating T-cells were found within the ILT, located at the growth-zones of the gills. These findings indicate a possibility of both external and internal recruitment of lymphocytes, as the ILT grows along with the gills. Ontogenetically, the ILT appears after the thymus. However, as the fish grew, the ILT became several times larger than the thymus, and the ILT underwent less size-reduction during sexual maturation than the thymus. The ILT was not found to possess transcription of genes that coincide with primary lymphoid functions as found in the thymus.

Apart from Atlantic salmon and rainbow trout, the presence of ILT-like tissues has so far not been described in any other species. To broaden the scope, the gills of the more recently

evolved common carp (*Cyprinus carpio* L.) were investigated, revealing similar lymphoid structures as found in the salmonids. However, in contrast to the observations in Atlantic salmon, the proximal ILT of common carp possessed three morphologically discernible compartments. The basal compartment contained moderate numbers of B-cells amongst the high numbers of T-cells, and was intimately associated with blood vessels. In addition to moderate numbers of lymphocytes, the intermediate and uppermost compartments contained elements of the innate immune system. The morphology of the intermediate and uppermost compartment extended into the distal ILT.

This thesis has produced new knowledge about the morphology and organization of the ILT in Atlantic salmon. The novel description of a more organized ILT in common carp raises the possibility of a continuum across fish species from a primitive salmonid ILT, towards more organized mucosa-associated lymphoid tissue (MALT) as seen in higher vertebrates. More studies are needed to reveal the immunological functions of the ILT in different species. However, with its extensive size, probable communication with the systemic circulation and its exposed location, the gills and the ILT of these two commercially important species emerge as an obvious candidate for further research on fish mucosal vaccines.

SUMMARY IN NORWEGIAN (SAMMENDRAG)

Akvakultur forventes å få økende betydning som kilde for fiskeprodukter etter hvert som fiske på viltlevende stammer overskrider bærekraftige nivåer. Vaksinasjon er et viktig sykdomsforebyggende tiltak i moderne akvakultur, men det er fortsatt behov for å utvikle mer effektive og praktisk anvendbare vaksiner. Slimhinnebaserte vaksiner kan bidra til dette, men for å kunne utvikle slike er det viktig med inngående forståelse av organisering og funksjon av slimhinneassosiert immunvev.

Det interbranchiale lymfoide vev (interbranchial lymphoid tissue; ILT) hos atlantisk laks og regnbueørret har blitt beskrevet som en intraepitelial ansamling av T-celler lokalisert til den distale enden av det interbranchiale septum. I denne avhandlingen viser morfologiske undersøkelser av gjeller hos atlantisk laks at ILT først blir synlig etter at fisken starter eksternt fôropptak og respirasjon over gjeller, det vil si etter plommesekkstadiet. Fra det juvenile stadiet (parr) ble en videre utbredelse av det tidligere beskrevne ILT funnet langs hele den frie del av filamentene som vender inn mot den branchiale kløft. ILT bekler derfor hele den branchiale kløften i hver gjelle, og en inndeling mellom det tidligere beskrevne ILT, betegnet som proksimalt ILT, og det nyoppdagede lymfoide vevet, betegnet som distalt ILT, ble foretatt. Videre ble det funnet at det distale ILT utgjør omtrent 80 % av det totale ILT samtidig som det ligger nært gjellens sekundære sirkulasjonssystem. Denne forlengelsen av ILT kan derfor representere stedet hvor ILT kommuniserer med systemisk sirkulasjon, noe som vil være viktig for å forstå funksjonen og dynamikken til ILT. Under normaltilstand ble det ikke observert forskjeller, hverken morfologisk eller i genuttrykk, mellom disse regionene. Videre ble avgrensede områder med T-celle-proliferasjon påvist i ILT, og disse områdene var sammenfallende med gjellenes vekstsoner. Lymfocytter kan derfor i teorien rekrutteres både internt og eksternt etter hvert som ILT vokser i den voksende gjellen. Utviklingsmessig blir ILT synlig senere enn tymus. Etter hvert som fisken vokser, utvikler ILT seg til å bli betydelig større enn tymus, og ILT gjennomgår mindre grad av størrelsesreduksjon enn tymus under kjønnsmodning. Genuttrykk sammenfallende med primær lymfoid funksjon tilsvarende tymus ble ikke påvist i ILT.

Fram til nå har ILT kun blitt beskrevet hos atlantisk laks og regnbueørret. For å utvide perspektivet ble det undersøkt gjeller fra karpe, en art som er evolusjonsmessig nyere enn

salmonider. Lignende lymfoide strukturer med samme anatomiske utbredelse som ILT hos laksefisker ble påvist, men i motsetning til hos atlantisk laks bestod det proksimale ILT hos karpe av tre morfologisk ulike avdelinger; den basale, den intermediære og den øvre. Den basale avdelingen bestod av et moderat antall B-celler og et høyt antall T-celler, og var nært assosiert til blodkar. I tillegg til moderate mengder lymfocytter inneholdt den intermediære og øvre avdeling innslag fra det medfødte immunsystemet. Morfologien fra den intermediære og øvre avdeling ble videreført i det distale ILT.

Denne avhandlingen frambringer ny kunnskap om morfologien og organiseringen av ILT hos atlantisk laks. Tilstedeværelsen av et ILT-vev med høyere grad av organisering hos karpe åpner for å diskutere en mulig evolusjonær utvikling av ILT hos fisk, fra en primitiv form, som hos laks, mot et organisert slimhinne-assosiert vev tilsvarende det som sees hos høyerestående virveldyr. Mer forskning er nødvendig for å klarlegge den immunologiske funksjonen for ILT hos ulike arter. Den omfattende størrelsen på ILT, den sannsynlige kommunikasjon mellom ILT og systemisk sirkulasjon samt ILTs eksponerte plassering tilsier likevel at gjeller og tilhørende ILT vil være en opplagt kandidat å utforske videre med tanke på å utvikle slimhinnebaserte vaksiner.

INTRODUCTION

Aquaculture

Aquaculture encompasses farmed aquatic organisms including fish, molluscs, crustaceans and aquatic plants. Farming implies intervention in the rearing process to enhance production, such as regular stocking, feeding, and protection from disease and predators (FAO, 2016d). However, in the following text, aquaculture is confined to farming of fishes.

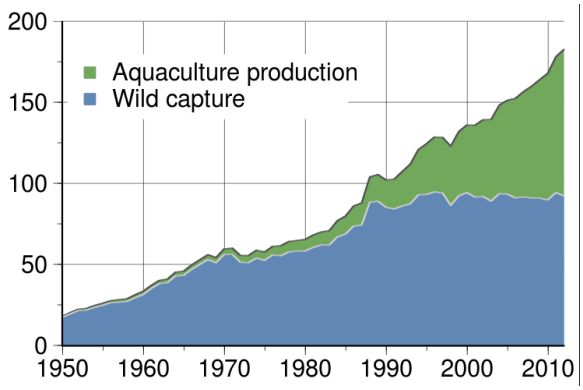

Fig. 1: Annual global harvest of fishes in million tonnes separated into aquaculture and wild capture (FAO, 2016c). The selection was based on all countries and fishing areas, and diadromous-, freshwater- and marine fishes between 1950 and 2014.

The global aquaculture industry is regarded as the fastest-growing food-producing sector with an annual growth of approximately 6 % over the last decade (Fig. 1). At the same time, the contribution of the wild-capture fisheries to the total fish consumption has decreased by 10 % from 2001 to 2011 (Turchini et al., 2010, Dhar et al., 2014). Altogether in 2014, aquaculture accounted for approximately 44 % of all fish consumed in the world (FAO, 2014). As most wild-capture fisheries have already reached or exceeded sustainable levels, the importance of aquaculture in providing fish food for the growing human population is estimated to increase according to the increased demand. By 2030 it is expected that aquaculture products will account for 62 % of the total fish consumption (World Bank, 2013).

Atlantic salmon

Culturing of Atlantic salmon began in the 19th century in the UK as a means of stocking waters for game fishing. In the 1960's, open sea cage culture for rearing marketable-size salmon was introduced in Norway (FAO, 2016b). Currently Norway is the leading producer of Atlantic salmon, with an estimated total annual production of 1.3 million tonnes representing a value of

5.8 billion United States dollar (USD) (2015) (Statistics Norway, 2015). With a global production of about 2.1 million tonnes (2012), Atlantic salmon was the eighth most cultured species in 2012. This production corresponded to an estimated value of 12.9 billion USD (FAO, 2014), making Atlantic salmon the highest valued cultured species.

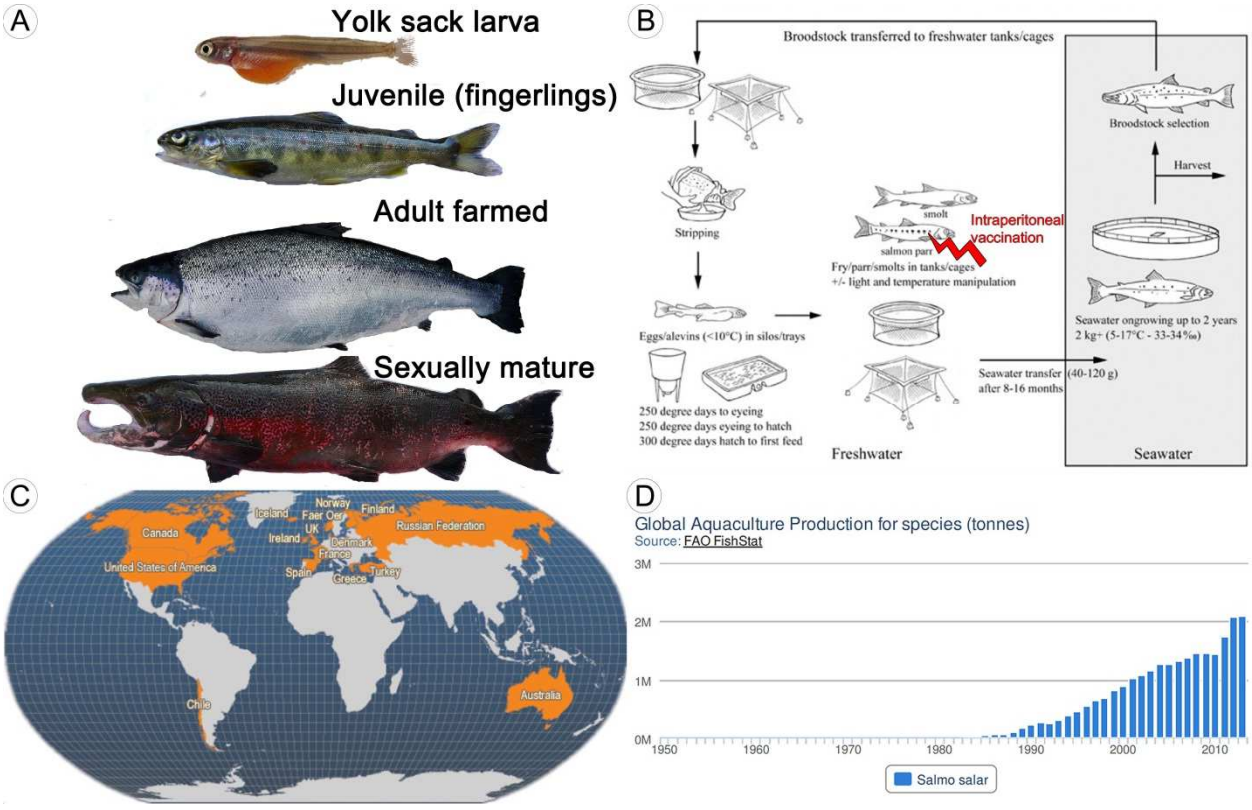

Fig. 2: Atlantic salmon and aquaculture. A) The various life-stages investigated (photographs by Professor Trygve T. Poppe). B) Production cycle of cultured Atlantic salmon. The fish is usually vaccinated once, with intraperitoneal injection at the juvenile fresh-water stage (source; (FAO, 2016b)). C) Global distribution of Atlantic salmon aquaculture (source; (FAO, 2016b)). D) Aquaculture statistics for global production of Atlantic salmon (source; (FAO, 2014)).

Aquaculture of Atlantic salmon is found on all continents except Africa and Antarctica. Salmon are anadromous, and growth can occur across a temperature-range of 0-25 °C with an optimum around 16 °C for the sea-living phase (Jonsson et al., 2001). All life-stages, and in particular the embryo, rely on water of relatively high levels of dissolved oxygen (Aas et al., 2011, Malcolm et al., 2005). The wild salmon yolk-sack larvae (alevins) hatch in gravel beds of river streams at about 500 degree days (dg) after fertilization. After another 300 dg living off their yolk-sack, they move up the water-column to start exogenous feeding as fry. Wild juvenile

fish remain in fresh-water for 2-5 years, until they undergo smoltification (sea-water preadaptation) from fingerlings (parr) into smolts, which migrate to the sea. After a growth period of up to 4 years, the salmon start spawning-migration, in which they usually return to their river of origin.

Under aquaculture conditions (Fig. 2B), the process is speeded up, and harvestable fish (2-6 kg) are produced over a period of 24-36 months. Especially the fingerling period is substantially reduced. Following sea-transfer, open net cages are the most usual facilities for growth.

Common carp

Common carp is one of the oldest domesticated fish species for food production, and it has been reared in China for more than 2.000 years (FAO, 2016a, Flajšhans and Hulata, 2007). Global production of common carp is estimated to 4.1 million tonnes, which makes it the third most farmed species on a weight-basis and the fifth most valuable at 5.7 billion USD in 2012 (FAO, 2014) .

The wild fresh-water living, omnivorous common carp thrives under warm-water conditions. Its tendency towards consumption of benthic organisms involves digging in the sediments in search for food items, which often contributes to turbid water. The highest growth rate for post yolk-sack life stages is obtained when water temperature ranges between 23 °C and 30 °C, but carp can survive cold winter periods and tolerate salinity up to 5 ‰. Furthermore, carp can survive in water of low levels of dissolved oxygen (0.3-0.5 mg/litre), as well as supersaturated water. A typical carp-pond is often shallow and eutrophic with a muddy bottom and dense aquatic vegetation (FAO, 2016e, FishBase, 2016). Typically, females mature after 11 000 – 12 000 dg in temperate and subtropical climatic zones, and they require a water-temperature of at least 18 °C to spawn (Flajšhans and Hulata, 2007).

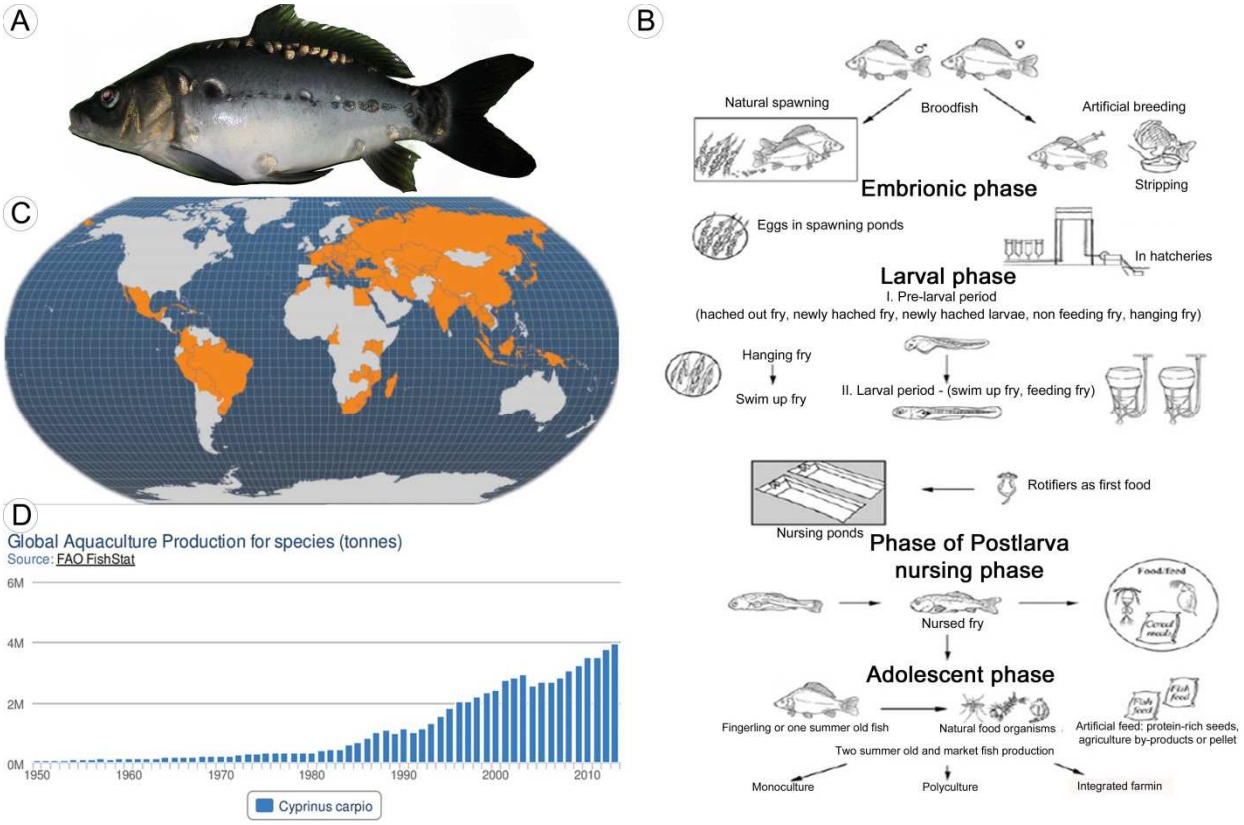

Fig. 3: Common carp and aquaculture. A) Adult common carp (photograph by Marleen Scheer). B) Production cycle of cultured common carp (source: (FAO, 2016a)). C) Global distribution of common carp aquaculture (source:(FAO, 2016e)). D) Aquaculture statistics for global production of common carp (source: (FAO, 2016a)).

In brood-stocks, females can lay more than one million eggs in one season. Embryonic growth takes 60-70 dg, and after a yolk-sack period of three days after hatching, the swim bladder appears and they start to move up in the water-column for exogenous feeding. Fingerlings (yearlings) of up to 30–100 g body-weight are produced in semi-intensive ponds, before transfer to extensive or semi-intensive ponds, either in monoculture or in polyculture with other cyprinids, for growth to market size. Growth in a temperate climate is slower, and the fish typically reaches 1.5 kg body weight after three rearing seasons (Flajšhans and Hulata, 2007).

Challenges in aquaculture

Despite the predicted increase in importance of aquaculture, the industry faces challenges. Infectious diseases are a significant problem in most intensive animal production systems. Salmon aquaculture has been confronted with bacterial, viral and parasitic diseases (Dhar et al., 2014). Vaccination by intraperitoneal injection of oil-adjuvanted vaccines was the salvation of

the industry, enabling effective control of bacterial diseases, and this approach holds hope for the control of viral and possibly even parasitic diseases (Brudeseth et al., 2013). However, injection-based vaccines are costly, labour intensive to administer and only feasible after the fish have reached a certain size. They are also associated with various side-effects (Midtlyng et al., 1996, Koppang et al., 2008), and these side-effects seem to be more substantial with decreasing size of the vaccinated fish (Berg et al., 2007). Mucosal vaccines are an attractive alternative, but they have so far proved to be less effective than injection-based vaccines. Development of effective mucosal vaccines would benefit from a better understanding of the organization and response of mucosal immune tissues, such as those in the gills, to infectious agents.

Pharyngeal arches, pouches and their derivatives- an overview

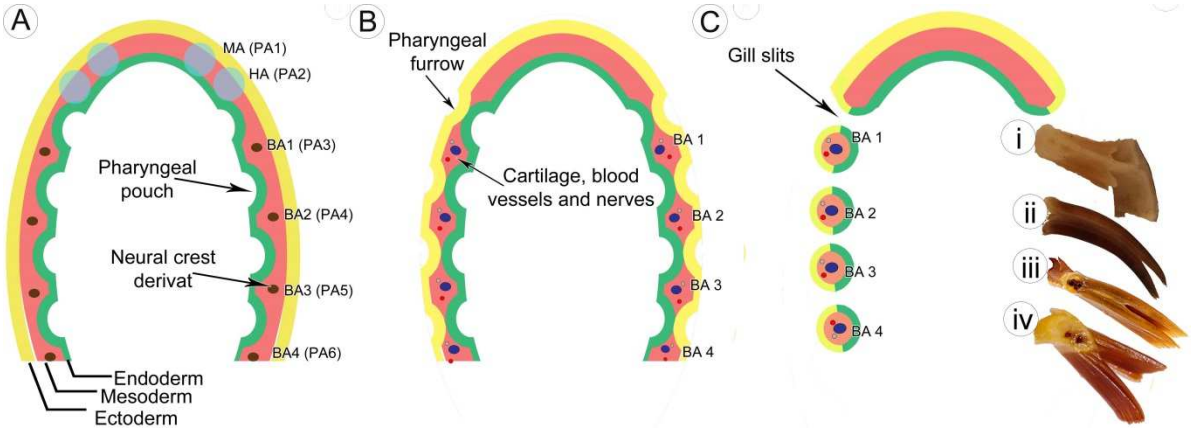

Fig. 4: Ontogeny of the gills and evolutionary development of the interbranchial septum. In the schematic figure, emphasis is placed on the gill-forming branchial arches one to four. A) Pharyngeal poaches form as outwards evaginations of the endodermal layer. B) Pharyngeal furrows form as inwards indentations of the ectodermal layer. C) Left side; gill slits formed as the pouches meet and fuse with the furrows, leaving open communications between the pharyngeal- and opercular cavities. Right side; gills cut in the transversal plane and viewed in transversal projections. Fishes of decreasing evolutionary age are depicted from gills one to four. Note the reduced length of the interbranchial septum. i) Cat shark (Scyliorhinus hesperius Springer, 1966), ii) Siberian sturgeon (Acipenser baerii Brandt, 1869), iii) Atlantic salmon, iv) European perch (Perca fluviatilis L.). MA; mandibular arch, HA; hyoid arch, BA; branchial arch, PA; pharyngeal arch. Figures and photographs by Alf Seljenes Dalum.

In fishes, seven paired pharyngeal arches form in the wall of the embryonic pharynx as a result of thickenings of mesenchymal tissue derived from neural crest cells in the mesoderm (Grevellec and Tucker, 2010). The two anterior-most pharyngeal arches (the mandibular and hyoid arches) form the jaws and associated supportive apparatus such as the operculum (Kimmel et al., 1995,

Wilson and Laurent, 2002). The pseudobranch originates from the posterior part of the mandibular arch. The next four pairs of arches give rise to the gills and are hence termed branchial arches (Fig. 4) (Hughes, 1984). The seventh pair of pharyngeal arches does not give rise to gills (Kimmel et al., 1995). Caudal to the hyoid arch, pharyngeal pouches form by outwards vertical-running evagination of the endodermic layer of the inner pharyngeal wall. Corresponding to each pouch, vertical-running indentations of the ectodermal layer of the outer pharyngeal wall give rise to the external pharyngeal furrows (Hyman, 1942, Hyttel, 2009). Gill slits are formed as the pouches meet and fuse with the corresponding furrows, leaving open communications between the pharyngeal cavity and the external environment (Hyman, 1942, Hyttel, 2009). In teleosts, the pharyngeal arches and the operculum confine the gill chamber, into which the gill filaments project.

Organs arising from the pharyngeal pouches are collectively referred to as branchiogenic organs (Hyman, 1942). Examples of specialized branchiogenic organs in mammals are the thymus and the palatine tonsils, but only the thymus has been identified in all jawed vertebrates including fishes. From an immunological perspective, the epithelial reticulum is suggested to be unique for the thymus and the palatine tonsils, as the connective tissue stroma of other primary or secondary lymphoid tissues are thought to be of mesenchymal origin (Pearse, 2006, Vejlsted, 2009).

The teleost thymus

Ontogeny

The term ontogeny is used to describe the formation and growth of an organism, organ or tissue from the time of fertilization to its mature form (Gould, 1977), while in the present thesis, development describes further morphological traits, including possible atrophy, for the rest of the organism's lifespan. The thymus is regarded as the first primary lymphoid organ to appear and the first to become lymphoid (Pearse, 2006, Chilmonczyk, 1992, Lam et al., 2002, Tatner, 1996). The epithelial reticulum of the thymus is of endodermal origin (Vejlsted, 2009, Ge and Zhao, 2013). Thymic tissue can arise from every pharyngeal pouch in certain cartilaginous fishes (Luer et al., 1995), from the second to fourth pouches in teleosts (Bowden et al., 2005), and from the

third pouch in mammals (Grevellec and Tucker, 2010, Hyttel, 2009). The timeframe for thymic ontogeny may vary significantly between teleost species (Bowden et al., 2005). In the common carp held at 23 °C, an epithelial primordium and the first lymphocytes were noted 3 and 4 days post-fertilization, respectively (Romano et al., 1999b). In Atlantic salmon held at 4-7 °C, lymphocytes had infiltrated the epithelial reticulum of the thymic primordium by 22 days pre-hatch (Ellis, 1977).

Anatomy

The paired thymus of fishes is superficially located in the dorso-lateral region of the gill chamber, closely associated with the gills and covered by the operculum (Bowden et al., 2005, Chilmonczyk, 1992). While the thymus is surrounded by a connective tissue capsule in higher vertebrates, such delineation is less obvious in fishes (Castillo et al., 1998). Laterally, the teleost thymus is covered by, and resides within, pharyngeal epithelium, which is in direct contact with the ambient water (Castillo et al., 1998). Medially, invaginations of underlying connective tissue into the basement membrane of the thymic epithelium produces trabeculae giving passage to blood vessels involved in the ingress of T-cell precursors and egress of mature, naive T-cells (Chilmonczyk, 1983). The thymic parenchyma of mammals can be divided into two different regions based on morphological properties of the lymphocytes; a darkly stained cortex that is dominated by T-cell precursors (thymocytes) of low cytoplasm-to-nucleus ratio, and the medulla that is less densely packed with differentiated T-cells of higher cytoplasm-to-nucleus ratio (Mescher and Junqueira, 2015). A similar pattern has been described in several teleosts (Bowden et al., 2005). Besides lymphocytes, cellular constituents of the teleost thymus includes epithelial cells, macrophages, dendritic (interdigitating) cells, fibroblasts, non-fibroblastic mesenchymal cells, nerve cells and endothelial cells (Bowden et al., 2005, Ge and Zhao, 2013), all of which form a dynamic environment for optimal T-cell maturation. Different subsets of each group of cells can be identified. In particular, the epithelial cells of the thymus are thought to be essential in T-cell maturation. In carp, differentiation of epithelial cells into cortical and medullary reticular cells, limiting cells of the capsule and trabeculae, nurse-like cells and Hassall`s body-like structures has been described (Romano et al., 1999b, Romano et al., 1999a). The internal

division of the thymus into a cortex and medulla is less evident in salmonids than in cyprinids (Romano et al., 1999b, Tatner and Manning, 1982, Chilmonczyk, 1983).

Function

As the primary site of T-cell differentiation and maturation, the function of the thymus is well-conserved in jawed vertebrates (Boehm et al., 2012, Boehm and Bleul, 2007, Ge and Zhao, 2013, Chilmonczyk, 1992). In higher vertebrates, T-cell precursors are recruited from haematopoietic tissues to the thymus, where they undergo positive- and negative selection (Anderson et al., 2007). In the cortex, T-cell precursors able to assemble a T-cell receptor (TCR) of low affinity for self-peptide- major histocompatibility complex (MHC) are selected for further differentiation, while T-cell precursors with no such affinity undergo apoptosis (Anderson et al., 2007). This is followed by negative selection in the medulla, whereby T-cells expressing potentially autoreactive TCR are induced to undergo apoptosis or become regulatory T-cells (Anderson et al., 2007). The same order of T-cell selection is thought to take place in fishes (Schorpp et al., 2002). This process of T-cell selection is associated with transcription of thymus-specific inherent genes, which in turn can be used to identify functional thymic tissue. Common to all primary lymphoid tissues is the transcription of recombination activating gene 1 and -2 (*RAG1* and *RAG2*, respectively), which gene-products are vital in somatic recombination of variable (diversity) joining gene segments of TCR and immunoglobulins (Hansen and Kaattari, 1995, Hansen and Kaattari, 1996). With regard to the thymus, transcription of *RAG1* and *-2* is confined to the cortex as shown in the zebrafish (*Danio rerio* Hamilton, 1822) (Lam et al., 2002, Schorpp et al., 2002). Others, such as forkhead box protein N1 (*FOXN1*) and proteasome subunit beta 11 (*PSMB11,* also referred to as *BETA-5T*) are associated with the specific function of the thymic epithelium both in fishes and higher vertebrates (Ma et al., 2012, Sutoh et al., 2012, Takahama et al., 2012, Bajoghli et al., 2009). *FOXN1,* transcribed both in the cortex and medulla, is regarded as the earliest thymus-specific gene to be transcribed, and its gene-product is required for the initial differentiation of thymic epithelium into cortical- and medullary subsets (Grevellec and Tucker, 2010, Nehls et al., 1994, Dooley et al., 2005). The gene-product of *PSMB11* is a catalytic subunit of a thymus proteasome involved in positive selection of the major repertoire of immunocompetent cluster of differentiation (CD)8^+ T-cells (Murata et al., 2007). Exclusively

transcribed in cortical thymic epithelial cells, *PSMB11* is one of the most specific markers for cortical thymic tissue in vertebrates (Takahama et al., 2010).

Atrophy

Just as in higher vertebrates, the thymus of most fishes atrophies with ageing and sexual maturation, although the time of onset and degree of atrophy varies significantly between species (Bowden et al., 2005). The exact mechanism of this atrophy is still unknown, but factors such as stress, season and hormones are suspected to influence this process (Chilmonczyk, 1992). The main characteristics of thymic atrophy in fishes are decrease in organ-size and lymphocyte-density, infiltration of adipocytes, increased proportion of reticular epithelial cells and collagenous fibres and formation of cystic spaces (Chilmonczyk, 1992).

The teleost gills- ontogeny and anatomy

Compared with the invaginated lungs of terrestrial vertebrates, the evaginated respiratory surface of the gills is particularly exposed to the surroundings (Maina, 2002). Apart from respiration, the gills perform functions including regulation of osmolarity and ionic composition, acid-base balance, excretion of ammonia, metabolism of circulating hormones, detoxification of plasma-born substances and immune functions (Maina, 2002, Rombough, 2007, Evans et al., 2005). Its anatomical complexity is thus a reflection of its functional diversity (Rombough, 2007).

Ontogeny of the fish gills

The above-mentioned four pairs of pharyngeal arches persist but are separated by the gill slits. Under the cover of endoderm and ectoderm, these arches are composed of connective tissue, endoskeleton, muscles, vessels and nerves (Hyman, 1942). Septum and filaments with lamellae grows out from these arches. Whether the epithelium of these structures is of endo- or ectodermal origin is a matter of debate, and it has even been claimed that this could vary between different species (Hughes, 1984). The prevailing view is that the gill epithelium of jawed fishes is formed

from the ectoderm (Laurent, 1984). Capacity for regulation of ionic composition appears in larvae before the respiratory function becomes of significance (Fu et al., 2010, Brauner and Rombough, 2012) (Rombough, 2007).

Gill anatomy

A great structural diversity of the fish gills is found depending on class, order and family considered. Generally, fish gills are commonly divided into three groups (Laurent, 1984); i) septal gills encountered in Cyclostomata and Elasmobranchii, where the interbranchial septum extends beyond the filaments, forming a connection between the gill arches and the outer body wall, ii) the branchial gills as found in Holostei, Chondrostei and Teleostei, where the interbranchial septum has a distal free end, and iii) the Dipnoi type gills which approach the arrangement seen in external amphibian gills. In this thesis, branchial gills of teleosts will be the main focus. The gill basket marks the border between the medial pharyngeal and the lateral opercular cavity, and it consists of four paired gills separated by gill slits (Laurent, 1984). Each gill has two rows of filaments (primary lamellas) connected to the gill arch. Each row of filaments is termed a hemibranch, while the two hemibranchs connected to one arch constitute the holobranch (Olson, 2000). Connecting the proximal part of the filaments of the hemibranchs, the interbranchial septum of branchial gills extends in parallel with the filaments for various lengths depending on the species, leaving the distal ends of the filaments free (Fig. 4). The branchial cleft is delimited by the end of the interbranchial septum and the free filaments of the opposing hemibranchs. The length of the interbranchial septum seems to be evolutionary determined, as more recently evolved species seem to have a shorter septum (Olson, 2000, Hughes, 1995). This septum contains both smooth and striated (adductor) musculature along with rich innervation and vascularization (Laurent, 1984). The filament is regarded as the functional unit of the gills, as it holds all structures needed for the physiological gill functions (Wilson and Laurent, 2002, Evans et al., 2005, Laurent, 1984). The filament leading and trailing edges are situated in the water inlet and outlet regions, respectively, and the latter faces the branchial cleft (see Fig. 7). An alternative designation is efferent and afferent side, respectively, with reference to the filament blood flow directions (Hughes, 1984, Laurent, 1984). Each filament is supported by a gill rod of cartilage

and holds and supplies two opposing rows of respiratory lamellae (secondary lamellae) (Laurent, 1984).

Gill vascularization

The branchial vasculature receives the entire cardiac output through the ventral aorta and the four paired afferent branchial arteries, before it is distributed into three different vascular networks inside the gills (Olson, 2002): i) The arterio-arterial (respiratory) pathway, ii) the interlamellar network and iii) the nutrient network. The arterio-arterial pathway is most prominent and consists of the afferent and efferent segments of branchial arteries, filament arteries and lamellar arterioles in addition to the respiratory capillaries of the lamellas. The interlamellar network is arranged as thin-walled vessels in a ladder-like pattern within the filaments, stretching out to surround the afferent and efferent filament arteries. It takes its origin from the medial side of the efferent filament arteries through narrow-bore feeder vessels along the whole length of the filaments. These feeder vessels regulate the entrance of blood cells into the secondary circulation. The nutrient network takes its origin from numerous narrow-bore tortuous arterioles, arising from the efferent filament artery proximally in the filament as well as from the efferent branchial artery.

Jointly, the interlamellar and nutrient network constitutes the arteriovenous pathway of the gills and has been considered to constitute the gill secondary circulation (Olson, 2002, Olson, 1996, Laurent, 1984, Brauner and Rombough, 2012). In all but a few species, these two networks join each other inside the filament before reaching the branchial vein (Olson, 2000). It should be noted that all the blood of the teleost circulation has to traverse the respiratory lamellas before entering the branchial artery. The only exception to this rule has been suggested for rainbow trout and some non-salmonid species where anastomosis between the afferent filament artery or afferent filament arterioles and the interlamellar network has been described (Laurent, 1984).

The existence of vessels analogous to mammalian lymph vessels has been a longstanding debate (Vogel, 2010). It has been argued that interlamellar vessels possess many attributes similar to mammalian lymphatic capillaries (Olson, 1996). However, the interlamellar vessels arise from arteries and not blindly, thus do not fulfil the requirement for true lymphatic vessels. Nevertheless, the interlamellar network has been suggested as a functional analogue (Olson,

1996, Olson, 2000, Olson, 2002). The secondary circulation preferentially drains the gills and the skin, and Rasmussen et al. (2013) suggested that this circulation was one of the elements linking the mucosal immune system to systemic immunity. Recently the physical transparency of the larvae stage and transgenic fish lines has enabled the existence of lymphatic vessels within the zebrafish to be claimed (Küchler et al., 2006, Yaniv et al., 2006). The existence of similar vessels in other teleost species awaits confirmation.

Gill epithelium

Five major types of differentiated epithelial cells have been described within the gills, namely squamous and columnar pavement cells, mucous (goblet) cells, chloride (mitochondria-rich) cells and neuro-epithelial cells (Laurent, 1984). To facilitate efficient diffusion, the respiratory squamous pavement cells are thin, but this thinness also renders the epithelium particularly vulnerable to breakdown in barrier function (Hughes and Morgan, 1973). The nature of epithelial cells associated with the gill-associated lymphoid tissue (GIALT) and ILT has so far not been defined.

The teleost gills- immune system

Lymphoid mucosal compartments in fishes

Most of the surface of the fish is covered by mucosal tissue, be it the gills, skin, gut, outlet of the urogenital tract, olfactory pits, gas bladder in physostomous species, or conjunctiva. Hence, mucosal immune defence should be of particular relevance in fishes. Anatomically the secondary lymphoid tissues of teleost MALT has been divided into GIALT, gut-associated lymphoid tissue, skin-associated lymphoid tissue and nasal-associated lymphoid tissue (Salinas et al., 2011, Gomez et al., 2013, Salinas, 2015, Tacchi et al., 2014). Due to the diffuse distribution of these tissues, no further subdivision has been assigned, except for the possible inclusion of the ILT of Atlantic salmon as a part of the GIALT (Salinas, 2015). Depending on level of architectural organization, mucosal lymphoid tissues can be divided into organized and apparently non-organized mucosal lymphoid tissues. In mammals organized lymphoid tissues involve the

presence of lymphoid nodules with germinal centres (Mescher and Junqueira, 2015), and the prevailing view has been that such tissues are not found in fishes (Zapata and Amemiya, 2000, Rombout et al., 2005). It has been suggested that organized MALT evolved from the primitive, semi-organized lymphoid nodules found in the mucosa of amphibians and anurans (Goldstine et al., 1975). However, recently a primitive organized MALT has been described in the nasal pits of African lungfish (*Protopterus dolloi* Boulenger, 1900 and *Protopterus annectens* Owen, 1839) (Tacchi et al., 2015).

Immune cells of the gill mucosal immune system

When dealing with the various subsets of immune cells it is important to realize that in many cases they represent continuum of intermediate stages (Forlenza et al., 2011), and that it is often the extremes of the continuum that define a subset. The subdivision and interaction of the various components of the mucosal immune system is as complicated, if not more so, as in the systemic immune system. The paucity of available molecular markers has hampered description of mucosa-associated immune cells. However, a short recapitulation of current knowledge of immune cell subsets commonly associated with the gill epithelium is presented. While lymphocytes are regarded as descendants of lymphoid progenitor cells, the remainder of the leukocytes belongs to the myeloid subset.

Lymphocytes

Lymphocytes are small rounded cells with prominent, spherical, basophilic and condensed nuclei. Functional roles include immune defence against invading microorganisms, foreign or abnormal antigens, and cancer cells. As for mammals, lymphocytes can be divided into T-cells, natural killer cell (NK-cells) and B-cells (Koppang et al., 2015). In the rainbow trout gills, T-cells have been claimed to be the most numerous resident lymphocyte population (Lin et al., 1999).

T-cells form the cellular arm of adaptive immunity. As the adaptive immune response to a large extent is restricted to antigens presented through MHC-molecules, each clone of lymphocytes usually displays a high degree of antigen specificity. The TCR is common to all T-cells and recognizes peptides presented by MHC-receptors, together with the co-receptor CD3

(Nakanishi et al., 2015). In particular, the CD3-receptor has been suggested as a pan-T-cell marker also in fishes, and antibodies against CD3 have been essential to study T-cell populations in species such as the Atlantic salmon (Koppang et al., 2010). Recently cloning and characterization of the zeta-chain-associated protein kinase 70 (ZAP-70), which belongs to the intracellular domain of the TCR, has revealed a high degree of conservation between human, zebrafish and common carp (Piazzon et al., 2015, Forlenza, 2009, Yoon et al., 2015). ZAP-70 is expressed in T-cells and NK-cells and antibodies against ZAP-70 can thus serve as another pan-T-cell marker. Also in fishes TCR-bearing T-cells can be further subdivided into two major subsets, namely $CD4^+CD8^-$ T helper cells (Th) and $CD4^-CD8^+$ cytotoxic T-cells (Nakanishi et al., 2015). It is becoming increasingly clear that Th-subsets of fishes can be further subdivided into Th1, Th2, Th17 and regulatory T-cells based on their cytokine- and gene transcription profiles in a similar fashion as seen in mammals (Wang and Secombes, 2013). In the normal-state salmonid gills high transcription of Th2- associated cytokines has led to the suggestion of a Th2-skewed environment protecting the gills against parasites and damage from aberrant Th1 and Th17 responses (Takizawa et al., 2011b).

In mammals the definition of T-cell subsets becomes increasingly complex as natural killer (NK) T-cells, mucosal-associated invariant T-cells and γ/δ T-cells diverge from the classical scheme established for systemic T-cells (D'Acquisto and Crompton, 2011).

NK-cells are lymphocytes belonging to the non-specific cytotoxic arm of the innate immune system. So far only two types of NK-cell homologues to NK-cells of mammals have been described in fishes; nonspecific cytotoxic cells and NK-like cells (Fischer et al., 2013). In common carp, natural killer cell enhancing factor (NKEF) has been shown to exist in two isoforms (*NKEF A* and *–B*). *NKEF A* was constitutively highly transcribed in normal-state gills, and *NKEF B* was significantly upregulated during infection with spring viremia of carp virus (Huang et al., 2009). Although functions such as enhancement of NK-cell cytotoxicity and protection of DNA and proteins from oxidative stress have been assigned to mammalian NK-cells, the function of teleost NKEF-A/B remains to be investigated (Huang et al., 2009). Beyond this study the tissue-distribution and function of NK-cell homologues in the gills is still at an early stage (Koppang et al., 2015).

B-cells and plasma cells form the humoral arm of adaptive immunity and are associated with three classes of immunoglobulins, namely IgM, IgD, and the latest, IgT (T for teleost) or IgZ (Z for zebrafish) (Wilson et al., 1997, Hansen et al., 2005, Danilova et al., 2005). For all three isotypes, both membrane-bound and secretory variants have been described (Ramirez-Gomez et al., 2012). IgT^+ B-cells are generally considered as both IgM^- and IgD^-. IgD^+ B-cells have generally been regarded as IgM^+ (IgM^+IgD^+), but recently an IgM^-IgD^+ subset highly present in the gills of European rainbow trout has been described (Castro et al., 2014). Although the function of IgD to a large degree remains unknown, recent indication on involvements in mucosal immunity has been presented (Makesh et al., 2015). IgM is the predominant isotype in blood and in mucus (Tadiso et al., 2011), while IgT (for those species possessing such) is thought to be the main isotype at mucosal surfaces (Parra et al., 2015, Salinas et al., 2011, Zhang et al., 2010). This distribution has recently been verified for the gills of rainbow trout, where IgT^+ B-cells in contrast to both IgM^+- and IgD^+ B-cells were found to proliferate locally during both parasitic and bacterial infections (Xu et al., 2016). The same report also showed that IgT was the major immunoglobulin coating the gill external microbiota thus identifying a major mucosal protective role undertaken by this isotype. In common carp, IgT is found as two subclasses where *IgT1* is preferably transcribed in systemic compartments while *IgT2* is dominant in mucosal tissues (Ryo et al., 2010).

B-cells are normally regarded as one of the prime constituents of adaptive immunity, but these cells also possess innate features such as phagocytic capability and secretion of natural antibodies (Parra et al., 2015, Sunyer, 2013). Thus, apart from immune responses such as antibodies targeting pathogens and marking them for phagocytosis and complement activation, the innate immune function of B-cells has been suggested to be particularly important in teleosts. Fish B-cells have been suggested to perform functions similar to human dendritic cells (Parra et al., 2015, Zhu et al., 2014).

Professional antigen presenting cells

Professional antigen presenting cells (APCs), including dendritic cells (DCs), macrophages and B-cells, are known for their superior ability to present antigens. Antigen presentation is mediated through MHC class I and -II, and results in either activation and proliferation or anergy of T-cells

(Granja et al., 2015). While it is supposed that all nucleated cells are able to display MHC class I on their cell surface (Dijkstra et al., 2003, Hewitt, 2003), expression of MHC class II under natural condition is largely confined to the professional APCs. However, exceptions such as the thymic epithelial cells and atypical MHC class II^+ cells exist in higher vertebrates (Kambayashi and Laufer, 2014). High numbers of MHC class II^+ cells have been detected in the epithelium of the ILT and gill epithelium in general in Atlantic salmon and rainbow trout (Haugarvoll et al., 2008, Koppang et al., 2003, Hetland et al., 2010, Olsen et al., 2011). Furthermore, high transcription of the costimulatory *CD40*, a membrane-bound receptor constitutively expressed in APCs in mammals (Elgueta et al., 2009), was found in the gills of Atlantic salmon (Lagos et al., 2012).

Mucosal antigen sampling in mammals has adapted to the diverse epithelial barriers that cover mucosal surfaces throughout the body, but all involve collaboration with DCs (Neutra and Kozlowski, 2006). The migratory capacity of DCs makes them particularly relevant as APCs compared with the tissue-resident macrophages (Jankovic et al., 2001). In mammals, DCs have been recognized as a critical link between innate and adaptive immunity (Mildner and Jung, 2014), and the same is anticipated for fish DCs (Esteban et al., 2015). The presence of teleost DCs has been a matter of debate, and their characterization has been elusive in the absence of specific markers (Granja et al., 2015). In salmonids existence of Langerhans-like DCs has been claimed based on the ultrastructural feature of cells containing Birbeck-like granules in microsporidia infected gills (Lovy et al., 2006, Lovy et al., 2007). In mammals CD83 is a standard lineage marker for activated or differentiated DCs, but it can also be expressed on other leukocytes. In fish high constitutive transcription of the *CD83* homologue has been detected in the gills of turbot (*Scophthalmus maximus* L.) (Hu et al., 2010), gilthead seabream (*Sparus aurata* L.) (Doñate et al., 2007) and in the elasmobranch nurse shark (*Ginglymostoma cirratum* Bonnaterre, 1788) (Ohta et al., 2004). Various hallmarks of mammalian DCs were identified in a functional approach employing enriched cultures of DCs from rainbow trout spleen, head kidney and anterior portion of trunk kidney (Bassity and Clark, 2012). Injecting enriched and labelled DCs intraperitoneally into allogeneic fish showed a preferred homing to the swim bladder, spleen and the gut, while the lowest number of homing DCs of the tissues investigated was found in the gills (Bassity and Clark, 2012). Recently, $CD8\alpha^+$ MHC class II^+ dendritic-like cells were identified in skin, gills and gut of rainbow trout (Granja et al., 2015), representing one

of few studies dedicated to DCs at fish mucosal surfaces and also the first description of a particular teleost DC subset. All the evidence for the existence of DCs in teleosts implies that this specialized APC evolved in concert with the emergence of adaptive immunity (Bassity and Clark, 2012), and that different subsets might be found in various organs and tissues.

The relative ease of isolating macrophages owing to their surface adherence in cell suspension has contributed to extensive exploration of their nature even in fishes. While monocytes are circulatory cells of the myeloid lineage, macrophages represent the extravasated, tissue-resident counterpart. Despite the high phenotypic plasticity of macrophages, it is usual to differentiate between (Forlenza et al., 2011, Hodgkinson et al., 2015); i) pro-inflammatory type (M1) promoting antimicrobial host defence operating in a Th1-environment, and ii) anti-inflammatory or regulatory types (M2) involved in resolving inflammation and tissue repair induced in a Th2-environment. Although not assigned to a particular cellular subset, the gill environment of rainbow trout is regarded as skewed in the Th2-direction (Takizawa et al., 2011b, Harun et al., 2011). Macrophage-like cells residing in the gills have been suggested to be important in particle-uptake (Goldes et al., 1986, Ototake et al., 1996, Zapata et al., 1987) as well as in clearing of apoptotic cells during normal epithelial-cell turnover in the gills of Mozambique tilapia (*Oreochromis mossambicus* Peters 1852) (Wendelaar Bonga and van der Mej, 1989). A profound upregulation of inducible nitric oxide synthase (*iNOS*) was found particularly in gills and kidney of rainbow trout exposed to the Gram-positive intracellular bacterium *Renibacterium salmoninarum*, which was suggested to stem from activation of tissue-resident macrophages (Campos-Perez et al., 2000). Considerable amounts of macrophages were reported in a study on cell-suspensions from gill tissues of Atlantic salmon and dab (*Limanda limanda* L.) (Lin et al., 1998).

The MHC class II^+ cells identified in the ILT of Atlantic salmon still remains to be characterized.

Eosinophilic granule cells

Eosinophilic granule cells (EGCs) are considered an innate cellular subset characterized by large oval or spindle-shaped cells with a small, spherical nucleus and numerous cytoplasmic

granules (Reite and Evensen, 2006, Lamas et al., 1991, Baccari et al., 2011). A comparison of EGCs to mammalian mast cells has been a longstanding matter of debate, partly fuelled by the variable staining properties of EGCs in different fish species and after different types of fixation (Reite and Evensen, 2006, Reite, 1996). It has been suggested that teleost EGCs are mast cells deprived of their basophilic granular material (Reite, 1996). The metachromatic granules of mammalian mast cells contain histamine, heparin and other bioactive components that are involved in inflammatory responses, innate and adaptive immunity, wound healing and tissue remodelling (Mescher and Junqueira, 2015, Baccari et al., 2011). Metachromatic staining of EGC cytoplasmic granules has been advocated in various fish species, including salmonids, upon applying appropriate alcoholic fixatives (Reite, 1997). However, histamine-content of teleost EGCs has so far only been claimed for species in the order of Perciformes (Mulero et al., 2007). Other bioactive compounds are commonly shared between EGCs and mammalian mast cells, while compounds such as the peptide antimicrobials (piscidins) appear to be a specific trait of fish EGCs (Silphaduang and Noga, 2001, Silphaduang et al., 2006). The differences in tissue-distribution of EGCs between species are thought to be a result of adaption to different environments (Nigam et al., 2012, Reite and Evensen, 2006). In general, EGCs occur commonly in association with blood vessels, nerves and in proximity to mucosal surfaces such as the intestine and the gills (Gomez et al., 2013, Mulero et al., 2007, Lamas et al., 1991). In normal-state salmonid gills EGCs are typically found in the connective tissue of filaments often surrounding blood vessels, while lower numbers are usually found in the gill epithelium (Reite, 1997, Holland and Rowley, 1998). This is contrary to findings in Mozambique tilapia, where motile and chemotactic EGCs were detected both within and on the surface of epithelium in addition to underlying connective tissue (Barnett et al., 1996). An increase in numbers of EGCs is often associated with various chronic inflammatory conditions (Baccari et al., 2011, Reite and Evensen, 2006, Dezfuli and Giari, 2008). Degranulation of EGCs in rainbow trout gill tissue explants was shown to induce increased resistance of the branchial vascular bed, thus eliciting vasomotor responses (Reite, 1996). Further, in salmonids and Nile tilapia (*Oreochromis niloticus* L.) degranulation of EGCs in the swim bladder was associated with release of leucocyte-chemotactic factors and increased vascular permeability (Reite, 1996, Matsuyama and Iida, 1999, Matsuyama and Iida, 2001).

Others

The elongated rodlet cells are associated with epithelial tissues and are characterized by their intracellular club-like inclusions of crystalline, dense inner core. The content of the inner core is secreted onto the epithelial surfaces upon stimulation (Reite and Evensen, 2006, Bielek, 2008). Rodlet cells have so far only been demonstrated in fishes, and tissue-distribution between and within species varies. An increased recruitment during helminthic infections has been noted (Reite, 2005, Reite, 1997). Although the true function of rodlet cells is still unknown, they are suggested to play a role in host defence, and a function as tissue-resident precursors for EGCs has been suggested (Reite and Evensen, 2006).

Granulocyte-like cells found in the blood of teleost fish include neutrophils, heterophils, eosinophils and basophils, but a great variability in composition and function exists (Hine, 1992, Koppang et al., 2015). As with the mammalian subsets neutrophils constitute the most abundant granulocyte type in fishes displaying phagocytosis and activity during early-phase of acute inflammations, although the characteristic myeloperoxidase-activity, as found in mammalian neutrophils, is low or lacking in several fish species (Hine and Wain, 1988). The normal-state gills is normally considered to contain low numbers of granulocytes (Koppang et al., 2015), although the numbers of acidophilic granulocytes (suggested by the authors to be functionally equivalent to higher vertebrate neutrophils) was shown to increase in seabream gills infected with ectoparasites (Lui et al., 2013).

Antigen uptake over the gills

The teleost gills have been identified as entry-point for a range of both local and systemic infections (Koppang et al., 2015, Ohtani et al., 2014), and as an important site of antigen uptake in the form of bacterins (Bowers and Alexander, 1981, Kato et al., 2013, Zapata et al., 1987). Factors shown to influence antigen-uptake from vaccine baths include those related to the fish (size, degree of stress, use of anaesthetics), water (temperature, pH, osmolality), time of exposure, vaccine concentration and -formulation (adjuvants or not, particulate or soluble) (Bowers and Alexander, 1981, Tatner and Horne, 1983, Nakanishi and Ototake, 1997). Selective mechanisms for antigen uptake across gills have been suggested, based on both differences in uptake between antigenic and non-antigenic material and differences in uptake of different bacterial species or

physiological states of the same strain of bacteria (Koppang et al., 2015, Torroba et al., 1993, Hodgkinson et al., 1987). Furthermore, several experiments have shown that after a short retention time in the gills the antigen reappears in various systemic lymphoid tissues (Smith, 1982, Takizawa et al., 2011b).

Cells involved in antigen uptake can differ depending on physical state of the antigen and site of antigen entry, but gill epithelial cells seems essential (Nakanishi and Ototake, 1997). In a mechanism termed branchial phagocytosis epithelial cells of the rainbow trout gills were observed to internalize mineral particles (inert suspended clay kaolin), followed by exocytosis and subsequent endocytosis in deeper tissue layers (Goldes et al., 1986). This mechanism was supported by Zapata et al. (1987) in Atlantic salmon and by Kato et al. (2013) in Japanese flounder (*Paralichthys olivaceus* Temminck & Schlegel, 1846). Both authors found *Yersinia ruckeri* O-antigen- and *Vibrio anguillarum* bacterin, respectively, adhering to or residing within gill epithelial cells. This was followed by uptake in mononuclear phagocytes both within the epithelium and underlying connective tissue. These antigens appeared immediately after bath immunization and were retained within the gill tissue only for a short time (Zapata et al., 1987, Kato et al., 2013). Followed by an initial period of immune exclusion in very young channel catfish (*Ictalurus punctatus* Rafinesque, 1818), epithelial cells emerged as the major cell type taking up fluorescent latex particles during immersion (Glenney and Petrie-Hanson, 2006). In a preliminary report rainbow trout gill epithelial cells with certain features of mammalian microfold cells (M-cells) were associated with uptake of *Aeromonas salmonicida* subsp. s*almonicida*-bacterin (Kato et al., 2016). M-like cells involved in antigen uptake have been claimed to exist in the gut of Atlantic salmon (Fuglem et al., 2010), and it has been considered highly probable that specialized gill epithelial cells similar to mammalian M-cells are present in the gills (Koppang et al., 2015). In mammals M-cells are associated with specialised mucosal immunological niches governing antigen uptake. They are situated overlying germinal centres in follicle-associated epithelium, and deliver intact macromolecules and microorganisms across the epithelial barrier to underlying lymphoid tissue for immune surveillance (Neutra et al., 2001).

In the preliminary report by Kato et al. (2016), a non-epithelial cellular subset involved in uptake of *Aeromonas salmonicida* subsp. *salmonicida*-bacterin was characterized by high transcription of *CD83* and interleukin-12 (*IL-12*). It was suggested that these cells could be either

macrophages or dendritic cells, but it was unclear whether these cells were associated with primary or secondary trapping of antigens. Altogether, current knowledge support that the epithelial surface of the gills appears as an important site for antigen sampling.

Immune responses induced by mucosal vaccine-models

Appearance of antigen-specific immunoglobulin-secreting B-cells in the gills after immersion vaccination draws attention to the potential of mucosal vaccines (dos Santos et al., 2001, Lumsden et al., 1993, Lumsden et al., 1995).

Induction of specific antibody responses have been demonstrated in small-sized fishes. An observed lack of immune response in rainbow trout fry below 0.14g after direct immersion with *Vibrio anguillarum*-bacterin was shown to result from lack of antigen uptake rather than tolerance. Once the fry reached a size at which bacterin was taken up, reasonable levels of protection were demonstrated, and based on this model it was suggested that 0.4g was the minimum weight of trout suitable for commercial immersion vaccination (Tatner and Horne, 1984). Sudheesh and Cain (2016) demonstrated onset of protective immunity in 0.5g rainbow trout fry after immersion vaccination with *Flavobacterium psychrophilum*-bacterin. Furthermore, onset of immunity correlates better with the weight of the fish than its age, as inferred by relative percentage survival (Johnson et al., 1982b, Johnson et al., 1982a, dos Santos et al., 2001). Although the direct involvement of the gills was not investigated in the aforementioned studies, they indicate the potential of mucosal vaccination in protecting small-sized fish.

Much less is known about the corresponding priming of the cellular arm of adaptive immunity during mucosal vaccination. This lack of knowledge is probably due to the more complicated task of directly measuring cell-mediated immunity (Nakanishi and Ototake, 1997). It has been suggested that the often-observed discrepancy between low serum antibody levels and high levels of protection after immersion or bath vaccination is a result of induced cellular immunity (Palm et al., 1998, Villumsen and Raida, 2013). During bath vaccination of Japanese flounder with *Vibrio anguillarum*-bacterin, up-regulation of inflammatory parameters together with transcripts associated with adaptive cellular immunity was noted in the gills but not in the skin or intestine

(Kato et al., 2013). However, an ILT has so far not been described in the gills of Japanese flounder.

Interbranchial lymphoid tissue

Haugarvoll and co-workers (2008) presented the first description of the ILT in Atlantic salmon in 2008. The ILT was described as an intraepithelial cell-aggregation on the caudal edge of the interbranchial septum. Abundant MHC class II^+ cells were seen within this aggregation together with proliferating cell nuclear antigen $(PCNA)^+$ cells, particularly in the basal layers. No labelling for IgM was demonstrated. Based on transcription analysis after laser microdissection of this cell aggregation, the presence of T-cells was suggested. This was the first description of lymphocyte aggregation within teleost gill epithelium, and it was suggested to illustrate a phylogenetic differentiation and compartmentalization of a respiratory organ immune apparatus (Haugarvoll et al., 2008). Subsequently the lymphocyte-like component of the cell-aggregation in the gills of Atlantic salmon and rainbow trout was shown to be primarily T-cells upon immunohistochemical labelling with a polyclonal CD3ε anti-salmon antibody (Koppang et al., 2010). These authors indicated that the ILT displayed some characteristics of a secondary lymphoid tissue with no primary lymphoid tissue attributes. The functional basis for this was not verified. In these studies neither the anatomical extent of the ILT nor its ontogeny were addressed. Furthermore, no comments were made on the possibility of communication between this lymphoid aggregate and the systemic circulation. High numbers of $CD8\alpha^+$ cells have been revealed within the ILT and along the filaments and lamellas in apparently healthy Atlantic salmon (Hetland et al., 2011, Hetland et al., 2010) and rainbow trout (Takizawa et al., 2011a). Dynamic properties of the ILT has been suggested, based on depletion of $CD8\alpha^+$ cells both during infection with infectious salmon anaemia virus (ISAV) in Atlantic salmon (Hetland et al., 2011, Hetland et al., 2010) and *Ichthyophthirius multifiliis* (Fouquet, 1876) in rainbow trout (Olsen et al., 2011), but the fate of these cells was not addressed. The presence of ILT-like tissue in other species than Atlantic salmon and rainbow trout has not been reported.

AIMS OF STUDY

The overall aim of the present thesis was to increase the knowledge and understanding of the ILT in teleosts by revealing novel anatomical and immunological characteristics of this gill lymphoid aggregate in the Atlantic salmon and the common carp.

Specific goals of the thesis were to investigate:

a) Distribution of the ILT within the gills of the Atlantic salmon.

b) Ontogeny and development of the ILT in different life-stages of the Atlantic salmon.

c) Possibilities for communication between the ILT and systemic circulation of the Atlantic salmon.

d) Relationship between the ILT and the thymus in the Atlantic salmon.

e) Whether an ILT exists in the gills of the more recently evolved common carp.

SUMMARY OF PAPERS

Paper I:

The teleost gill forms an extensive, semi-permeable barrier that must tolerate intimate contact with the surrounding environment and be able to protect the body from external pathogens. The recent discovery of the ILT has initiated an anatomical and functional investigation of the lymphoid tissue of the salmonid gills. In this article, sectioning of gills in all three primary planes revealed an elongation of the ILT extending along the trailing edges of the primary filaments to the very distal end, a finding not previously described. This newly found lymphoid tissue was investigated using a range of morphological and transcriptional tools. To avoid potential salinity-related effects, the study focused on two fresh-water life-stages, namely smoltifying juveniles and mature adults. Aggregates of T-cells continuous with the ILT were found within the thick epithelial lining of the trailing edge of the filament in considerably larger numbers than seen in the epithelium of the leading edge and of the interlamellar area. Only a few of these cells were identified as $CD8\alpha^+$-cells, and there was a significantly ($P<0.05$) higher relative transcription of *CD4*- than of *CD8*-related genes in all gill segments investigated. Numerous major histocompatibility complex class II^+-cells were distributed uniformly throughout the filament epithelial tissue. Few Ig^+-cells were detected. Overall, the morphological features and comparable immune gene transcription of the previously described ILT and the filament trailing edge lymphoid tissue suggest a close functional and anatomical relationship. It was proposed that the anatomical definition of the ILT must be broadened to include both the previously described ILT (to be renamed proximal ILT) and the trailing edge lymphoid tissue (to be named distal ILT). This extended anatomical localization identifies the ILT as a widely distributed mucosal lymphoid tissue in the gills of Atlantic salmon.

Paper II:

The interbranchial lymphoid tissue of Atlantic salmon originates from an embryological location that in higher vertebrates gives rise to both primary and secondary lymphoid tissues. Still much is unknown about the morphological and functional development of

the ILT. In this article a standardized method of organ volume determination was established to study the development of ILT in relation to the development of the gill and the thymus. Based on morphological findings and gene transcription data, the ILT shows no signs of primary lymphoid function. In contrast to the thymus, an ILT-complex first became discernible after the yolk-sack period. After its appearance, the ILT-complex constitutes 3-7 % of the total volume of the gill (excluding the gill arch) with the newly described distal ILT constituting a major part. In adult fish the ILT was approximately 13 times larger than the thymus. Confined regions of T-cell proliferation were present within the ILT. Communication with systemic circulation through the distal ILT was also found highly plausible, thus suggesting that both internal and external recruitment of immune cells is possible in the growing ILT.

Paper III:

The gills of fish constitute a significant proportion of the total mucosal surface, and their immunological potential has been substantiated by the discovery of the ILT in salmonids. We hypothesised that other fish species would possess similar lymphoid aggregations. Employing different morphological techniques we identified and characterized ILT in common carp. As in salmonids carp ILT consists of proximal and distal regions of intraepithelial lymphocyte aggregations lining the branchial cleft. However, the carp proximal ILT could be divided into three morphologically distinct compartments. The basal compartment contained high numbers of ZAP-70^+ cells (putative T-cells), moderate numbers of IgT-1^+ B-cells, and was traversed by blood vessels. The intermediate and uppermost compartments contained moderate numbers of ZAP-70^+ cells, low numbers of IgT-1^+ B-cells and appeared devoid of blood vessels. Furthermore, the intermediate compartment was distinctive due to the presence of $WCL38^+$ cells (putative mucosal T-cells) and high numbers of EGCs. The morphology of the intermediate and uppermost compartments was propagated into the distal ILT. These findings show that the ILT of the more recently-evolved common carp has a higher degree of organization than the ILT of salmonids.

METHODOLOGICAL CONSIDERATIONS

Material

In this thesis the fishes examined were not immunized or otherwise immunological stimulated, and were exposed to relatively clean water and low crowding density. The intention was to investigate apparently healthy fish under normal-state conditions. Thus, the fishes investigated in this thesis are referred to as apparently healthy, and tissue thereof is referred to as being in normal-state. The inclusion criteria were no history of disease or mortality above the normal in the populations, no external or internal gross pathology, and no histopathological changes in the gills. In paper I and II both wild-caught and reared Atlantic salmon were included, while paper III was based solely on reared common carp. Captivity has been shown to influence the transcript-levels of various immune-related genes in the gut mucosa of Atlantic salmon, as compared with their wild counterpart (Løkka et al., 2014). Whether the same applies to the gill mucosa remains to be investigated.

Atlantic salmon

Yolk-sack larvae and juveniles were sampled from either a cultivation plant (Hellefossen hatcheries, Hokksund, Norway) or a research station (IMR Matre research station, Matredal, Norway) with continuous flow-through of fresh-water, while adult pre-sexually mature individuals were sampled from sea-cages (LetSea, Sandnessjøen, Norway). Wild sexually mature individuals were captured after returning to the river (Drammen river, Drammen, Norway).

To increase the validity of the study when addressing the distribution of the ILT (paper I) widely separated life-stages, but in as similar environments as possible, were sought. Salinity is known to be an important factor influencing the immune system in teleosts (Cuesta et al., 2005), and therefore pre- and post-sea life-stages were chosen. For the pre-sea stage juveniles about to smoltify were chosen so that the gills were of a reasonable size. For the post-sea life stage wild sexually mature individuals were collected. While the juvenile group was uniform in size, the mature group varied considerably. Mature fish commonly return to the river during early summer to autumn but otherwise it is not possible to know the more exact time spent in fresh-water. Furthermore, the normal starvation during sexually maturation (Thorstad et al., 2011) might have had an effect on the immune system of the mature salmon.

For the investigation of the volume of the ILT (paper II) the same reasoning as for paper I was followed, although in this study yolk-sack larvae and sea-transferred fish before sexual maturation were included. Juveniles were sampled from Hellefossen hatcheries. As both season and temperature are known to influence the immune system (Chilmonczyk, 1992), great care was taken to sample fish from as similar water-temperatures as possible, and the sampling was done at the same time of the year.

Common carp

In the study on the ILT of common carp (paper III) fish was sampled from the facilities of 'de Haar Vissen', department of Animal Sciences of Wageningen University (The Netherlands). The fish was held under strictly controlled water conditions, and the water quality was essentially the same prior to and during the sampling period. It is emphasised that the water employed in this facility probably is much cleaner than what would be expected in most natural carp habitats or under aquaculture conditions.

Ethical considerations

Handling, anaesthesia and euthanasia were performed in accordance with regulations of the Norwegian Directorate of Fisheries (Norway) and the Centrale Commissie Dierproeven (CCW) (the Netherlands).

Methods

In general histology was prepared from paraffin-embedded material by standard methods (Bancroft and Gamble, 2008). Sections of all fishes were stained with haematoxylin and eosin (HE) which was the method of choice during point-counting for volume-estimations in paper II. Special staining techniques were additionally used on the material of paper I and III to reveal histochemical properties within the tissues. Immunohistochemistry (IHC) was used to describe tissue-distribution of different epitopes (all papers), and immunofluorescence (IF) double-labelling was used to investigate possible co-localization of selected markers (paper II and III). Other morphological techniques included vascular casting combined with scanning electron microscopy, to describe details concerning vascular structures adjacent to the distal ILT in

Atlantic salmon (paper I) or associated with the basal proximal ILT in common carp (paper III). Transmission electron microscopy further revealed ultrastructural details of these vascular structures (paper II and III). Quantitative real-time polymerase chain reaction (qPCR) was used to address possible differences in gene transcription levels between proximal and distal ILT (paper I), and also to investigate whether the ILT could be associated with a primary lymphoid function (paper II).

HE-staining, special staining, and scanning electron- and transmission electron microscopy were performed according to standard procedures as previously described by others (Bancroft and Gamble, 2008, Haugarvoll et al., 2008).

Immunohistochemistry and immunofluorescence

The purpose of IHC and IF is to identify discrete tissue components by the interaction of target epitopes with specific antibodies tagged with a reporter system that either produces a colour product (IHC) (all papers) or fluorescence (IF) (paper II and III). These techniques make it possible to visualize the distribution and localization of specific epitopes within cells and in the proper tissue context. Formalin fixed, paraffin-embedded material was chosen over cryo-sectioned material due to superior morphologic quality obtained with the former method. As formalin-induced cross-binding might mask epitopes, heat-induced epitope-retrieval by autoclavation was included in the procedures.

One of the major obstacles in research on fish immunology is the shortage of specific antibodies (Mulero et al., 2008). One possible factor delaying this progress might be the heavily glycosylated surface of fish cells, which diverts the antibody response towards these molecules instead of specific epitopes (Yamaga et al., 1978). Another factor is the high occurrence of gene duplications as a result of several rounds of whole-genome duplications (Flajnik and Kasahara, 2010). This is the case for the various subclasses of teleost immunoglobulin isotypes (Hedfors et al., 2012, Tadiso et al., 2011).

In this thesis, both commercially and non-commercially available antibodies were used. Validation of specificity and sensitivity is essential and should preferably be done by several methods such as western blot, flow cytometry, immunofluorescence on transfected cells or verification of conserved genes across species (Howat et al., 2014). For description of validations,

the reader is referred to the references given in each paper. Some antibodies with species cross reactivity were used. The anti-PCNA antibody was produced against rat PCNA-A fusion protein, but this nuclear protein has been shown to be highly conserved (Suzuka et al., 1989), even in fishes (Gu et al., 2013). The specificity of the anti-pan-cytokeratin antibody produced against human epidermal skin has been evaluated on the basis on labelling pattern by several authors (Bunton, 1993, Haugarvoll et al., 2008, Løkka et al., 2013). The anti-ZAP-70 antibody targets the cytoplasmic signalling domain of the T-cell receptor complex (Wang et al., 2010, Chan et al., 1991). While great species-variability exists in extracellular domains, intracellular domains are often found to be highly conserved (Forlenza, 2009), and the specificity of anti-ZAP-70 towards common carp- (Forlenza, 2009) and zebrafish (Yoon et al., 2015) T-cells or NK-cells has been confirmed. However, the resulting pattern of each labelling must be subjected to critical judgement. Furthermore, inclusion of positive and negative controls in each labelling batch is important for proper interpretation of results. Positive controls included sections from tissue known to contain the epitope in question. Negative controls included tissue known not to contain the epitope, use of pre-immune serum as primary antibody, irrelevant primary antibody of the same isotype (isotype-control) and incubation with only buffer omitting the primary antibody (Howat et al., 2014).

Only unconjugated primary antibodies were used in the study, necessitating an indirect procedure utilising secondary antibodies targeting the relevant isotype (and subclass) of the primary antibody. While this offers the advantage of signal amplification, it also introduces an additional step with the possibility of non-specific labelling by the secondary antibody. Therefore, a prior blocking-stage with normal serum from the same species as the secondary antibody originated from was included.

Quantitative real-time polymerase chain reaction

Nucleic acid quantification was performed with qPCR, which is a molecular technique that monitors the amplification of a target DNA molecule as the PCR-reaction proceeds and hence allows evaluation of the transcription level of certain genes within a tissue homogenate. This is done by determining the time point during cycling when the amplification of the nucleic acid target reaches a threshold value (threshold cycle (Ct) or quantification cycle (Cp) (Bustin et al.,

2009)). This value is defined as the point at which the detection signal rises appreciably above the background level (Pfaffl, 2001). The methodology is based on the fluorescence signal produced by reporter molecules, and the strength of this signal increases with the increase of amplicon (amount of DNA templates) in each reaction. Two fundamentally different reporter molecule systems exist; non-sequence-specific fluorescent intercalating double-stranded DNA-binding dyes and sequence-specific fluorescent probes (Pfaffl, 2004). In this thesis, sequence-specific fluorescent probes were employed in the form of hydrolysing probes (TaqMan® probes). The level of fluorescence detected is directly proportional to the amount of fluorophore released from the probes as a result of the 5´–3´ exonuclease activity of Taq polymerase, which depends on the amount of amplicon in the PCR reaction (van Guilder et al., 2008). Due to the sequence-specific binding of the hydrolysis-probe, this system is regarded as more specific than systems using non-sequence-specific probes. Furthermore, by designing primers or probes to span exon-exon junctions, unintentional binding of contaminating genomic DNA can be avoided.

Two different quantification methods in real-time qPCR are possible; absolute quantification is based on either an internal or an external calibration curve, while relative quantification is based on the relative transcription of a target gene *versus* a reference gene (Pfaffl, 2001). Although the relative quantification-approach is less complicated, it presupposes stabile transcription of the reference gene(s) in the different tissues under investigation.

One has to be careful when comparing qPCR results with immuno-labelling. These two methodologies measure two different time-points during protein synthesis (transcription *versus* translation), and several post-transcriptional mechanisms exist before the final protein can be detected. Furthermore, during work-up the sampled tissue is homogenized, meaning that there is no way of knowing whether a majority or only a small fraction of cells are responsible for the detected nucleic acid (Bassity and Clark, 2012). Homogenization also dilutes the sequence of interest if it *in vivo* occurred in certain cells only. Several other possible shortcomings are reviewed by the MIQE guidelines (Bustin et al., 2009). However, in the absence of appropriate molecular markers, qPCR has brought important knowledge into the field of fish immunology and will certainly continue to do so in the future.

Vascular corrosion casting

Vascular corrosion casting has been an indispensable technique helping researchers to describe the immensely complicated vasculature found in the gills of various species (Laurent, 1984). This is achieved by introducing low-viscosity resin into the vascular space, and after polymerization of the resin and maceration of surrounding tissue, the vascular corrosion casting can be investigated either macroscopically or aided by microscope techniques.

Optimally, the resin should fulfil several criteria. Non-toxicity, low viscosity, high resilience towards breaking as well as tear- and corrosion resistance are all essential factors. Furthermore, the resin should not penetrate tissue barriers, not cause morphological or physiological changes to the vessel walls and not shrink during polymerization, while it should maintain structural configuration while drying and conduct electrons (Verli et al., 2007, Meyer et al., 2007). While probably no resin fulfils all these criteria, the polyurethane elastomer PUii from VasQtec (Zurich, Switzerland) was found to perform well for most of these factors.

Complete evacuation of the vascular space is important to produce representative castings. Important preliminary steps in the preparation of vascular casting include injection of anticoagulants followed by thorough flushing of the vascular bed. Inclusion of fixatives such as formalin during flushing can decrease the fragility of thin walled structures (Verli et al., 2007). Optimally infusion should always be performed at controlled, physiological pressure. However, often slightly higher pressure is needed, increasing the probability of over-extension of thin-walled structures. Thus, pressure-measurement during the procedure is important to achieve reproducible results. Injection of resin into afferent and efferent vessels supplying a capillary bed in different preparations may serve as a control of artifacts.

Scanning electron microscopy has proven invaluable in revealing microscopic details in vascular corrosion casting. It is important to obtain proper electrical conductivity within the specimen and connection to the sample holder (Macchiarelli et al., 2015). Coating with a 30 nm thick layer of palladium was found sufficient in most cases, and the conductivity to the sample holder was increased by bending the carbon conductive tabs, increasing the contact surface with the thread-like gill vascular corrosion castings.

Morphometric measurements

Volume estimation from vertical sections offers a straightforward and reproducible method for measuring the size of various objects (Mühlfeld, 2014, Baddeley et al., 1986). Contrary to measuring area and length, volume measurements do not require isotropic random orientation of the object to be measured (Baddeley et al., 1986).

One potential source of error using paraffin section might be tissue shrinkage during fixation and further processing, and stretching of the section during preparation (Dorph-Petersen et al., 2001). However, it has been claimed that stretching in the water-bath to a large extent compensates for the shrinkage during fixation (Da Costa et al., 2007). Regarding the gills, it is plausible that the cartilaginous or bony filaments would behave different from surrounding soft tissues during processing. For this reason the gill arches were omitted from the volume estimations. In order to achieve reproducible results, standardized treatment of tissues during all steps is crucial. One major benefit of using paraffin sections instead of plastic sections is the possibility to perform immunohistochemistry on consecutive sections, ensuring proper classification of tissues.

RESULTS AND GENERAL DISCUSSION

In order to perform sound functional studies on the ILT, a thorough understanding of its anatomy is crucial. This thesis presents new knowledge about the anatomical distribution (paper I), ontogeny and development (paper II) of the ILT in Atlantic salmon. In the post yolk-sack larvae stages, the ILT was found to constitute a significant part of the total salmonid gill volume (paper II). There were indications of communication between the newly described distal ILT (paper I) and the gill secondary vessels (paper II). The gills and thymus share an anatomical proximity in the gill chamber but differences in volume-properties with age and transcription of primary lymphoid tissue- associated genes did not provide evidence for a functional connection between the gills and the thymus (paper II). As the anatomy of the ILT in Atlantic salmon started to unfold, the question of whether similar structures exist in other fish species became increasingly relevant. To address this issue, the gills of common carp were investigated and found to hold an ILT with similar branchial distribution albeit of higher morphological complexity than the ILT found in Atlantic salmon (paper III).

Distribution of the ILT within the gills of the Atlantic salmon

An elongation of the ILT along the free filament trailing edges of the Atlantic salmon gills was revealed, meaning that the ILT lines the whole branchial cleft (paper I). Based on this finding the size of the ILT was shown to be four times larger than initially described (paper II), and the ILT emerges as one of the most extensive aggregations of T-cells in post yolk-sack larvae life-stages. A distinction between the previously described proximal ILT, and the newly described distal ILT was made (paper I). Similar lymphoid aggregates were not found in other parts of the Atlantic salmon gills. No differences in morphology, immuno-labelling or gene transcription of selected immune genes were found between these two regions in the normal-state salmonid gills (paper I). The use of antibodies against CD8α (Hetland et al., 2010) and the pan T-cell marker CD3ε (Koppang et al., 2010) showed fewer $CD8\alpha^+$- than $CD3^+$-cells in the ILT. Caution should be exercised when interpreting the remaining $CD3^+$ to be $CD4^+$- T-cells since some subsets of NK-cells can display parts of the membrane bound CD3- complex, at least in higher vertebrates (Lanier et al., 1992). Hence, the definite demonstration of T-cells would require the co-localization of both CD3 and CD28 together with CD4- or CD8. However, a higher transcription

of CD4-2a than both CD8α and CD8β was found in the normal-state gills containing ILT of Atlantic salmon (paper I). Again caution is necessary, as various myeloid cell lines are known to express CD4 both in humans (Biswas et al., 2003) and fish (Takizawa et al., 2016). Another example is the $CD45^+$ $CD4^+$ $CD3^-$ lymphoid tissue-inducer cells as found in mammals (Drayton et al., 2006). Despite this, $CD4^+$ T-cells have been reported as the major T-cell subset within the rainbow trout gills (Takizawa et al., 2011a). The suggested higher ratio of $CD4^+$- compared with $CD8^+$ T-cells in the ILT is in contrast to the nature of intraepithelial lymphocytes in most other vertebrates, as the majority of these lymphocytes are normally regarded as $CD8^+$- T-cells (Rombout et al., 2014, Pabst et al., 2005). However, the extensive intraepithelial lymphoid aggregation of the ILT appears largely unprecedented, making comparative considerations challenging.

Ontogeny and development of the ILT in Atlantic salmon

The presence of a discernible ILT was first evident in juveniles that had commenced exogenous feeding and extensive branchial breathing (paper II). Thus lymphoid infiltration in the ILT appeared later than in the thymus (paper II), head-kidney and spleen (Alf Seljenes Dalum, own unpublished result, Fig. 5), coinciding with the time frame of systemic lymphoid tissue ontogeny as described by others (Zapata et al., 2006). External exposure to antigens might therefore be an important trigger for the appearance of the ILT as well as maintaining its size. One can only speculate on whether the ILT would appear if fish were maintained under completely sterile conditions, as such conditions are challenging to achieve.

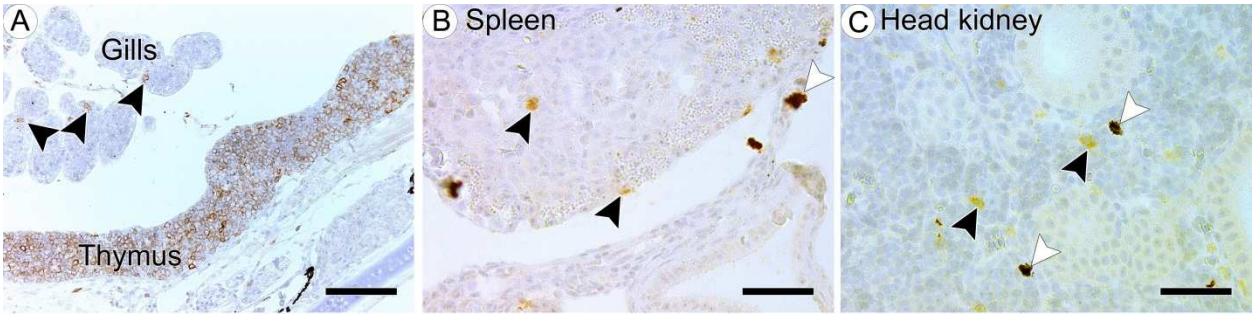

Fig. 5: $CD3\varepsilon^+$ T-cells (brown) in Atlantic salmon yolk-sack larva occurs as aggregates in the thymus and scattered in the gills (A) and in the spleen (B) and head kidney (C) while no ILT is discernible. Scale bars: A; 200 µm, B and C; 50 µm. Photographs by Alf Seljenes Dalum.

Knowledge about the ontogeny of lymphoid tissues and their attainment of full immune-competence is important in order to determine their suitability as potential targets for immune-prophylactic measures. However, functional evidence of full immune-competence is needed rather than just morphological documentation of a tissue's presence (Zapata et al., 2006). It is becoming increasingly clear that fish too small to be vaccinated by injection are able to mount protective immune responses after immersion vaccination (Tatner and Horne, 1984, dos Santos et al., 2001, Johnson et al., 1982b, Johnson et al., 1982a, Sudheesh and Cain, 2016). The involvement of ILT in such immune responses remains to be investigated. The ontogeny of the ILT in salmonids has not previously been addressed, and our findings suggest that full immune-competence of the ILT tissue cannot be expected before the post yolk-sack life-stages (paper II).

After its initial appearance, the ILT constitutes a significant part of the gills, ranging from 3 to 7 % excluding gill arches. A relatively constant ratio between the volume of proximal ILT and distal ILT was found regardless of the size and stage of the post yolk-sack Atlantic salmon. Furthermore, the ratio was maintained during the size-reduction of the ILT that occurred with sexual maturation. Relative and absolute reduction in volume of the ILT, as seen in spawners, is not necessarily a sign of forthcoming atrophy. In relative and absolute terms the volume of the thymus declined more drastically when comparing adults with mature fish. In general it is known that sex steroids modulate fish immune responses (Chaves-Pozo et al., 2012). Further studies might shed light on whether the ILT regains its volume in fish surviving the spawning period. This thesis has shown that the absolute volume of the ILT increased along with the growing gills whereas the relative volumes were the same in juveniles and adults, and that proliferating T-cells were present in discrete regions of the ILT (paper II), coinciding with the growth-zones of the gills (Hughes, 1984, Zenker et al., 1987). Whether the receptor repertoire of these proliferating T-cells can be shaped by external stimuli remains to be investigated. The significant size of ILT, as revealed in this thesis, suggests a significant role in the gill immune system and in the general mucosal immune system as a whole.

Communication between the ILT and systemic circulation of the Atlantic salmon

Although proliferation of T-cells takes place within the ILT, a possible route of communication between the salmonid ILT and the systemic circulation through the distal ILT was described (paper II). Such a mechanism could explain the apparent decrease in size of the proximal ILT during ISAV-infection and disease, as apparently no apoptosis in the proximal ILT accompanied this size reduction (Aas et al., 2014). The existence of communication between the ILT and the systemic circulation has considerable practical implications for strategies involving vaccine delivery via the mucosa, particularly for the feasibility of vaccine delivery to the gills and ILT resulting in systemic and broad mucosal protection.

In higher vertebrates the term "common mucosal immune system" (CMIS) describes the integration between various induction sites and remote effector sites (McDermott and Bienenstock, 1979). To date no evidence of a fish common mucosal immune system exists (Rombout et al., 2014), although indications have been presented (Rombout et al., 1986). Systemic immune responses have been shown after immersion vaccination with confirmed antigen-uptake over the gills although uptake might have occurred in other places as well (Kato et al., 2013, Zapata et al., 1987). Trafficking of immune cells between the site of antigen-uptake and site of immune induction must take place for a systemic immune response to occur. In organized MALT of higher vertebrates high endothelial venules (HEV) are crucial in lymphocyte trafficking, and naive lymphocytes are only able to enter secondary lymphoid tissue through HEV (Wardlaw et al., 2005). These particular vessels are recognized by their exceptional high endothelium (Hayasaka et al., 2010) and constitutive transcription of the chemokines C-C motif chemokine ligand *(CCL)-19* and *CCL21,* both ligands for the C-C chemokine receptor type 7 (CCR7). CCL19 and -21 directs CCR7-carrying lymphocytes across vascular walls and hence ensure recruitment and clustering of circulating lymphocytes to secondary lymphoid tissues (Förster et al., 2008, Ordás et al., 2012). Presence of HEV has not been confirmed in fish, but the gill secondary vasculature close to the distal ILT could be a possible candidate (paper II). Interestingly, a study of mucosal lymphoid aggregates in African lungfish used an anti-mouse peripheral lymph node addressin antibody (MECA-79) to label vessels surrounding nasal

lymphoid aggregates (Tacchi et al., 2015). However, the specificity of this antibody towards African lungfish tissues were not further investigated.

The presence of a *CCR7*-homologue has been described in rainbow trout (Ordás et al., 2012), and in a study by Castro et al., (2014), the gene transcription of *CCR7* was found to be high in IgD^+IgM^- B-cells in the gills. It was also shown that the $CCR7^+$ cells of the gills transcribed both *CD83* and *MHC class II* at high levels. In a sorted $CCR7^+$-cell subset, transcripts of *CD3* were not found at detectable levels (Castro et al., 2014), but it is uncertain whether the ILT was included in the tissue extract. The possibility for upregulation of *CCR7* in $CD3^+$ -cells of the ILT following immune stimulation of the gills should be investigated.

It is highly likely that the vascular structures in close connection to the distal ILT of Atlantic salmon could be engaged in transport of immune cells and signalling molecules to and from the ILT. Further investigations of this possibility may provide important insights into the function and dynamics of the ILT. It has been emphasised that the proximal part of the ILT is distinctly separated from blood vessels (Haugarvoll et al., 2008). Thus the distal ILT might be essential for the interaction between the ILT and the systemic circulation in Atlantic salmon, and it will be essential to include this region in further functional studies on the ILT.

ILT in Atlantic salmon lacks attributes of a primary lymphoid tissue

The gene transcription studies in this thesis (paper I and II) have added to the evidence that the ILT or gills of Atlantic salmon are not involved in primary lymphoid functions (Aas et al., 2014). Despite the morphological closeness no physical connection was found between the ILT and the thymus in Atlantic salmon (paper II). These findings are contrary to reports in European brook lamprey (*Lampetra planeri* Bloch, 1784), where thymus-like tissue (thymoid) was found at the distal end of the gill filaments (Bajoghli et al., 2011). The difference between the thymus and ILT in Atlantic salmon was further demonstrated by comparing the volume of these two tissues in developing fish. No discernible ILT was found in the yolk-sack salmon larvae, which was in contrast to the well-defined thymus present at this life-stage. With the approach of sexual maturity, the ILT outgrew the thymus several fold, and following maturation the volume decrease was less pronounced for the ILT compared with the thymus (paper II).

Adaptive humoral immunity in the ILT of Atlantic salmon

Both the proximal and distal ILT of the normal-state Atlantic salmon gills was found to contain few IgM^+ cells (paper I). However, this interpretation might be precluded by the occurrence of several sub-populations of each immunoglobulin isotype (Hedfors et al., 2012, Tadiso et al., 2011). In a recent report, substantial transcription of both *IgM* and *IgT* was demonstrated in the proximal ILT of both ISAV-infected and uninfected Atlantic salmon (Austbø et al., 2014). Interestingly, in the same study a slight up-regulation of *IgT*-transcripts was noted in the proximal ILT in the final stages of the ISAV-infection trial. Altogether IgT has been proposed to be essential for mucosal defence in teleosts (Zhang et al., 2010, Salinas et al., 2011, Gomez et al., 2013) including the gills (Xu et al., 2016, Makesh et al., 2015). Research on IgT has, however, been hampered by the lack of available molecular markers. Preliminary studies employing an anti-rainbow trout IgT-antibody (Olsen et al., 2011) on the same ISAV infected material as described by Austbø et al. (2014) showed a marked increase in IgT^+ cells, particularly in the distal ILT (Alf Seljenes Dalum, own unpublished results, Fig. 6). This observation indicates a possible influx of IgT^+ cells through the suggested communication between the distal ILT and the gill secondary vascularization. Importantly, no such increase in IgT^+ cells could be detected in the proximal ILT of infected fish despite the increase in *IgT*-transcript recorded for this region (Austbø et al., 2014). As such, it seems likely that the measured increase of *IgT*-transcript would have been more substantial if the distal ILT had been included. The anti-rainbow trout IgT-antibody used in the preliminary study has since been shown to be specific for Atlantic salmon IgT by western blot (Elin Christine Valen, personal communication). Thus, despite the apparent homogeneity of the ILT in the normal-state gills, differences between proximal- and distal ILT might appear during immunological stimulation.

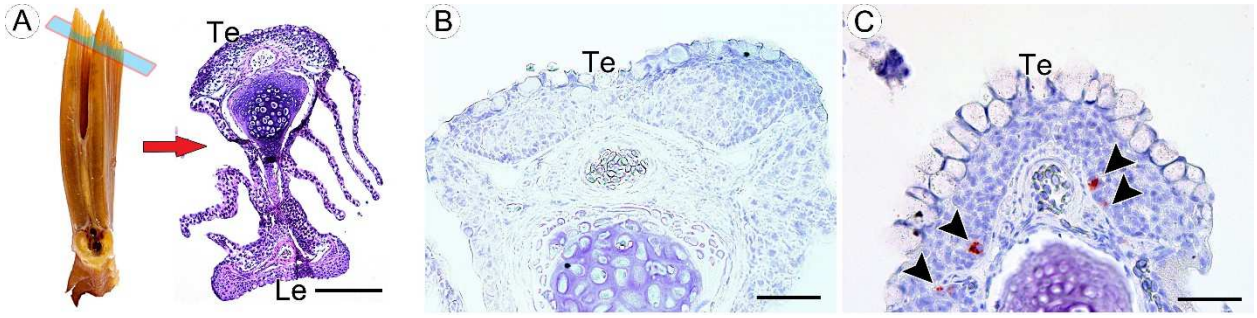

Fig. 6: Putative IgT$^+$ cells in the distal ILT of ISAV-infected Atlantic salmon in material described by Austbø et al. (2014). (A) Atlantic salmon gills cut and oriented in transversal projection, with dorsal section plane depicted. HE; free filament cut in dorsal plane with trailing edge (Te) and leading edge (Le) depicted. (B) Te distal ILT of control fish, showing no labelling. (C) Te of ISAV-infected fish (20 days post challenge) showing putative IgT$^+$ cells (red, black arrowheads) within the distal ILT. Scale bars: A; 200 µm, B and C; 50 µm. Photographs by Alf Seljenes Dalum.

It is still unknown why mainly T-cells and very few B-cells have been observed in the Atlantic salmon normal-state ILT. The other MALTs of rainbow trout have been shown to harbour considerable amounts of IgT (Tacchi et al., 2014, Salinas, 2015). However, a high T-cell to B-cell ratio is also described in the mucosal respiratory lymphoid tissue in higher vertebrates (Wardlaw et al., 2005). Due to the extensive interaction between the water and the gills one could argue that secretion of antibodies into mucus would be expensive because of the continuous "wash-out" of mucus. It might be that the IgT-bearing B-cells are only recruited to the gill mucosal lining in times of need, and that the cellular arm of the adaptive immunity forms the baseline of the ILT normal-state defence.

ILT in the gills of common carp

A compartmentalized ILT in common carp was an unexpected observation. As in salmonids the ILT of common carp was situated in the epithelium lining the branchial cleft. The basal compartment of the common carp proximal ILT consisted of high numbers of putative T-cells (ZAP-70$^+$ cells) and moderate numbers of IgT1-positive cells, and was closely associated with blood vessels (paper III). Further research is needed to reveal the functions of the basal proximal ILT-associated vessels and whether any similarity to HEV in mammals exists. In the intermediate and uppermost proximal ILT, as well as in the distal ILT, a tissue organization more in line with

that in Atlantic salmon was seen, although there was a considerable presence of EGCs in the intermediate compartment (paper III). The presence of EGCs might point to different species-specific strategies in protecting the vulnerable gill tissues (Sollid et al., 2003, Sollid and Nilsson, 2006). Altogether, the ILT of common carp appeared more morphological complex compared with Atlantic salmon, which might be a reflection upon common carp being more recently evolved. Other morphological indications of further immunological evolvement in cyprinids as compared with salmonids could be the higher degree of organization of the melano-macrophage centres (Agius and Roberts, 2003, Vigliano et al., 2006) and the more internalized thymus (Lam et al., 2002, Tatner, 1996). It should be kept in mind that the investigations presented in this thesis are based on reared fish from only one population kept in relatively clean water. Therefore, further research on the ILT in wild and farmed carp living in water of different qualities, as well as fish with mucosal infection and inflammation, is needed.

It was surprising to find $IgT1^+$ cells preferably localized in the basal, vessel-associated compartment of the common carp proximal ILT (paper III). However, the presence of this antibody producing cell population within the ILT does not compromise the "wash-out" hypothesis which has been proposed for Atlantic salmon, as the basal compartment is well shielded from ambient water by the two overlaying compartments. One might speculate if the more organized ILT with increased presence of B-cells in the more recently evolved common carp represents a step further in the evolution towards organized MALT, as found in higher vertebrates, or whether it is a result of species-specific adaption to different environments. An answer to this question might lie in the gills of even more recently evolved fish species.

ILT- a common feature in Atlantic salmon and common carp

The anatomical distribution of the ILT in both Atlantic salmon and common carp was found to coincide (paper I and III). Despite variations in cellular subsets and architecture a reticular epithelium formed the framework for the immune cells in both species (paper I and III). In contrast to other fish MALTs, the architecture of the ILT possess many similarities with the thymus. This resemblance became even more apparent with the discovery of blood vessels associated with the basal proximal ILT of common carp (paper III). However, similar to the

Atlantic salmon (paper II), the ILT in the common carp appears to lack primary lymphoid function, as carp gills have been found not to transcribe *RAG-1* (Huttenhuis et al., 2005). Furthermore, the seemingly constant presence of ILT in normal-state gills of Atlantic salmon (from juveniles and onwards) and common carp excludes a role as a tertiary lymphoid tissue, and it has been stated that the ILT of Atlantic salmon most likely is a secondary lymphoid tissue (Aas et al., 2014, Austbø et al., 2014, Koppang et al., 2010). One can only speculate whether a phylogenetic relationship exists between the thymus, ILT and organized MALT. The thymus appears early in the evolution of vertebrate adaptive immunity (Boehm and Bleul, 2007). Hypothetically, a tissue derived from it would offer the same three-dimensional network, facilitating extensive cell-cell interaction even though the primary lymphoid function was lost. Also, the pharyngeal region experiences extensive antigen exposure both during respiration and food intake, which would make it a potential site for the initial evolvement of MALT (Matsunaga and Rahman, 2001, Varga et al., 2008). Even though a primary lymphoid function of the gills and ILT seems unlikely, the absence of evidence of this function does not exclude a possible evolutionary relationship between the epithelial reticulum of the thymus and the ILT. An epithelial reticulum represents a unique entity among immune tissues, only paralleled by the palatine tonsils in higher vertebrates (Vejlsted, 2009).

Increased knowledge about the anatomical distribution of the ILT encourages the discussion about ontogenetically and developmental driving-forces and functions of this lymphoid tissue. The prevailing theory is that during respiration water flows from the leading to the trailing edges of both lateral and medial hemibranchs, and the water streams meet in the branchial cleft. In the gills of fishes with a long interbranchial septum an upwelling of water must be expected along the septal water channels before it reaches the branchial cleft (Fig. 7) (Olson, 2000). For this reason the branchial cleft has been suggested as a site of extensive water-mixing (Hughes, 1984). Such mixing further implies an increased contact possibility between water-borne compounds and the branchial cleft mucosal surface. This could necessitate aggregations of lymphoid tissue in terms of inducing both tolerance to innocuous content and immunological reactivity to potential pathogens in the water. This reasoning is in line with the predominant locations of lymphoid tissues in the respiratory pathways of higher vertebrates. Ontogeny and development of both nasopharynx-associated lymphoid tissue, bronchus-associated lymphoid tissue and tonsils have been reported to be highly dependent of environmental influences (Pabst, 2007,

Gebert and Pabst, 1999, Iwata and Sato, 1991) and typically appear at branching-points with increased interaction between the respiratory medium and the mucosal lining (Cesta, 2006).

Many studies have been conducted that treated the gills as a homogenous organ. This thesis clearly demonstrates that the ILT constitutes a well-defined immunological tissue of significant size within the gills of two extensively studied species. Inclusion or not of ILT in investigations on gills may give significantly different results. This difference would be particularly true if T-cell populations, the major lymphocyte subset of the ILT in both Atlantic salmon and common carp, were the matter of interest. As an example, the contribution of ILT is unclear in the report which stated that the rainbow trout gills lymphocyte-population consisted of only 3-9 % T-cells (Boardman et al., 2012).

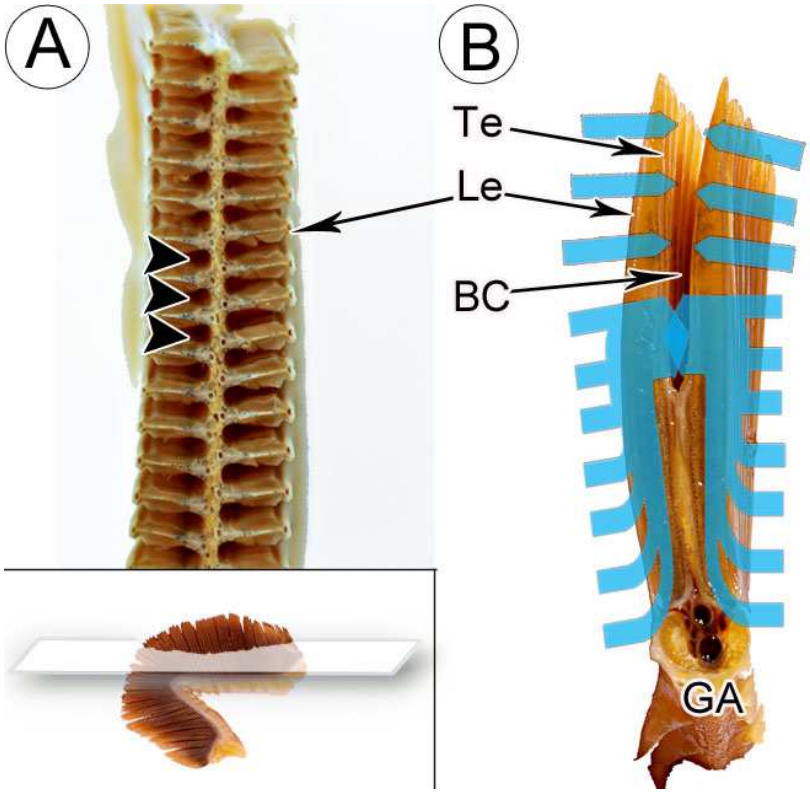

Fig. 7: Upwelling theory in the Atlantic salmon gills. (A) A gill sectioned in dorsal plane and oriented in dorsal projection towards the gill arch (dorsal section plane indicated in the inset below). Evident are the septal water channels between the lamellae and septum (black arrowheads) allowing upwelling of water along the interbranchial septum before the branchial cleft is reached. (B) A gill sectioned in transversal plane and oriented in transversal projection. Blue arrows indicates hypothetical streams of water from the pharyngeal cavity and the gill slits, crossing from leading edges (Le) to trailing edges (Te) into the branchial cleft (BC). Water is forced along the septal water channels before reaching the distal end of the interbranchial septum and, accordingly, the proximal part of the branchial cleft. Extensive interaction between water and the surface of the branchial cleft epithelium holding the ILT is thought to take place. GA; gill arch. Figures and photographs by Alf Seljenes Dalum.

The present thesis has targeted lymphoid aggregations in the gills of Atlantic salmon and the common carp. Both species belong to the ray finned (Actinopterygii) fishes, which is the largest single class of extant vertebrates and consists of over 22,000 species divided into approximately 40 orders and 400 families (Nelson, 2006). As such, this class represents more than half of the extant species of vertebrates, and the majority of these are found in the infraclass of Teleostei, which holds the orders of both salmonids and carp (Zapata and Amemiya, 2000). Thus, it is at best speculative to draw general conclusions and trends based on two species only. However, pending knowledge on the presence or absence of similar structures in other fish species, the ILT represents a unique target to be investigated for mucosal-delivery of vaccines and could contribute to understanding evolution toward organized MALT.

MAIN CONCLUSIONS

This thesis provides novel information about the ILT in two distant teleost species. The conclusions can be summarized as follows:

a) Beyond the previously described proximal ILT residing at the distal end of the interbranchial septum in Atlantic salmon, the newly described distal ILT is distributed through the trailing edge of the free filaments, and together these regions constitute the ILT. Furthermore, the distal ILT accounts on average for 80 % of the ILT in post yolk-sack larvae life-stages.

b) ILT could not be detected in the Atlantic salmon yolk-sack larvae, but after its appearance as the fish commence exogenous feeding and extensive branchial respiration, the ILT constitutes a significant part of the total gill volume:
   - Sizes of ILT and gills increased in parallel. Discrete regions of putative T cell proliferation within the ILT were identified in all post yolk-sack larvae life-stages investigated, which suggest discrete growth zones within the ILT.
   - Despite decreased volume of the ILT relative to the volume of the gills in spawners, the ratio between the proximal- and distal ILT was constant for all post yolk-sack larvae life-stages.

c) Morphological evidence of an association between the distal ILT and the secondary vasculature of gills of the Atlantic salmon was found, suggesting a possible communication between the mucosal lymphoid tissue and the systemic circulation.

d) Transcription of genes specific for primary lymphoid tissue or for thymic tissue in particular, was not detected in the gills of any Atlantic salmon life-stage. The different nature of thymus and the ILT was further supported by the difference in development. From their near equal volumes at the juvenile stage the ILT outgrew the thymus with increasing size of the fish. The noted volume-reduction in spawners was less extensive for the ILT

compared with the thymus. Hence, there is at present no support of primary lymphoid functions in the ILT.

e) ILT was for the first time described in common carp, and various morphological techniques revealed an organized lymphoid tissue. The proximal ILT could be divided into three morphologically distinct intraepithelial compartments: a basal compartment characterized by high numbers of lymphocytes and intimate association with blood vessels, an intermediate compartment characterized by high numbers of EGCs and an uppermost compartment forming the outer surface to ambient water. The intermediate and uppermost compartments extended into the distal ILT.

FUTURE PERSPECTIVES:

- A further characterization of the various T-cell subsets in the ILT is warranted. For Atlantic salmon a first step should be to address the nature of $CD3^+$ $CD8\alpha^-$ T-cells. Pending T-cell subset specific markers, gene transcriptional techniques could be employed in the further investigations on the ZAP-70^+ cells of the common carp ILT. Furthermore, the reactivity of the putative mucosal T-cell marker WCL38 in common carp ILT needs further characterization.

- By employing the CCR7-antibody targeting homing lymphocytes along with the range of other immune related molecular markers available for rainbow trout, this species could be used as a model for further studies on lymphocyte-trafficking between the ILT and the systemic circulation.

- The extensive lymphoid aggregations in the gills of two major cultured fish species are an obvious target for mucosal vaccine delivery. Specific points to address:
    - Minimum size of the fish where the ILT is able to respond immunologically.
    - Balance between induction of tolerance and immunological reactivity, and whether novel adjuvants are able to tailor the immunological milieu of the ILT in a desirable immunological direction.
    - Antigen sampling in the ILT, where the MHC class II^+ cells which has been described in Atlantic salmon represents a particular interesting subset.

- Laser microdissection and transcriptome analyses on RNA sequenced tissues of the different ILT compartments of common carp should be conducted. This could reveal the transcriptional fundament for the morphological differences observed.

- Lastly, the search for ILT-like tissue in other fish species could open new and interesting aspects regarding the evolution of the mucosal immune system.

REFERENCE LIST

AAS, I. B., AUSTBØ, L., KÖNIG, M., SYED, M., FALK, K., HORDVIK, I. & KOPPANG, E. O. 2014. Transcriptional characterization of the T cell population within the salmonid interbranchial lymphoid tissue. *J Immunol,* 193**,** 3463-9.

AAS, Ø., EINUM, S., KLEMETSEN, A. & SKURDAL, J. 2011. Freshwater habitat requirements of Atlantic salmon. *In:* AAS, Ø., EINUM, S., KLEMETSEN, A. & SKURDAL, J. (eds.) *Atlantic salmon ecology.* Chichester, Wiley-Blackwell, 67-87.

AGIUS, C. & ROBERTS, R. J. 2003. Melano-macrophage centres and their role in fish pathology. *J Fish Dis,* 26**,** 499-509.

ANDERSON, G., LANE, P. J. & JENKINSON, E. J. 2007. Generating intrathymic microenvironments to establish T-cell tolerance. *Nat Rev Immunol,* 7**,** 954-63.

AUSTBØ, L., AAS, I. B., KÖNIG, M., WELI, S. C., SYED, M., FALK, K. & KOPPANG, E. O. 2014. Transcriptional response of immune genes in gills and the interbranchial lymphoid tissue of Atlantic salmon challenged with infectious salmon anaemia virus. *Dev Comp Immunol,* 45**,** 107-14.

BACCARI, G. C., PINELLI, C., SANTILLO, A., MINUCCI, S. & RASTOGI, R. K. 2011. Mast cells in nonmammalian vertebrates: an overview. *Int Rev Cell Mol Biol,,* 290**,** 1-53.

BADDELEY, A. J., GUNDERSEN, H. J. & CRUZ-ORIVE, L. M. 1986. Estimation of surface area from vertical sections. *J Microsc,* 142**,** 259-76.

BAJOGHLI, B., AGHAALLAEI, N., HESS, I., RODE, I., NETUSCHIL, N., TAY, B. H., VENKATESH, B., YU, J. K., KALTENBACH, S. L., HOLLAND, N. D., DIEKHOFF, D., HAPPE, C., SCHORPP, M. & BOEHM, T. 2009. Evolution of genetic networks underlying the emergence of thymopoiesis in vertebrates. *Cell,* 138**,** 186-97.

BAJOGHLI, B., GUO, P., AGHAALLAEI, N., HIRANO, M., STROHMEIER, C., MCCURLEY, N., BOCKMAN, D. E., SCHORPP, M., COOPER, M. D. & BOEHM, T. 2011. A thymus candidate in lampreys. *Nature,* 470**,** 90-4.

BANCROFT, J. D. & GAMBLE, M. 2008. *Theory and practice of histological techniques.* 6 ed. Philadelphia, Churchill Livingstone/Elsevier.

BARNETT, R. R., AKINDELE, T., ORTE, C. & SHEPHARD, K. L. 1996. Eosinophilic granulocytes in the epidermis of Oreochromis mossambicus gill filaments studied in situ. *J Fish Biol,* 49**,** 148-56.

BASSITY, E. & CLARK, T. G. 2012. Functional identification of dendritic cells in the teleost model, rainbow trout (*Oncorhynchus mykiss*). *PLoS One,* 7**,** e33196.

BERG, A., RØDSETH, O. M. & HANSEN, T. 2007. Fish size at vaccination influence the development of side-effects in Atlantic salmon (*Salmo Salar* L.). *Aquaculture,* 265**,** 9-15.

BIELEK, E. 2008. Membrane transformations in degenerating rodlet cells in fishes of two teleostean families (Salmonidae, Cyprinidae). *Anat Rec (Hoboken),* 291**,** 1693-706.

BISWAS, P., MANTELLI, B., SICA, A., MALNATI, M., PANZERI, C., SACCANI, A., HASSON, H., VECCHI, A., SANIABADI, A., LUSSO, P., LAZZARIN, A. & BERETTA, A. 2003. Expression of CD4 on human peripheral blood neutrophils. *Blood,* 101**,** 4452-6.

BOARDMAN, T., WARNER, C., RAMIREZ-GOMEZ, F., MATRISCIANO, J. & BROMAGE, E. 2012. Characterization of an anti-rainbow trout (*Oncorhynchus mykiss*) CD3epsilon monoclonal antibody. *Vet Immunol Immunopathol,* 145**,** 511-5.

BOEHM, T. & BLEUL, C. C. 2007. The evolutionary history of lymphoid organs. *Nat Immunol,* 8**,** 131-5.

BOEHM, T., HESS, I. & SWANN, J. B. 2012. Evolution of lymphoid tissues. *Trends Immunol,* 33**,** 315-21.

BOWDEN, T. J., COOK, P. & ROMBOUT, J. H. W. M. 2005. Development and function of the thymus in teleosts. *Fish Shellfish Immunol,* 19**,** 413-27.

BOWERS, A. & ALEXANDER, J. B. 1981. Hyperosmotic infiltration: immunological demonstration of infiltrating bacteria in brown trout, *Salmo trutta* L. *J Fish Biol,* 18**,** 9-13.

BRAUNER, C. J. & ROMBOUGH, P. J. 2012. Ontogeny and paleophysiology of the gill: new insights from larval and air-breathing fish. *Respir Physiol Neurobiol,* 184**,** 293-300.

BRUDESETH, B. E., WIULSRØD, R., FREDRIKSEN, B. N., LINDMO, K., LØKLING, K. E., BORDEVIK, M., STEINE, N., KLEVAN, A. & GRAVNINGEN, K. 2013. Status and future perspectives of vaccines for industrialised fin-fish farming. *Fish Shellfish Immunol,* 35**,** 1759-68.

BUNTON, T. E. 1993. The immunocytochemistry of cytokeratin in fish tissues. *Vet Pathol,* 30**,** 418-25.

BUSTIN, S. A., BENES, V., GARSON, J. A., HELLEMANS, J., HUGGETT, J., KUBISTA, M., MUELLER, R., NOLAN, T., PFAFFL, M. W., SHIPLEY, G. L., VANDESOMPELE, J. & WITTWER, C. T. 2009. The MIQE guidelines: minimum information for publication of quantitative real-time PCR experiments. *Clin Chem,* 55**,** 611-22.

CAMPOS-PEREZ, J. J., WARD, M., GRABOWSKI, P. S., ELLIS, A. E. & SECOMBES, C. J. 2000. The gills are an important site of iNOS expression in rainbow trout *Oncorhynchus mykiss* after challenge with the gram-positive pathogen *Renibacterium salmoninarum*. *Immunology,* 99**,** 153-61.

CASTILLO, A., RAZQUIN, B., VILLENA, A. J., ZAPATA, A. G. & LÓPEZ-FIERRO, P. 1998. Thymic barriers to antigen entry during the post-hatching development of the thymus of rainbow trout, *Oncorhynchus mykiss*. *Fish Shellfish Immunol,* 8**,** 157-70.

CASTRO, R., BROMAGE, E., ABOS, B., PIGNATELLI, J., GONZALEZ GRANJA, A., LUQUE, A. & TAFALLA, C. 2014. CCR7 is mainly expressed in teleost gills, where it defines an IgD+IgM- B lymphocyte subset. *J Immunol,* 192**,** 1257-66.

CESTA, M. F. 2006. Normal structure, function, and histology of mucosa-associated lymphoid tissue. *Toxicol Pathol,* 34**,** 599-608.

CHAN, A. C., IRVING, B. A., FRASER, J. D. & WEISS, A. 1991. The zeta chain is associated with a tyrosine kinase and upon T-cell antigen receptor stimulation associates with ZAP-70, a 70-kDa tyrosine phosphoprotein. *Proc Natl Acad Sci U S A,* 88**,** 9166-70.

CHAVES-POZO, E., CABAS, I. & GARCÍA-AYALA, A. 2012. Sex steroids modulate fish immune response. *In:* KAHN, S. M. (ed.) *Sex steroids.* InTech, 199-220.

CHILMONCZYK, S. 1983. The thymus of the rainbow trout (*Salmo gairdneri*)- light and electron microscopic study. *Dev Comp Immunol,* 7**,** 59-68.

CHILMONCZYK, S. 1992. The thymus in fish: Development and possible function in the immune response. *Annu Rev Fish Dis,* 2**,** 181-200.

CUESTA, A., LAIZ-CARRION, R., DEL RIO, M. P., MESEGUER, J., MANCERA, J. M. & ESTEBAN, M. A. 2005. Salinity influences the humoral immune parameters of gilthead seabream (*Sparus aurata* L.). *Fish Shellfish Immunol,* 18**,** 255-61.

D'ACQUISTO, F. & CROMPTON, T. 2011. CD3+CD4-CD8- (double negative) T cells: saviours or villains of the immune response? *Biochem Pharmacol,* 82**,** 333-40.

DA COSTA, O. T., PEDRETTI, A. C., SCHMITZ, A., PERRY, S. F. & FERNANDES, M. N. 2007. Stereological estimation of surface area and barrier thickness of fish gills in vertical sections. *J Microsc,* 225**,** 1-9.

DANILOVA, N., BUSSMANN, J., JEKOSCH, K. & STEINER, L. A. 2005. The immunoglobulin heavy-chain locus in zebrafish: identification and expression of a previously unknown isotype, immunoglobulin Z. *Nat Immunol,* 6**,** 295-302.

DEZFULI, B. S. & GIARI, L. 2008. Mast cells in the gills and intestines of naturally infected fish: evidence of migration and degranulation. *J Fish Dis,* 31**,** 845-52.

DHAR, A. K., MANNA, S. K. & THOMAS ALLNUTT, F. C. 2014. Viral vaccines for farmed finfish. *VirusDis,* 25**,** 1-17.

DIJKSTRA, J. M., KÖLLNER, B., AOYAGI, K., SAWAMOTO, Y., KURODA, A., OTOTAKE, M., NAKANISHI, T. & FISCHER, U. 2003. The rainbow trout classical MHC class I molecule Onmy-UBA*501 is expressed in similar cell types as mammalian classical MHC class I molecules. *Fish Shellfish Immunol,* 14**,** 1-23.

DOÑATE , C., ROHER, N., BALASCH, J. C., RIBAS, L., GOETZ, F. W., PLANAS, J. V., TORT, L. & MACKENZIE, S. 2007. CD83 expression in sea bream macrophages is a marker for the LPS-induced inflammatory response. *Fish Shellfish Immunol,* 23**,** 877-85.

DOOLEY, J., ERICKSON, M. & FARR, A. G. 2005. An organized medullary epithelial structure in the normal thymus expresses molecules of respiratory epithelium and resembles the epithelial thymic rudiment of nude mice. *J Immunol,* 175**,** 4331-7.

DORPH-PETERSEN, K. A., NYENGAARD, J. R. & GUNDERSEN, H. J. 2001. Tissue shrinkage and unbiased stereological estimation of particle number and size. *J Microsc,* 204**,** 232-46.

DOS SANTOS, N. M., TAVERNE-THIELE, J. J., BARNES, A. C., VAN MUISWINKEL, W. B., ELLIS, A. E. & ROMBOUT, J. H. 2001. The gill is a major organ for antibody secreting cell production following direct immersion of sea bass (*Dicentrarchus labrax*, L.) in a *Photobacterium damselae* ssp. *piscicida* bacterin: an ontogenetic study. *Fish Shellfish Immunol,* 11**,** 65-74.

DRAYTON, D. L., LIAO, S., MOUNZER, R. H. & RUDDLE, N. H. 2006. Lymphoid organ development: from ontogeny to neogenesis. *Nat Immunol,* 7**,** 344-53.

ELGUETA, R., BENSON, M. J., DE VRIES, V. C., WASIUK, A., GUO, Y. & NOELLE, R. J. 2009. Molecular mechanism and function of CD40/CD40L engagement in the immune system. *Immunol Rev,* 229**,** 152-72.

ELLIS, A. E. 1977. Ontogeny of the immune response in *Salmo salar*: histogenesis of the lymphoid organs and appearance of membrane immunoglobulin and mixed leucocyte reactivity. *In:* SOLOMON, J. B. & HORTON, J. D. (eds.) *Developmental immunobiology.* Amsterdam, Elsevier Biomedical Press, 225–31.

ESTEBAN, M. Á., CUESTA, A., CHAVES-POZO, E. & MESEGUER, J. 2015. Phagocytosis in teleosts. Implications of the new cells Involved. *Biology (Basel),* 4**,** 907-22.

EVANS, D. H., PIERMARINI, P. M. & CHOE, K. P. 2005. The multifunctional fish gill: dominant site of gas exchange, osmoregulation, acid-base regulation, and excretion of nitrogenous waste. *Physiol Rev,* 85**,** 97-177.

FAO 2014. *Fishery and Aquaculture Statistics, FAO yearbook 2012*. Rome.

FAO. 2016a. *Cultured aquatic species information programme- Cyprinus carpio (Linnaeus, 1758)* [Online]. Available: http://www.fao.org/fishery/culturedspecies/Cyprinus_carpio/en [Accessed 25.08.2016].

FAO. 2016b. *Cultured aquatic species information programme- Salmo salar (Linnaeus, 1758)* [Online]. Available: http://www.fao.org/fishery/culturedspecies/Salmo_salar/en [Accessed 25.08.2016].

FAO. 2016c. *Fisheries and aquaculture departments, global statistical collections online, query panels* [Online]. Fisheries and aquaculture department. Available: http://www.fao.org/fishery/topic/16140/en [Accessed 31.08.2016].

FAO. 2016d. *Fishery statistical collections- global aquaculture production* [Online]. Fisheries and aquaculture department. Available: http://www.fao.org/fishery/statistics/global-aquaculture-production/en [Accessed 25.08.2016 2016].

FAO. 2016e. *Species fact sheets Cyprinus carpio (Linnaeus, 1758)* [Online]. Available: http://www.fao.org/fishery/species/2957/en [Accessed 25.08.2016].

FISCHER, U., KOPPANG, E. O. & NAKANISHI, T. 2013. Teleost T and NK cell immunity. *Fish Shellfish Immunol,* 35**,** 197-206.

FISHBASE. 2016. *Cyprinus carpio Linnaeus, 1758, Common carp* [Online]. FishBase.org. Available: http://www.fishbase.org/Summary/SpeciesSummary.php?ID=1450&AT=carp [Accessed 31.08.2016].
FLAJNIK, M. F. & KASAHARA, M. 2010. Origin and evolution of the adaptive immune system: genetic events and selective pressures. *Nat Rev Genet,* 11**,** 47-59.
FLAJŠHANS, M. & HULATA, G. 2007. Common carp – *Cyprinus carpio*. *In:* SVÅSAND, T., CROSETTI, D., GARCÍA-VÁZQUEZ, E. & VERSPOOR, E. (eds.) *Genetic impact of aquaculture activities on native populations. Genimpact final scientific report (EU contract n. RICA-CT-2005-022802).* Institute of marine research, Norway, 32-9.
FORLENZA, M. 2009. *Immune responses of carp - A molecular and cellular approach to infections.* Thesis, Wageningen University.
FORLENZA, M., FINK, I. R., RAES, G. & WIEGERTJES, G. F. 2011. Heterogeneity of macrophage activation in fish. *Dev Comp Immunol,* 35**,** 1246-55.
FU, C., WILSON, J. M., ROMBOUGH, P. J. & BRAUNER, C. J. 2010. Ions first: Na+ uptake shifts from the skin to the gills before O2 uptake in developing rainbow trout, *Oncorhynchus mykiss*. *Proc Biol Sci,* 277**,** 1553-60.
FUGLEM, B., JIRILLO, E., BJERKÅS, I., KIYONO, H., NOCHI, T., YUKI, Y., RAIDA, M., FISCHER, U. & KOPPANG, E. O. 2010. Antigen-sampling cells in the salmonid intestinal epithelium. *Dev Comp Immunol,* 34**,** 768-74.
FÖRSTER, R., DAVALOS-MISSLITZ, A. C. & ROT, A. 2008. CCR7 and its ligands: balancing immunity and tolerance. *Nat Rev Immunol,* 8**,** 362-71.
GE, Q. & ZHAO, Y. 2013. Evolution of thymus organogenesis. *Dev Comp Immunol,* 39**,** 85-90.
GEBERT, A. & PABST, R. 1999. M cells at locations outside the gut. *Semin Immunol,* 11**,** 165-70.
GLENNEY, G. W. & PETRIE-HANSON, L. 2006. Fate of fluorescent microspheres in developing *Ictalurus punctatus* following prolonged immersion. *Fish Shellfish Immunol,* 20**,** 758-68.
GOLDES, S. A., FERGUSON, H. W., DAOUST, P. Y. & MOCCIA, R. D. 1986. Phagocytosis of the inert suspended clay kaolin by the gills of rainbow trout, *Salmo gairdneri* Richardson. *J Fish Dis,* 9**,** 147-51.
GOLDSTINE, S. N., MANICKAVEL, V. & COHEN, N. 1975. Phylogeny of gut-associated lymphoid tissue. *Am Zool,* 15**,** 107-18.
GOMEZ, D., SUNYER, J. O. & SALINAS, I. 2013. The mucosal immune system of fish: the evolution of tolerating commensals while fighting pathogens. *Fish Shellfish Immunol,* 35**,** 1729-39.
GOULD, S. J. 1977. *Ontogeny and phylogeny.* London, The Belknap Press of Harverd University Press.
GRANJA, A. G., LEAL, E., PIGNATELLI, J., CASTRO, R., ABÓS, B., KATO, G., FISCHER, U. & TAFALLA, C. 2015. Identification of teleost skin CD8α+ dendritic-like cells, representing a potential common ancestor for mammalian cross-presenting dendritic cells. *J Immunol,* 195**,** 1825-37.
GREVELLEC, A. & TUCKER, A. S. 2010. The pharyngeal pouches and clefts: Development, evolution, structure and derivatives. *Semin Cell Dev Biol,* 21**,** 325-32.
GU, J., KROGDAHL, Å., SISSENER, N. H., KORTNER, T. M., GELENCSER, E., HEMRE, G. I. & BAKKE, A. M. 2013. Effects of oral Bt-maize (MON810) exposure on growth and health parameters in normal and sensitised Atlantic salmon, *Salmo salar* L. *Br J Nutr,* 109**,** 1408-23.
HANSEN, J. D. & KAATTARI, S. L. 1995. The recombination activation gene 1 (RAG1) of rainbow trout (*Oncorhynchus mykiss*): cloning, expression, and phylogenetic analysis. *Immunogenetics,* 42**,** 188-95.
HANSEN, J. D. & KAATTARI, S. L. 1996. The recombination activating gene 2 (RAG2) of the rainbow trout *Oncorhynchus mykiss*. *Immunogenetics,* 44**,** 203-11.

HANSEN, J. D., LANDIS, E. D. & PHILLIPS, R. B. 2005. Discovery of a unique Ig heavy-chain isotype (IgT) in rainbow trout: Implications for a distinctive B cell developmental pathway in teleost fish. *Proc Natl Acad Sci U S A,,* 102**,** 6919-24.

HARUN, N. O., WANG, T. & SECOMBES, C. J. 2011. Gene expression profiling in naive and vaccinated rainbow trout after *Yersinia ruckeri* infection: insights into the mechanisms of protection seen in vaccinated fish. *Vaccine,* 29**,** 4388-99.

HAUGARVOLL, E., BJERKÅS, I., NOWAK, B. F., HORDVIK, I. & KOPPANG, E. O. 2008. Identification and characterization of a novel intraepithelial lymphoid tissue in the gills of Atlantic salmon. *J Anat,* 213**,** 202-9.

HAYASAKA, H., TANIGUCHI, K., FUKAI, S. & MIYASAKA, M. 2010. Neogenesis and development of the high endothelial venules that mediate lymphocyte trafficking. *Cancer Sci,* 101**,** 2302-8.

HEDFORS, I. A., BAKKE, H., SKJØDT, K. & GRIMHOLT, U. 2012. Antibodies recognizing both IgM isotypes in Atlantic salmon. *Fish Shellfish Immunol,* 33**,** 1199-206.

HETLAND, D. L., DALE, O. B., SKJØDT, K., PRESS, C. M. & FALK, K. 2011. Depletion of CD8 alpha cells from tissues of Atlantic salmon during the early stages of infection with high or low virulent strains of infectious salmon anaemia virus (ISAV). *Dev Comp Immunol,* 35**,** 817-26.

HETLAND, D. L., JØRGENSEN, S. M., SKJØDT, K., DALE, O. B., FALK, K., XU, C., MIKALSEN, A. B., GRIMHOLT, U., GJØEN, T. & PRESS, C. M. 2010. In situ localisation of major histocompatibility complex class I and class II and CD8 positive cells in infectious salmon anaemia virus (ISAV)-infected Atlantic salmon. *Fish Shellfish Immunol,* 28**,** 30-9.

HEWITT, E. W. 2003. The MHC class I antigen presentation pathway: strategies for viral immune evasion. *Immunology,* 110**,** 163-9.

HINE, P. M. 1992. The granulocytes of fish. *Fish Shellfish Immunol,* 2**,** 79-98.

HINE, P. M. & WAIN, J. M. 1988. Observations on the granulocyte peroxidase of teleosts: a phylogenetic perspective. *J Fish Biol,* 33**,** 247-54.

HODGKINSON, J. L., BUCKE, D. & AUSTIN, B. 1987. Uptake of the fish pathogen, *Aeromonas salmonicida*, by rainbow trout (*Salmo gairdneri* L.). *FEMS Microbiol Lett,* 40**,** 207-10.

HODGKINSON, J. W., GRAYFER, L. & BELOSEVIC, M. 2015. Biology of bony fish macrophages. *Biology (Basel),* 4**,** 881-906.

HOLLAND, J. W. & ROWLEY, A. F. 1998. Studies on the eosinophilic granule cells in the gills of the rainbow trout, *Oncorhynchus mykiss*. *Comp Biochem Physiol C Pharmacol Toxicol Endocrinol,* 120**,** 321-8.

HOWAT, W. J., LEWIS, A., JONES, P., KAMPF, C., PONTÉN, F., VAN DER LOOS, C. M., GRAY, N., WOMACK, C. & WARFORD, A. 2014. Antibody validation of immunohistochemistry for biomarker discovery: recommendations of a consortium of academic and pharmaceutical based histopathology researchers. *Methods,* 70**,** 34-8.

HU, Y. H., ZHANG, M. & SUN, L. 2010. Expression of *Scophthalmus maximus* CD83 correlates with bacterial infection and antigen stimulation. *Fish Shellfish Immunol,* 29**,** 608-14.

HUANG, R., GAO, L. Y., WANG, Y. P., HU, W. & GUO, Q. L. 2009. Structure, organization and expression of common carp (*Cyprinus carpio* L.) NKEF-B gene. *Fish Shellfish Immunol,* 26**,** 220-9.

HUGHES, G. M. 1984. General anatomy of the gills. *In:* HOAR, W. S. & RANDALL, D. J. (eds.) *Fish physiology. Volume X. Gills. Part A. Anatomy, gas transfer, and acid-base regulation.* New York, Academic Press, 1-63.

HUGHES, G. M. 1995. The gills of the coelacanth, Latimeria chalumnae, a study in relation to body size. *Philos Trans R Soc Lond B Biol Sci,* 347**,** 427-38.

HUGHES, G. M. & MORGAN, M. 1973. The structure of fish gills in relation to their respiratory function. *Biol Rev Camb Philos Soc,* 48**,** 419-75.

HUTTENHUIS, H. B., HUISING, M. O., VAN DER MEULEN, T., VAN OOSTERHOUD, C. N., SANCHEZ, N. A., TAVERNE-THIELE, A. J., STROBAND, H. W. & ROMBOUT, J. H. 2005. Rag expression identifies B and T cell lymphopoietic tissues during the development of common carp (*Cyprinus carpio*). *Dev Comp Immunol,* 29**,** 1033-47.

HYMAN, L. H. 1942. *Comparative vertebrate anatomy.* 2 ed. Chicago IL., University of Chicago Press.

HYTTEL, P. 2009. Development of the gastro-pulmonary system. *In:* HYTTEL, P. (ed.) *Essentials of domestic animal embryology.* Edinburgh Saunders, 216-51.

IWATA, M. & SATO, A. 1991. Morphological and immunohistochemical studies of the lungs and bronchus-associated lymphoid tissue in a rat model of chronic pulmonary infection with *Pseudomonas aeruginosa*. *Infect Immun,* 59**,** 1514-20.

JANKOVIC, D., LIU, Z. & GAUSE, W. C. 2001. Th1- and Th2-cell commitment during infectious disease: asymmetry in divergent pathways. *Trends Immunol,* 22**,** 450-7.

JOHNSON, K. A., FLYNN, J. K. & AMEND, D. F. 1982a. Duration of immunity in salmonids vaccinated by direct immersion with *Yersinia ruckeri* and *Vibrio anguillarum* bacterins. *J Fish Dis,* 5**,** 207-13.

JOHNSON, K. A., FLYNN, J. K. & AMEND, D. F. 1982b. Onset of immunity in salmonid fry vaccinated by direct immersion in *Vibrio anguillarum* and *Yersinia ruckeri* bacterins. *J Fish Dis,* 5**,** 197-205.

JONSSON, B., FORSETH, T., JENSEN, A. J. & NÆSJE, T. F. 2001. Thermal performance of juvenile Atlantic Salmon, *Salmo salar* L. *Funct Ecol,* 15**,** 701-11.

KAMBAYASHI, T. & LAUFER, T. M. 2014. Atypical MHC class II-expressing antigen-presenting cells: can anything replace a dendritic cell? *Nat Rev Immunol,* 14**,** 719-30.

KATO, G., MIYAZAWA, H., YAMAGUCHI, T., KONDO, H., SANO, M. & FISCHER, U. 2016. Characterization of antigen sampling cells in rainbow trout gill epithelium. *Fish Shellfish Immunol,* 53**,** 82-3.

KATO, G., TAKANO, T., SAKAI, T., MATSUYAMA, T. & NAKAYASU, C. 2013. *Vibrio anguillarum* bacterin uptake via the gills of Japanese flounder and subsequent immune responses. *Fish Shellfish Immunol,* 35**,** 1591-7.

KIMMEL, C. B., BALLARD, W. W., KIMMEL, S. R., ULLMANN, B. & SCHILLING, T. F. 1995. Stages of embryonic development of the zebrafish. *Dev Dyn,* 203**,** 253-310.

KOPPANG, E. O., BJERKÅS, I., HAUGARVOLL, E., CHAN, E. K., SZABO, N. J., ONO, N., AKIKUSA, B., JIRILLO, E., POPPE, T. T., SVEIER, H., TORUD, B. & SATOH, M. 2008. Vaccination-induced systemic autoimmunity in farmed Atlantic salmon. *J Immunol,* 181**,** 4807-14.

KOPPANG, E. O., FISCHER, U., MOORE, L., TRANULIS, M. A., DIJKSTRA, J. M., KÖLLNER, B., AUNE, L., JIRILLO, E. & HORDVIK, I. 2010. Salmonid T cells assemble in the thymus, spleen and in novel interbranchial lymphoid tissue. *J Anat,* 217**,** 728-39.

KOPPANG, E. O., HORDVIK, I., BJERKÅS, I., TORVUND, J., AUNE, L., THEVARAJAN, J. & ENDRESEN, C. 2003. Production of rabbit antisera against recombinant MHC class II beta chain and identification of immunoreactive cells in Atlantic salmon (*Salmo salar*). *Fish Shellfish Immunol,* 14**,** 115-32.

KOPPANG, E. O., KVELLESTAD, A. & FISCHER, U. 2015. Fish mucosal immunity: gill. *In:* BECK, B. H. & PEATMAN, E. (eds.) *Mucosal health in aquaculture.* Amsterdam, Elsevier Academic Press, 93-133.

KÜCHLER, A. M., GJINI, E., PETERSON-MADURO, J., CANCILLA, B., WOLBURG, H. & SCHULTE-MERKER, S. 2006. Development of the zebrafish lymphatic system requires VEGFC signaling. *Curr Biol,* 16**,** 1244-8.

LAGOS, L. X., ILIEV, D. B., HELLAND, R., ROSEMBLATT, M. & JØRGENSEN, J. B. 2012. CD40L-a costimulatory molecule involved in the maturation of antigen presenting cells in Atlantic salmon (*Salmo salar*). *Dev Comp Immunol,* 38**,** 416-30.

LAM, S. H., CHUA, H. L., GONG, Z., WEN, Z., LAM, T. J. & SIN, Y. M. 2002. Morphologic transformation of the thymus in developing zebrafish. *Dev Dyn,* 225**,** 87-94.

LAMAS, J., BRUNO, D. W., SANTOS, Y., ANADÓN, R. & ELLIS, A. E. 1991. Eosinophilic granular cell response to intraperitoneal injection with *Vibrio anguillarum* and its extracellular products in rainbow trout, *Oncorhynchus mykiss*. *Fish Shellfish Immunol,* 1**,** 187-94.

LANIER, L. L., CHANG, C., SPITS, H. & PHILLIPS, J. H. 1992. Expression of cytoplasmic CD3 epsilon proteins in activated human adult natural killer (NK) cells and CD3 gamma, delta, epsilon complexes in fetal NK cells. Implications for the relationship of NK and T lymphocytes. *J Immunol,* 149**,** 1876-80.

LAURENT, P. 1984. Gill internal morphology. *In:* HOAR, W. S. & RANDALL, D. J. (eds.) *Fish physiology. Volume X. Gills. Part A. Anatomy, gas transfer, and acid-base regulation.* New York, Academic Press Inc, 73-183.

LIN, S. H., DAVIDSON, G. A., SECOMBES, C. J. & ELLIS, A. E. 1998. A morphological study of cells isolated from the perfused gill of dab and Atlantic salmon. *J Fish Biol,* 53**,** 560-8.

LIN, S. H., ELLIS, A. E., DAVIDSON, G. A. & SECOMBES, C. J. 1999. Migratory, respiratory burst and mitogenic responses of leucocytes isolated from the gills of rainbow trout (*Oncorhynchus mykiss*). *Fish Shellfish Immunol,* 9**,** 211-26.

LOVY, J., WRIGHT, G. M. & SPEARE, D. J. 2006. Morphological presentation of a dendritic-like cell within the gills of chinook salmon infected with *Loma salmonae*. *Dev Comp Immunol,* 30**,** 259-63.

LOVY, J., WRIGHT, G. M. & SPEARE, D. J. 2007. Ultrastructural examination of the host inflammatory response within gills of netpen reared chinook salmon (*Oncorhynchus tshawytscha*) with Microsporidial Gill Disease. *Fish Shellfish Immunol,* 22**,** 131-49.

LUER, C. A., WALSH, C. J., BODINE, A. B., WYFFELS, J. T. & SCOTT, T. R. 1995. The elasmobranch thymus: Anatomical, histological, and preliminary functional characterization. *J Exp Zool,* 273**,** 342-54.

LUI, A., MANERA, M., GIARI, L., MULERO, V. & DEZFULI, B. S. 2013. Acidophilic granulocytes in the gills of gilthead seabream *Sparus aurata*: evidence for their responses to a natural infection by a copepod ectoparasite. *Cell Tissue Res,* 353**,** 465-72.

LUMSDEN, J. S., OSTLAND, V. E., BYRNE, P. J. & FERGUSON, H. W. 1993. Detection of a distinct gill-surface antibody response following horizontal infection and bath challenge of brook trout *Salvelinus fontinalis* with *Flavobacterium branchiophilum*, the causative agent of bacterial gill disease. *Dis Aquat Organ,* 16**,** 21-7.

LUMSDEN, J. S., OSTLAND, V. E., MACPHEE, D. D. & FERGUSON, H. W. 1995. Production of gill-associated and serum antibody by rainbow trout (*Oncorhynchus mykiss*) following immersion immunization with acetone-killed *Flavobacterium branchiophilum* and the relationship to protection from experimental challenge. *Fish Shellfish Immunol,* 5**,** 151-65.

LØKKA, G., AUSTBØ, L., FALK, K., BJERKÅS, I. & KOPPANG, E. O. 2013. Intestinal morphology of the wild Atlantic salmon (*Salmo salar*). *J Morphol,* 274**,** 859-76.

LØKKA, G., AUSTBØ, L., FALK, K., BROMAGE, E., FJELLDAL, P. G., HANSEN, T., HORDVIK, I. & KOPPANG, E. O. 2014. Immune parameters in the intestine of wild and reared unvaccinated and vaccinated Atlantic salmon (*Salmo salar* L.). *Dev Comp Immunol,* 47**,** 6-16.

MA, D., WANG, L., WANG, S., GAO, Y., WEI, Y. & LIU, F. 2012. Foxn1 maintains thymic epithelial cells to support T-cell development via mcm2 in zebrafish. *Proc Natl Acad Sci U S A,* 109**,** 21040-5.

MACCHIARELLI, G., PALMERINI, M. G. & NOTTOLA, S. A. 2015. Scanning electron microscopy of blood vascular corrosion casts in mammals. *In:* SLEVIN, M. & MCDOWELL, G. (eds.) *Handbook of vascular biology techniques.* Dordrecht, Springer, 153-71.

MAINA, J. N. 2002. Structure, function and evolution of the gas exchangers: comparative perspectives. *J Anat,* 201**,** 281-304.

MAKESH, M., SUDHEESH, P. S. & CAIN, K. D. 2015. Systemic and mucosal immune response of rainbow trout to immunization with an attenuated *Flavobacterium psychrophilum* vaccine strain by different routes. *Fish Shellfish Immunol,* 44**,** 156-63.

MALCOLM, I. A., SOULSBY, C., YOUNGSON, A. F. & HANNAH, D. M. 2005. Catchment-scale controls on groundwater–surface water interactions in the hyporheic zone: implications for salmon embryo survival. *River Res Appl,* 21**,** 977-89.

MATSUNAGA, T. & RAHMAN, A. 2001. In search of the origin of the thymus: the thymus and GALT may be evolutionarily related. *Scand J Immunol,,* 53**,** 1-6.

MATSUYAMA, T. & IIDA, T. 1999. Degranulation of eosinophilic granular cells with possible involvement in neutrophil migration to site of inflammation in tilapia. *Dev Comp Immunol,* 23**,** 451-7.

MATSUYAMA, T. & IIDA, T. 2001. Influence of tilapia mast cell lysate on vascular permeability. *Fish Shellfish Immunol,* 11**,** 549-56.

MCDERMOTT, M. R. & BIENENSTOCK, J. 1979. Evidence for a common mucosal immunologic system. I. Migration of B immunoblasts into intestinal, respiratory, and genital tissues. *J Immunol,* 122**,** 1892-8.

MESCHER, A. L. & JUNQUEIRA, L. C. 2015. *Junqueira's basic histology: text and atlas* 14 ed. New York, McGraw-Hill

MEYER, E. P., BEER, G. M., LANG, A., MANESTAR, M., KRUCKER, T., MEIER, S., MIHIC-PROBST, D. & GROSCURTH, P. 2007. Polyurethane elastomer: a new material for the visualization of cadaveric blood vessels. *Clin Anat,* 20**,** 448-54.

MIDTLYNG, P. J., REITAN, L. J., LILLEHAUG, A. & RAMSTAD, A. 1996. Protection, immune responses and side effects in Atlantic salmon (*Salmo salar* L.) vaccinated against furunculosis by different procedures. *Fish Shellfish Immunol,* 6**,** 599-613.

MILDNER, A. & JUNG, S. 2014. Development and function of dendritic cell subsets. *Immunity,* 40**,** 642-56.

MULERO, I., PILAR SEPULCRE, M., ROCA, F. J., MESEGUER, J., GARCÍA-AYALA , A. & MULERO, V. 2008. Characterization of macrophages from the bony fish gilthead seabream using an antibody against the macrophage colony-stimulating factor receptor. *Dev Comp Immunol,* 32**,** 1151-9.

MULERO, I., SEPULCRE, M. P., MESEGUER, J., GARCÍA-AYALA, A. & MULERO, V. 2007. Histamine is stored in mast cells of most evolutionarily advanced fish and regulates the fish inflammatory response. *Proc Natl Acad Sci U S A,* 104**,** 19434-9.

MURATA, S., SASAKI, K., KISHIMOTO, T., NIWA, S., HAYASHI, H., TAKAHAMA, Y. & TANAKA, K. 2007. Regulation of CD8+ T cell development by thymus-specific proteasomes. *Science,* 316**,** 1349-53.

MÜHLFELD, C. 2014. Quantitative morphology of the vascularisation of organs: a stereological approach illustrated using the cardiac circulation. *Ann Anat,* 196**,** 12-9.

NAKANISHI, T. & OTOTAKE, M. 1997. Antigen uptake and immune responses after immersion vaccination. *In:* GUDDING, R., LILLEHAUG, A., MIDTLYNG, P. J. & BROWN, F. (eds.) *Fish vaccinology.* Basel, Karger, 59-68.

NAKANISHI, T., SHIBASAKI, Y. & MATSUURA, Y. 2015. T Cells in Fish. *Biology (Basel),* 4**,** 640-63.

NEHLS, M., PFEIFER, D., SCHORPP, M., HEDRICH, H. & BOEHM, T. 1994. New member of the winged-helix protein family disrupted in mouse and rat nude mutations. *Nature,* 372**,** 103-7.

NELSON, J. S. 2006. *Fishes of the world.* 4 ed. New York, John Wiley.

NEUTRA, M. R. & KOZLOWSKI, P. A. 2006. Mucosal vaccines: the promise and the challenge. *Nat Rev Immunol,* 6**,** 148-58.

NEUTRA, M. R., MANTIS, N. J. & KRAEHENBUHL, J. P. 2001. Collaboration of epithelial cells with organized mucosal lymphoid tissues. *Nat Immunol,* 2**,** 1004-9.

NIGAM, A. K., KUMARI, U., MITTAL, S. & MITTAL, A. K. 2012. Comparative analysis of innate immune parameters of the skin mucous secretions from certain freshwater teleosts, inhabiting different ecological niches. *Fish Physiol Biochem,* 38**,** 1245-56.

OHTA, Y., LANDIS, E., BOULAY, T., PHILLIPS, R. B., COLLET, B., SECOMBES, C. J., FLAJNIK, M. F. & HANSEN, J. D. 2004. Homologs of CD83 from elasmobranch and teleost fish. *J Immunol,* 173**,** 4553-60.

OHTANI, M., VILLUMSEN, K. R., STRØM, H. K. & RAIDA, M. K. 2014. 3D Visualization of the initial *Yersinia ruckeri* infection route in rainbow trout (*Oncorhynchus mykiss*) by optical projection tomography. *Plos One,* 9**,** e89672.

OLSEN, M. M., KANIA, P. W., HEINECKE, R. D., SKJØDT, K., RASMUSSEN, K. J. & BUCHMANN, K. 2011. Cellular and humoral factors involved in the response of rainbow trout gills to *Ichthyophthirius multifiliis* infections: molecular and immunohistochemical studies. *Fish Shellfish Immunol,* 30**,** 859-69.

OLSON, K. R. 1996. Secondary circulation in fish: Anatomical organization and physiological significance. *J Exp Zool,* 275**,** 172-85.

OLSON, K. R. 2000. Respiratory system. *In:* OSTRANDER, G. K. (ed.) *The laboratory fish.* San Diego, California, Academic Press 151-9.

OLSON, K. R. 2002. Vascular anatomy of the fish gill. *J Exp Zool,* 293**,** 214-31.

ORDÁS, M. C., CASTRO, R., DIXON, B., SUNYER, J. O., BJORK, S., BARTHOLOMEW, J., KORYTAR, T., KÖLLNER, B., CUESTA, A. & TAFALLA, C. 2012. Identification of a novel CCR7 gene in rainbow trout with differential expression in the context of mucosal or systemic infection. *Dev Comp Immunol,* 38**,** 302-11.

OTOTAKE, M., IWAMA, G. K. & NAKANISHI, T. 1996. The uptake of bovine serum albumin by the skin of bath-immunised rainbow trout *Oncorhynchus mykiss*. *Fish Shellfish Immunol,* 6**,** 321-33.

PABST, O., HERBRAND, H., WORBS, T., FRIEDRICHSEN, M., YAN, S., HOFFMANN, M. W., KORNER, H., BERNHARDT, G., PABST, R. & FORSTER, R. 2005. Cryptopatches and isolated lymphoid follicles: dynamic lymphoid tissues dispensable for the generation of intraepithelial lymphocytes. *Eur J Immunol,* 35**,** 98-107.

PABST, R. 2007. Plasticity and heterogeneity of lymphoid organs. What are the criteria to call a lymphoid organ primary, secondary or tertiary? *Immunol Lett,* 112**,** 1-8.

PALM, R. C., JR., LANDOLT, M. L. & BUSCH, R. A. 1998. Route of vaccine administration: effects on the specific humoral response in rainbow trout *Oncorhynchus mykiss*. *Dis Aquat Organ,* 33**,** 157-66.

PARRA, D., REYES-LOPEZ, F. E. & TORT, L. 2015. Mucosal immunity and B cells in teleosts: effect of vaccination and stress. *Front Immunol,* 6**,** 354.

PEARSE, G. 2006. Normal structure, function and histology of the thymus. *Toxicol Pathol,* 34**,** 504-14.

PFAFFL, M. W. 2001. A new mathematical model for relative quantification in real-time RT-PCR. *Nucleic Acids Res,* 29**,** e45.

PFAFFL, M. W. 2004. Quantification strategies in real-time PCR. *In:* BUSTIN, S. A. (ed.) *A-Z of quantitative PCR.* La Jolla, CA, International University Line, 87-112.

PIAZZON, M. C., SAVELKOUL, H. S., PIETRETTI, D., WIEGERTJES, G. F. & FORLENZA, M. 2015. Carp Il10 has anti-inflammatory activities on phagocytes, promotes proliferation of memory T cells, and regulates B cell differentiation and antibody secretion. *J Immunol,* 194**,** 187-99.

RAMIREZ-GOMEZ, F., GREENE, W., REGO, K., HANSEN, J. D., COSTA, G., KATARIA, P. & BROMAGE, E. S. 2012. Discovery and characterization of secretory IgD in rainbow trout: secretory IgD is produced through a novel splicing mechanism. *J Immunol,* 188**,** 1341-9.

RASMUSSEN, K. J., STEFFENSEN, J. F. & BUCHMANN, K. 2013. Differential occurrence of immune cells in the primary and secondary vascular systems in rainbow trout, *Oncorhynchus mykiss* (Walbaum). *J Fish Dis,* 36**,** 675-9.

REITE, O. B. 1996. The mast cell nature of granule cells in the digestive tract of the pike *Esox lucius*: similarity to mammalian mucosa mast cells and globule leucocytes. *Fish Shellfish Immunol,* 6**,** 363-9.

REITE, O. B. 1997. Mast cells/eosinophilic granule cells of salmonids: staining properties and responses to noxious agents. *Fish Shellfish Immunol,* 7**,** 567-84.
REITE, O. B. 2005. The rodlet cells of teleostean fish: their potential role in host defence in relation to the role of mast cells/eosinophilic granule cells. *Fish Shellfish Immunol,* 19**,** 253-67.
REITE, O. B. & EVENSEN, Ø. 2006. Inflammatory cells of teleostean fish: a review focusing on mast cells/eosinophilic granule cells and rodlet cells. *Fish Shellfish Immunol,* 20**,** 192-208.
ROMANO, N., FANELLI, M., MARIA DEL PAPA, G., SCAPIGLIATI, G. & MASTROLIA, L. 1999a. Histological and cytological studies on the developing thymus of sharpsnout seabream, *Diplodus puntazzo*. *J Anat,* 194 (Pt 1)**,** 39-50.
ROMANO, N., TAVERNE-THIELE, A. J., FANELLI, M., BALDASSINI, M. R., ABELLI, L., MASTROLIA, L., VAN MUISWINKEL, W. B. & ROMBOUT, J. H. 1999b. Ontogeny of the thymus in a teleost fish, *Cyprinus carpio* L.: developing thymocytes in the epithelial microenvironment. *Dev Comp Immunol,* 23**,** 123-37.
ROMBOUGH, P. 2007. The functional ontogeny of the teleost gill: which comes first, gas or ion exchange? *Comp Biochem Physiol A Mol Integr Physiol,* 148**,** 732-42.
ROMBOUT, J. H., HUTTENHUIS, H. B., PICCHIETTI, S. & SCAPIGLIATI, G. 2005. Phylogeny and ontogeny of fish leucocytes. *Fish Shellfish Immunol,* 19**,** 441-55.
ROMBOUT, J. H., YANG, G. & KIRON, V. 2014. Adaptive immune responses at mucosal surfaces of teleost fish. *Fish Shellfish Immunol,* 40**,** 634-43.
ROMBOUT, J. W., BLOK, L. J., LAMERS, C. H. & EGBERTS, E. 1986. Immunization of carp (*Cyprinus carpio*) with a *Vibrio anguillarum* bacterin: indications for a common mucosal immune system. *Dev Comp Immunol,* 10**,** 341-51.
RYO, S., WIJDEVEN, R. H., TYAGI, A., HERMSEN, T., KONO, T., KARUNASAGAR, I., ROMBOUT, J. H., SAKAI, M., VERBURG-VAN KEMENADE, B. M. & SAVAN, R. 2010. Common carp have two subclasses of bonyfish specific antibody IgZ showing differential expression in response to infection. *Dev Comp Immunol,* 34**,** 1183-90.
SALINAS, I. 2015. The mucosal immune system of teleost fish. *Biology (Basel),* 4**,** 525-39.
SALINAS, I., ZHANG, Y. A. & SUNYER, J. O. 2011. Mucosal immunoglobulins and B cells of teleost fish. *Dev Comp Immunol,* 35**,** 1346-65.
SCHORPP, M., LEICHT, M., NOLD, E., HAMMERSCHMIDT, M., HAAS-ASSENBAUM, A., WIEST, W. & BOEHM, T. 2002. A zebrafish orthologue (whnb) of the mouse nude gene is expressed in the epithelial compartment of the embryonic thymic rudiment. *Mech Dev,* 118**,** 179-85.
SILPHADUANG, U., COLORNI, A. & NOGA, E. J. 2006. Evidence for widespread distribution of piscidin antimicrobial peptides in teleost fish. *Dis Aquat Organ,* 72**,** 241-52.
SILPHADUANG, U. & NOGA, E. J. 2001. Peptide antibiotics in mast cells of fish. *Nature,* 414**,** 268-9.
SMITH, P. D. 1982. Analysis of the hyperosmotic and bath methods for fish vaccination - comparison of uptake of particulate and non-particulate antigens. *Dev Comp Immunol Supl 2.* 181-6.
SOLLID, J., DE ANGELIS, P., GUNDERSEN, K. & NILSSON, G. E. 2003. Hypoxia induces adaptive and reversible gross morphological changes in crucian carp gills. *J Exp Biol,* 206**,** 3667-3673.
SOLLID, J. & NILSSON, G. E. 2006. Plasticity of respiratory structures-adaptive remodeling of fish gills induced by ambient oxygen and temperature. *Respir Physiol Neurobiol,* 154**,** 241-51.
STATISTICS NORWAY. 2015. *Aquaculture, 2015, preliminary figures* [Online]. Oslo: Statistics Norway. Available: https://www.ssb.no/en/jord-skog-jakt-og-fiskeri/statistikker/fiskeoppdrett [Accessed 19.07.2016].
SUDHEESH, P. S. & CAIN, K. D. 2016. Optimization of efficacy of a live attenuated *Flavobacterium psychrophilum* immersion vaccine. *Fish Shellfish Immunol,* 56**,** 169-80.
SUNYER, J. O. 2013. Fishing for mammalian paradigms in the teleost immune system. *Nat Immunol,* 14**,** 320-6.

SUTOH, Y., KONDO, M., OHTA, Y., OTA, T., TOMARU, U., FLAJNIK, M. F. & KASAHARA, M. 2012. Comparative genomic analysis of the proteasome beta5t subunit gene: implications for the origin and evolution of thymoproteasomes. *Immunogenetics,* 64**,** 49-58.

SUZUKA, I., DAIDOJI, H., MATSUOKA, M., KADOWAKI, K., TAKASAKI, Y., NAKANE, P. K. & MORIUCHI, T. 1989. Gene for proliferating-cell nuclear antigen (DNA polymerase delta auxiliary protein) is present in both mammalian and higher plant genomes. *Proc Natl Acad Sci U S A,* 86**,** 3189-93.

TACCHI, L., LARRAGOITE, E. T., MUÑOZ, P., AMEMIYA, C. T. & SALINAS, I. 2015. African lungfish reveal the evolutionary origins of organized mucosal lymphoid tissue in vertebrates. *Curr Biol,* 25**,** 2417-24.

TACCHI, L., MUSHARRAFIEH, R., LARRAGOITE, E. T., CROSSEY, K., ERHARDT, E. B., MARTIN, S. A., LAPATRA, S. E. & SALINAS, I. 2014. Nasal immunity is an ancient arm of the mucosal immune system of vertebrates. *Nat Commun,* 5**,** 5205.

TADISO, T. M., LIE, K. K. & HORDVIK, I. 2011. Molecular cloning of IgT from Atlantic salmon, and analysis of the relative expression of τ, μ, and δ in different tissues. *Vet Immunol Immunopathol,* 139**,** 17-26.

TAKAHAMA, Y., NITTA, T., MAT RIPEN, A., NITTA, S., MURATA, S. & TANAKA, K. 2010. Role of thymic cortex-specific self-peptides in positive selection of T cells. *Semin Immunol,* 22**,** 287-93.

TAKAHAMA, Y., TAKADA, K., MURATA, S. & TANAKA, K. 2012. β5t-containing thymoproteasome: specific expression in thymic cortical epithelial cells and role in positive selection of CD8+ T cells. *Curr Opin Immunol,* 24**,** 92-8.

TAKIZAWA, F., DIJKSTRA, J. M., KOTTERBA, P., KORYTÁŘ, T., KOCK, H., KÖLLNER, B., JAUREGUIBERRY, B., NAKANISHI, T. & FISCHER, U. 2011a. The expression of CD8alpha discriminates distinct T cell subsets in teleost fish. *Dev Comp Immunol,* 35**,** 752-63.

TAKIZAWA, F., KOPPANG, E. O., OHTANI, M., NAKANISHI, T., HASHIMOTO, K., FISCHER, U. & DIJKSTRA, J. M. 2011b. Constitutive high expression of *interleukin-4/13A* and *GATA-3* in gill and skin of salmonid fishes suggests that these tissues form Th2-skewed immune environments. *Mol Immunol,* 48**,** 1360-8.

TAKIZAWA, F., MAGADAN, S., PARRA, D., XU, Z., KORYTÁŘ, T., BOUDINOT, P. & SUNYER, J. O. 2016. Novel teleost CD4-bearing cell populations provide insights into the evolutionary origins and primordial roles of CD4+ lymphocytes and CD4+ macrophages. *J Immunol,* 196**,** 4522-35.

TATNER, M. F. 1996. Natural changes in the immune system of fish. *In:* IWAMA, G. & NAKANISHI, T. (eds.) *Fish Physiology. Volume 15. The fish immune system: organism, pathogen, and environment.* San Diego, California, Academic Press, 255-87.

TATNER, M. F. & HORNE, M. T. 1983. Factors influencing the uptake of ^{14}C-labelled *Vibrio anguillarum* vaccine in direct immersion experiments with rainbow trout, *Salmo gairdneri* Richardson. *J Fish Biol,* 22**,** 585-91.

TATNER, M. F. & HORNE, M. T. 1984. The effects of early exposure to *Vibrio anguillarum* vaccine on the immune response of the fry of the rainbow trout, *Salmo gairdneri* Richardson. *Aquaculture,* 41**,** 193-202.

TATNER, M. F. & MANNING, M. J. 1982. The morphology of the trout, *Salmo gairdneri* Richardson, thymus: some practical and theoretical considerations. *J Fish Biol,* 21**,** 27-32.

THORSTAD, E. B., WHORISKEY, F., RIKARDSEN, A. H. & AARESTRUP, K. 2011. Aquatic nomads: the life and migrations of Atlantic salmon. *In:* AAS, Ø., EINUM, S., KLEMETSEN, A. & SKURDAL, J. (eds.) *Atlantic salmon ecology.* Blackwell Publishing Ltd, 1-32.

TORROBA, M., ANDERSON, D. P., DIXON, O. W., CASARES, F., VARAS, A., ALONSO, L., DEL MORAL, M. G. & ZAPATA, A. G. 1993. *In vitro* antigen trapping by gill cells of the rainbow trout: an immunohistochemical study. *Histology and Histopathology,* 8**,** 363-367.

TURCHINI, G. M., NG, W. & TOCHER, D. R. 2010. *Fish oil replacement and alternative lipid sources in aquaculture feeds* Boca Raton, CRC Press.
VAN GUILDER, H. D., VRANA, K. E. & FREEMAN, W. M. 2008. Twenty-five years of quantitative PCR for gene expression analysis. *Biotechniques,* 44**,** 619-26.
VARGA, I., POSPÍŠILOVÁ, V., GMITTEROVÁ, K., GÁLFIOVÁ, P., POLÁK, Š. & GALBAVÝ, Š. 2008. The phylogenesis and ontogenesis of the human pharyngeal region focused on the thymus, parathyroid, and thyroid glands. *Neuro Endocrinol Lett,* 29**,** 837-45.
VEJLSTED, M. 2009. Development of the immune system. *In:* HYTTEL, P. (ed.) *Essentials of domestic animal embryology.* Edinburgh, Saunders, 208-215.
VERLI, F. D., ROSSI-SCHNEIDER, T. R., SCHNEIDER, F. L., YURGEL, L. S. & DE SOUZA, M. A. 2007. Vascular corrosion casting technique steps. *Scanning,* 29**,** 128-32.
VIGLIANO, F. A., BERMÚDEZ, R., QUIROGA, M. I. & NIETO, J. M. 2006. Evidence for melano-macrophage centres of teleost as evolutionary precursors of germinal centres of higher vertebrates: an immunohistochemical study. *Fish Shellfish Immunol,* 21**,** 467-71.
VILLUMSEN, K. R. & RAIDA, M. K. 2013. Long-lasting protection induced by bath vaccination against *Aeromonas salmonicida* subsp. *salmonicida* in rainbow trout. *Fish Shellfish Immunol,* 35**,** 1649-53.
VOGEL, W. O. 2010. Zebrafish and lymphangiogenesis: a reply. *Anat Sci Int,* 85**,** 118-9.
WANG, H., KADLECEK, T. A., AU-YEUNG, B. B., GOODFELLOW, H. E., HSU, L. Y., FREEDMAN, T. S. & WEISS, A. 2010. ZAP-70: an essential kinase in T-cell signaling. *Cold Spring Harb Perspect Biol,* 2**,** a002279.
WANG, T. & SECOMBES, C. J. 2013. The cytokine networks of adaptive immunity in fish. *Fish Shellfish Immunol,* 35**,** 1703-18.
WARDLAW, A. J., GUILLEN, C. & MORGAN, A. 2005. Mechanisms of T cell migration to the lung. *Clin Exp Allergy,* 35**,** 4-7.
WENDELAAR BONGA, S. E. & VAN DER MEJ, C. J. M. 1989. Degeneration and death, by apoptosis and necrosis, of the pavement and chloride cells in the gills of the teleost *Oreochromis mossambicus*. *Cell Tissue Res,* 255**,** 235-243.
WILSON, J. M. & LAURENT, P. 2002. Fish gill morphology: inside out. *J Exp Zool,* 293**,** 192-213.
WILSON, M., BENGTEN, E., MILLER, N. W., CLEM, L. W., DU PASQUIER, L. & WARR, G. W. 1997. A novel chimeric Ig heavy chain from a teleost fish shares similarities to IgD. *Proc Natl Acad Sci U S A,* 94**,** 4593-7.
WORLD BANK 2013. FISH TO 2030: Prospects for fisheries and aquaculture. *In:* VOEGELE, J. (ed.) *World bank report number 83177-GLB.* Washington DC, The World Bank.
XU, Z., TAKIZAWA, F., PARRA, D., GOMEZ, D., VON GERSDORFF JØRGENSEN, L., LAPATRA, S. E. & SUNYER, J. O. 2016. Mucosal immunoglobulins at respiratory surfaces mark an ancient association that predates the emergence of tetrapods. *Nat Commun,* 7**,** 10728.
YAMAGA, K. M., KUBO, R. T. & ETLINGER, H. M. 1978. Studies on the question of conventional immunoglobulin on thymocytes from primitive vertebrates. I. Presence of anti-carbohydrate antibodies in rabbit anti-trout Ig sera. *J Immunol,* 120**,** 2068-73.
YANIV, K., ISOGAI, S., CASTRANOVA, D., DYE, L., HITOMI, J. & WEINSTEIN, B. M. 2006. Live imaging of lymphatic development in the zebrafish. *Nat Med,* 12**,** 711-6.
YOON, S., MITRA, S., WYSE, C., ALNABULSI, A., ZOU, J., WEERDENBURG, E. M., VAN DER SAR, A. M., WANG, D., SECOMBES, C. J. & BIRD, S. 2015. First demonstration of antigen induced cytokine expression by CD4-1+ lymphocytes in a poikilotherm: studies in zebrafish (*Danio rerio*). *PLoS One,* 10**,** e0126378.
ZAPATA, A. & AMEMIYA, C. T. 2000. Phylogeny of lower vertebrates and their immunological structures. *Curr Top Microbiol Immunol,* 248**,** 67-107.

ZAPATA, A., DIEZ, B., CEJALVO, T., GUTIERREZ-DE FRIAS, C. & CORTES, A. 2006. Ontogeny of the immune system of fish. *Fish Shellfish Immunol,* 20**,** 126-36.

ZAPATA, A. G., TORROBA, M., ALVAREZ, F., ANDERSON, D. P., DIXON, O. W. & WISNIEWSKI, M. 1987. Electron microscopic examination of antigen uptake by salmonid gill cells after bath immunization with a bacterin. *J Fish Biol,* 31**,** 209-17.

ZENKER, W. G., FERGUSON, H. W., BARKER, I. K. & WOODWARD, B. 1987. Epithelial and pillar cell replacement in gills of juvenile trout, *Salmo gairdneri* Richardson. *Comp Biochem Physiol A Comp Physiol,* 86**,** 423-8.

ZHANG, Y. A., SALINAS, I., LI, J., PARRA, D., BJORK, S., XU, Z., LAPATRA, S. E., BARTHOLOMEW, J. & SUNYER, J. O. 2010. IgT, a primitive immunoglobulin class specialized in mucosal immunity. *Nat Immunol,* 11**,** 827-35.

ZHU, L. Y., LIN, A. F., SHAO, T., NIE, L., DONG, W. R., XIANG, L. X. & SHAO, J. Z. 2014. B cells in teleost fish act as pivotal initiating APCs in priming adaptive immunity: an evolutionary perspective on the origin of the B-1 cell subset and B7 molecules. *J Immunol,* 192**,** 2699-714.

ERRATA

APPENDIX: ENCLOSED PAPERS I-III

I

The Interbranchial Lymphoid Tissue of Atlantic Salmon (*Salmo salar* L) Extends as a Diffuse Mucosal Lymphoid Tissue throughout the Trailing Edge of the Gill Filament

Alf S. Dalum,[1] Lars Austbø,[1] Håvard Bjørgen,[1] Karsten Skjødt,[2] Ivar Hordvik,[3] Tom Hansen,[4] Per G. Fjelldal,[4] Charles McL Press,[1] David J. Griffiths,[1] and Erling O. Koppang[1]*

[1]*Faculty of Veterinary Medicine and Biosciences, Department of Basic Sciences and Aquatic Medicine, Norwegian University of Life Sciences, Oslo, Norway*
[2]*Faculty of Health Science, Department of Cancer and Inflammation Research, Institute of Molecular Medicine, University of Southern Denmark, Odense, Denmark*
[3]*Faculty of Mathematics and Natural Sciences, Department of Biology, University of Bergen, Bergen, Norway*
[4]*Matre Research Station, Institute of Marine Research, Matre, Norway*

ABSTRACT The teleost gill forms an extensive, semipermeable barrier that must tolerate intimate contact with the surrounding environment and be able to protect the body from external pathogens. The recent discovery of the interbranchial lymphoid tissue (ILT) has initiated an anatomical and functional investigation of the lymphoid tissue of the salmonid gill. In this article, sectioning of gill arches in all three primary planes revealed an elongation of the ILT outward along the trailing edge of the primary filament to the very distal end, a finding not previously described. This newly found lymphoid tissue was investigated using a range of morphological and transcriptional tools. Avoiding potential salinity-related effects, the study focused on two fresh-water life stages—smoltifying juveniles and mature adults. Aggregates of T-cells continuous with the ILT were found within the thick epithelial lining of the trailing edge of the filament in considerably larger numbers than seen in the epithelium of the leading edge and of the interlamellar area. Only a few of these cells were identified as CD8α^+-cells, and there was a significantly ($P < 0.05$) higher relative expression of CD4- than of CD8- related genes in all gill segments investigated. Numerous major histocompatibility complex class II$^+$-cells were distributed uniformly throughout the filament epithelial tissue. Few Ig$^+$-cells were detected. Overall, the morphological features and comparable immune gene expression of the previously described ILT and the filament trailing edge lymphoid tissue suggest a close functional and anatomical relationship. We propose that the anatomical definition of the ILT must be broadened to include both the previously described ILT (to be renamed proximal ILT) and the trailing edge lymphoid tissue (to be named distal ILT). This extended anatomical localisation identifies the ILT as a widely distributed mucosal lymphoid tissue in the gill of Atlantic salmon. J. Morphol. 000:000–000, 2015. © 2015 Wiley Periodicals, Inc.

KEY WORDS: B-cell; gill anatomy; intraepithelial lymphocytes; mucosa; T-cell; teleost

INTRODUCTION

The vertebrate adaptive immune system occurs in its earliest form in the *Cyclostomata* with variable lymphocyte receptor molecules (Kasahara and Sutoh, 2014). In the cyclomate lamprey, tissue loosely resembling thymus has been identified in the terminal portion of gill filaments (Bajoghli et al., 2011). Adaptive immune molecules of the immunoglobulin superfamily are first seen in cartilaginous fish, which also develop a proper thymus. However, both cartilaginous fish and the more modern teleosts (bony fish) lack several components of the adaptive immune system found in higher vertebrates, including lymph nodes and complex mucosa-associated lymphoid tissue (MALT) with germinal centres of B-cell proliferation (Zapata and Amemiya, 2000; Rombout et al., 2005; Fischer et al., 2013). Recently, aggregates of lymphoid cells, the interbranchial

Author Contributions: ASD worked on all aspects of the study including design of the project, sampling of material, morphological, immunohistochemical, and gene expression study, interpretation of results as well as statistical analysis and writing of the manuscript. LA participated in study design, primer and probe design for gene expression study and writing of the manuscript. HB contributed with laboratory assistance. DJG contributed with macroscopic pictures and scanning electron microscopy of vascular casts. KS contributed with monoclonal antibody against CD8α. IH participated in design of the project and interpretation of findings. TH and PGA provided research material for the study. CMP participated in interpretation of findings and writing of the manuscript. EOK was project leader. All authors approved the final manuscript.

Contract grant sponsor: Research Council of Norway; Contract grant number: FRIMEDBIO-222207/F20.

*Correspondence to: Erling Olaf Koppang, Section of Anatomy and Pathology, School of Veterinary Medicine, Norwegian University of Life Sciences, Norway Ullevålsveien 72, Box 8146 Dep, 0033 Oslo, Norway. E-mail: erling.o.koppang@nmbu.no

Received 16 December 2014; Revised 10 April 2015;
Accepted 29 April 2015.

Published online 00 Month 2015 in
Wiley Online Library (wileyonlinelibrary.com).
DOI 10.1002/jmor.20403

lymphoid tissue (ILT), were discovered in the gills of salmonids (Haugarvoll et al., 2008; Koppang et al., 2010) and to our knowledge, similar structures have not been recorded in other teleosts.

The teleost gill is physiologically one of the most diversified organs among vertebrates and it possesses an intricate vasculature (Olson, 2002). The teleost gill contributes about 90% of the outer surface area of the fish (Hughes, 1984), and consists of four-paired arches, each having two rows of filaments (often referred to as primary lamellae). In salmonids, the proximal third of the filaments are fused by the tissue of the interbranchial septum, leaving only the distal two-thirds free. The filament, regarded as the functional unit of the gill (Wilson and Laurent, 2002; Evans et al., 2005), harbours two rows of lamellae (also referred to secondary lamellae) on each side where the main part of gas exchange occurs. The intimate interaction between the gills and the external milieu makes it a frontline of defence against potential pathogens and a strategic site for lymphoid tissue. The gills develop from the pharyngeal pouches, which are also thought to be of crucial importance in the development of the adaptive immune system (Matsunaga and Rahman, 2001). In mammals, the thymus, which is a primary lymphoid organ, develops from the embryological pharyngeal pouches as does the palatine tonsil, which is a secondary lymphoid organ (Varga et al., 2008). As the ILT seems to be of secondary lymphoid character (Aas et al., 2014; Austbø et al., 2014), the pharyngeal region of teleosts, as with the pharynx of mammals, appears to give rise to both a primary (thymus) and secondary (ILT) lymphoid organ.

With the recent discovery of thymus-analogous tissue in the distal ends of lamprey filaments (Bajoghli et al., 2011), a more thorough investigation of the anatomy of the ILT in salmonid gill filaments is warranted. In this article, we describe lymphoid tissue in the free end of the gill filament of Atlantic salmon (*Salmo salar* L.) and address its cellular composition using molecular markers and gene expression approaches. The choice of genes is based on previous studies showing that the ILT is rich in T-cells (Haugarvoll et al., 2008; Koppang et al., 2010). In addition, B-cell associated genes and genes involved in the function of primary lymphoid tissues were included. We show that lymphoid tissue discovered along the trailing edge of the salmon gill filament is continuous with the previously described ILT, which broadens the concept of mucosal immune tissue in the defence of the teleost respiratory organ.

MATERIALS AND METHODS

Fish

Unvaccinated, juvenile Atlantic salmon fingerlings approaching smoltification were collected from the Matre Research Station, Institute of Marine Research, Norway, in March 2013 ($n = 12$, average weight: 56.0 ± 7.0 g, average length: 172 ± 9.5 mm, average condition factor: 1.1 ± 0.1; approved by the Norwegian Research Animal Council, FOTS id 5817 2013/64255-2 of date 25.04.2013). In addition, wild, sexually mature Atlantic salmon were caught by dip-net at Hellefossen in the river Drammenselva, Norway, in December 2012 ($n = 6$, weight ranging from 1,800 g to 3,000 g, average weight $2{,}320 \pm 495$ g, average length 707 ± 130 mm, average condition factor 0.81 ± 0.1). Both groups were, thus, taken from freshwater. Each fish was anaesthetised in an aqueous solution of 100 mg/ml MS-222 (Tricaine methanesulfonate, Sigma-Aldrich, MO) and then decapitated. The second, left gill arch, the left thymus, and parts of the head kidney were sampled and stored in 10% buffered formalin for 72 h, or on RNAlater (Sigma-Aldrich, MO) and stored at −20°C until further processing. All fish were euthanized according to regulations of the Norwegian Directorate of Fisheries (Forskrift om drift av akvakulturanlegg §34. Avlivning av fisk). No mortality or disease outbreak had been recorded in the research facility of Matre or in the river Drammenselva in the recent past.

Histology

Formalin-fixed tissue was paraffin-embedded and processed for histological analysis using standard procedures (Bancroft and Gamble, 2008). Gill sections were cut in three different orientations in relation to the gill arch, namely sagittal, transverse, and dorsal. To obtain the different levels of dorsal sections (ILT-region, proximal- and distal-free filament), the regions as indicated in Figure 1 were excised from paraffin blocks of transversely oriented tissue using a razorblade. The sections were orientated in the dorsal plane and re-embedded. Together with the thymus and head kidney, 2.5 μm thick sections were made from the different gill orientations and stained with haematoxylin and eosin (H&E), van Gieson method (vG), periodic acid-methenamine silver, and Periodic acid-Schiff (PAS).

Immunohistochemistry

The different orientations of formalin-fixed, paraffin-embedded gill tissue (processed as described above) were sectioned at 4 μm thickness and mounted on poly-L-lysine-coated slides (Superfrost Plus, Thermo scientific, Braunschweig, Germany). The slides were incubated at 37°C for 24 h, followed by 58°C for 24 h, before deparaffinisation in xylene and hydration in graded alcohols to distilled water. Heat-induced epitope retrieval (HIER) was performed at 121°C for 10 min in citrate buffer pH 6 or tris-ethylenediaminetetraacetic acid (tris-EDTA) buffer pH 9.2 (Table 1). The slides were subsequently washed in phosphate-buffered saline (PBS). Inhibition was obtained with 50 mmol l^{-1} Phenylhydrazine (Sigma-Aldrich Chemistry, MO) in PBS, preheated to 37°C, for 40 min and then washed with PBS and stored at 4°C overnight. On the following day, the slides were blocked for 20 min with 0.2% goat normal serum in 5% bovine serum albumin (BSA)/tris-buffered saline (TBS) before incubation with primary antibody of appropriate concentrations diluted in 1% BSA/TBS. For staining with monoclonal antibodies, labelled polymer-HRP anti-mouse (Dako EnVison+ System-HRP, Dako, Glostrup, Denmark) was used as the secondary antibody. For staining with polyclonal antibodies, labelled polymer-HRP anti-rabbit (Dako EnVison+ System-HRP) was used as the secondary antibody. Either 3,3′-diaminobenzidine (DAB) or 3-amino-9-ethyl carbazol (AEC) was used as substrate (Table 1). Between each step, the slides were rinsed in TBS. Counterstaining was performed with haematoxylin, followed by washing in distilled water and mounting with polyvinyl alcohol (Apotekproduksjon, Oslo, Norway). The primary antibodies used are listed in Table 1.

Scanning Electron Microscopy on Gill Vascular Casting

One juvenile fish was anaesthetised as described above and decapitated. A 0.9 mm vascular catheter (Braun VasoVet, Jan F Andersen, Hønefoss, Norway) was inserted into the dorsal aorta

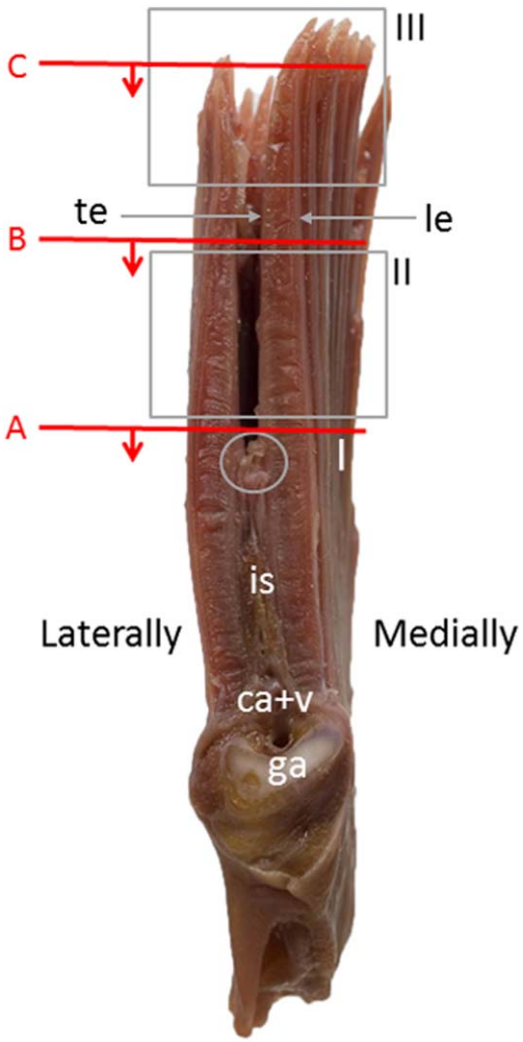

Fig. 1. Macroscopic presentation of a gill arch from mature Atlantic salmon cut in the transverse plane. Circle I indicates the proximal ILT-area, which together with box II and III define the regions targeted for mRNA extraction. Red lines A, B, and C represent dorsal section orientation for ILT, proximal- and distal filament, respectively. Red arrows indicate sectioning directions. The free end of the filament stretches from the level of the ILT and distally. Note that the filaments belonging to the medial hemibranch in general are longer than corresponding filaments of the lateral hemibranch; together they constitute the distal part of the holobranch of the gill. Trailing edge (te; also known as afferent edge with regard to blood flow direction) leading edge (le; also known as efferent edge with regard to blood flow direction), interbranchial septum (is), central branchial artery and -vein (ca+v), gill arch (ga).

and glued in place with a large drop of cyanoacrylate glue (Zap-a-Gap CA+, SmallSize Hobbyland, Oslo, Norway). Five millilitres of saline were carefully injected into the artery to flush the vascular system of the gills, followed by 1.5 ml of red-coloured epoxy solution (Axson RSF-816 laminating epoxy + 1% Ciba-Geigy DW-0133 red colouring paste, Wilh Willumsen AS, Stabekk, Norway) until colour was clearly visible in the filaments. After hardening of the epoxy for a day in water at room temperature, the casting was transferred to a 3% aqueous solution of potassium hydroxide at room temperature and agitated twice daily for 3 days until all tissue was gone. Small pieces of casting were critical-point dried, fastened to an aluminium stub, sputter-coated, and examined with a Cambridge stereoscan 90 scanning electron microscope (SEM).

Gene Expression

Six individuals from each group were subjected to total RNA extraction from the different gill filament parts (box II and III in Fig. 1 define the regions targeted for mRNA extraction from sexually mature individuals, while in juvenile fish the whole free end of the gill filament was chosen due to its small size), ILT-area (the area indicated by circle I in Fig. 1), thymus, and head kidney. The extracts were produced using the QIAzol-method (QUIAGEN Sciences, MD) and cleaned with NucleoSpin RNAII (Macherey-Nagel, Düren, Deutschland) according to the manufacturer's protocol and including an integrated rDNase digestion step (Macherey-Nagel, Düren, Deutschland). Total RNA concentration and purity were measured with a spectrophotometer (Biospec-Nano, Shimadzu Corporation, Kyoto, Japan) reading at optical density 260/280 nm and the integrity of RNA was evaluated qualitatively by electrophoresis on 2% agarose gel. First-strand cDNA synthesis was performed using M-MLV Reverse Transcriptase RNase H Minus, Point Mutation kit (Promega Corporation, WI) with Oligo dT15 and random hexamer primers. cDNA was amplified using TaqMan Gene Expression Master Mix (Life Technologies, CA) combined with 400 nmol/l forward and reverse primers, 100 nmol/l hydrolysis probes and 15 ng template in a total reaction volume of 13 μl. Each sample was amplified in triplicates, and the expression level for each tissue was evaluated as the relative ratio of cycle threshold between the gene of interest and elongation factor 1Ab (EF1Ab) as the reference gene (Olsvik et al., 2005). The following PCR profile was used (on a 7900HT fast real-time PCR system, Applied Biosystems, CA): 1) denaturation at 95°C for 10 min, 2) 40 cycles of 95°C for 15 s, 58°C for 15 s, and 60°C for 1 min. Primers and hydrolysis probes used are listed in Table 2. When possible, they were designed to span exon–intron junctions. Controls including no reverse transcriptase and nontemplate controls were included in the study.

Statistical Analysis

Prior to statistical analyses, Gaussian distribution was confirmed in all data sets using the Kolmogorov–Smirnov normality test. Differences in expression across tissues (Fig. 8) and between gene (Fig. 9) expression ratios were evaluated with one-way ANOVA followed by Tukey's multiple comparisons test. Differences in gene expression between tissues were considered significant at $P < 0.05$. The statistical calculations and graphical presentation in Figures 8 and 9 were performed using Prism® (Version 6.02; GraphPad Software, CA).

RESULTS

Unless stated otherwise, the histological and immunohistochemical findings applied to both juvenile and mature Atlantic salmon.

Histology

The macroscopic presentation of a gill arch and anatomical terms employed during this study are presented in Figure 1. HE-staining of transverse (Fig. 2A,H), dorsal (Fig. 2B–G), and sagittal (Fig. 2I) gill sections revealed a substantial numbers of intraepithelial cells with morphology resembling lymphocytes (determined by a prominent, dense nucleus surrounded by a narrow brim of free cytoplasm). These cells were distributed continuously from the proximal ILT and along the entire trailing edge of the gill filament to its distal end (Fig. 2A).

TABLE 1. List of primary antibodies used for immunohistochemical analysis

Primary antibody, HIER buffer, and substrate used	Reactivity	Reference/producer
Anti-CD3ε (rabbit polyclonal)-Citrate buffer pH6-DAB	Reactive against the CD3ε-chain of the CD3 complex, and is a highly specific marker during all developmental stages of T-cells in Atlantic salmon	(Koppang et al., 2010)
MHC class II β (rabbit polyclonal) -Tris-EDTA pH 9,1-AEC	Reactive against the β-chain of the MHC class II complex in Atlantic salmon	(Koppang et al., 2003)
Pan cytokeratin (clone AE1/AE3) (mouse monoclonal)-Citrate buffer pH6-DAB	Mix of monoclonal antibodies reacting with a broad range of keratins visualising normal simple epithelial cells; AE1 recognizes keratins 10, 14, 15, 16, and 19 in the acidic subfamily, and AE3 recognises the entire basic subfamily of keratins	Invitrogen Corporation 1600 Faraday avenue Carlsbad, CA 92008
Sasa CD8 F1-29 (mouse monoclonal)-Citrate buffer pH6–DAB	Reactive against CD8α, a part of the CD8 complex found both in the homodimeric (i.e., CD8αα) and heterodimeric (i.e., CD8αββ) isoforms. CD8 is predominantly expressed on the surface of cytotoxic T-lymphocytes and serves as *CORECEPTOR* for the T-cell receptor	(Hetland et al., 2010)
Mouse anti-Salmonid Ig, IgG1, clone 3D1 (mouse monoclonal)-Citrate buffer pH6-DAB	Anti-salmonid immunoglobulin (H chain) monoclonal antibody with specificity toward Salmo- and Oncorhynchus serum immunoglobulins	ImmunoPrecise Antibodies, Vancouver Island, Canada

Cluster of differentiation, CD; major histocompatibility complex, MHC; immunoglobulin M, IgM; 3,3‘-diaminobenzidine, DAB; 3-amino-9-ethyl carbazol, AEC.

TABLE 2. Primers and probes used for RT-qPCR assay. Primers or probes were designed to span internal exon-exon junctions

Gene	Gene bank accession number	Sequence (5′–3′)	Reference
EF1Ab	BG933853	F–TGCCCCTCCAGGATGTCTAC, R–CACGGCCCACAGGTACTG, P–FAM-AAATCGGCGGTATTGG-MGB	(Olsvik et al., 2005)
CD3ζ	BT060238	F–AACAGGGATCCAGAGAGTGCTG, R–AAGGGACGTGTAAGTGTCGTCA, P–FAM-ACGGCACGCGATAATCGCAGGA-BHQ1	(Austbø et al., 2014)
CD4-2a	EU409792	F–GCCCCTGAAGTCCAACGAC, R–AGGCTTCTCTCACTGCGTCC, P–FAM-CCGCACACTAGAGGGTCCACCACG-BHQ1	(Løkka et al., 2014)
CD8α	NM_001123583	F–ACTTGCTGGGCCAGCC, R–CACGACTTGGCAGTTGTAGA, P–FAM-CGACAACAACAACCACCACG-BHQ1	(Løkka et al., 2014)
CD8β	AY693394	F–TTCTTCTCAGACCCGGAGAA, R–ATCGTTCCTTTTGGTGCAG, P–FAM-CAACATTAACCCCTGTCACGAAGC-BHQ1	(Aas et al., 2014)
TCR α	AY552002	F–AACTGGTATTTTGACACAGATGC, R–ATCAGCACGTTGAAAACGAT, P–FAM-ACCATTCTGGGCCTGAGAATTCTGT-BHQ1	(Løkka et al., 2014)
TCR δ	EG821964	F–AGCGTTGTGAGATGGATGGC, R–GCAGTTGTAGCCGTGGTGTTATAG, P–FAM-AGCCGCCCGTTGATGATAAAGATGATTC-BHQ1	(Løkka et al., 2014)
IgM A/B	Y12456, Y12457	F–TGTAAAGAGAGCAGACTGGGACAG, R–GAGACGGGTGCTGCAGATATTC, P–FAM-TGTTCCACGGCGCATTCAAAGATTT-BHQ1	(Austbø et al., 2014)
IgT A/B	GQ907003, GQ907004	F–CAGCAGTCTGCTGAAGGTC, R–GGTTCTGTTTTGGAGATCG, P–FAM-CTGCACCACACAGCTGTACTTGACC-BHQ1	(Austbø et al., 2014)
RAG-1	NM_001124737	F–GAGGCCATGATGCAAGGC, R–CTTGACGGTGCGGTACATCT, P–FAM-ATCCTGCTGTGTGTCTGGCCATC-BHQ1	(Løkka et al., 2014)
RAG-2	DY697789	F–GTTCTTCGAGACGTTCAAACAG, R–TTCACTGCAGTCAGTGGTTG, P–FAM-ACGTTAGCTACTTGAGCAGGAGCCAC-BHQ1	(Løkka et al., 2014)

Primers (400 nmol/l each) and probes (100 nmol/l) used for RT-qPCR assay on immune-related genes in the different parts of the free gill filament and ILT, thymus, and pronephros.
Elongation factor, EF; cluster of differentiation, CD; T-cell receptor, TCR; immunoglobulin M, IgM; immunoglobulin T, IgT; recombination activating gene, RAG; 6-carboxyfluorescein, FAM; Black Hole Quencher®, BHQ; Minor groove binding, MGB.

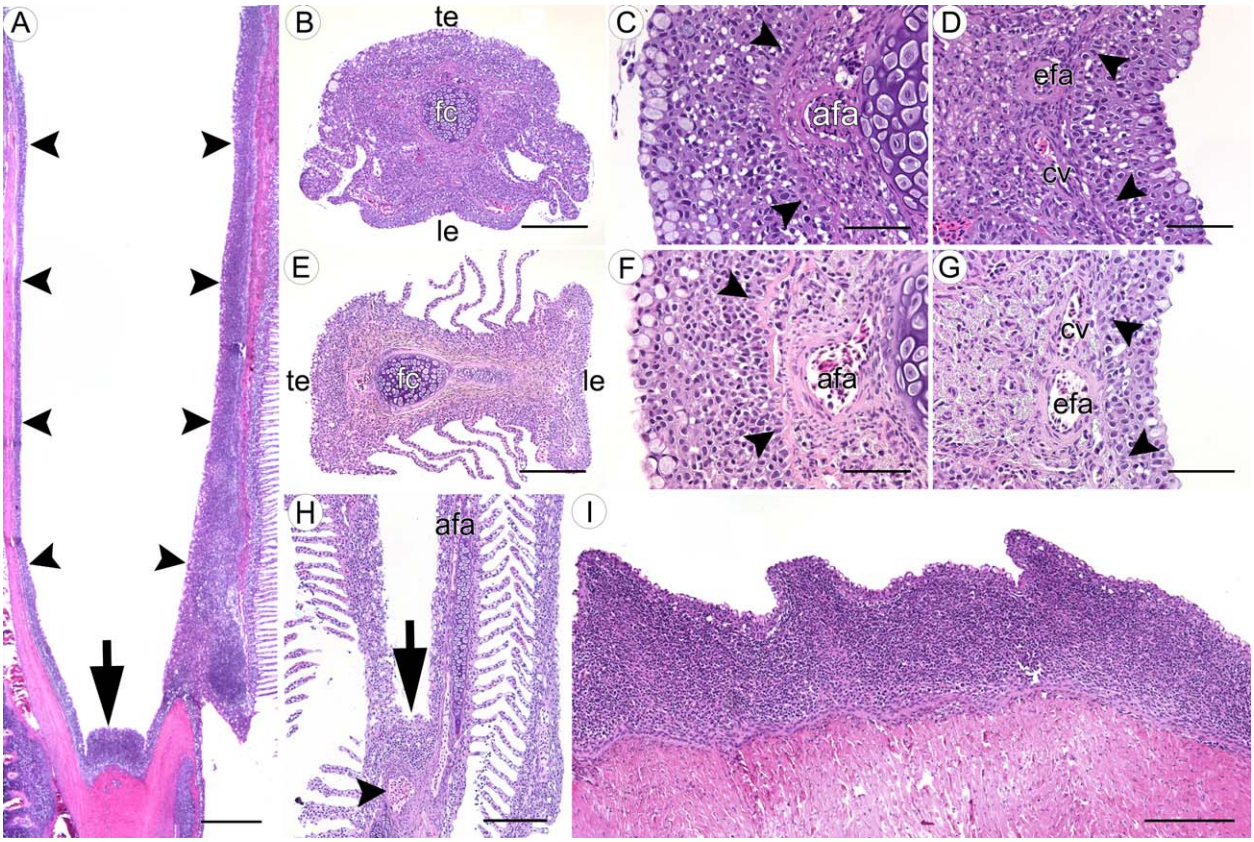

Fig. 2. Distribution of lymphoid tissue in HE stained gills: (**A**) Transverse view of the gill with the proximal ILT (arrow) and its extension along the trailing edge (arrowheads) toward the distal end of the filaments. (**B**) Overview of dorsal section of the distal end of the gill filament with higher magnification of the trailing edge (**C**) and leading edge (**D**) showing lymphoid-like cells in the gill epithelium, confined by a layer of mucous cells and a basement membrane. Note the single row of oriented epithelial cells with low nuclear density (arrowheads) covering the apical basement membrane. (**E**, **F,** and **G**) corresponds to (B, C, and D) and representing the middle part of the free filament. (**H**) Transverse section of juvenile salmon gill, depicting a less-prominent proximal ILT (arrow). Arrowhead points to afferent vascular ampulla filled with nucleated erythrocytes. (**I**) Sagittal montage of the ILT, demonstrating the large amounts of lymphoid cells confined by epithelial cell framework. Trailing edge (te), leading edge (le), filamentous cartilage (fc), afferent filamentous artery (afa), efferent filamentous artery (efa), collateral vessels (cv). (A) Scale bar = 1000 μm, (B and E) scale bar = 400 μm, (C, D, F, and G) scale bar =**=** 100 μm, (H) scale bar = 200 μm, (I) scale bar = 600 μm.

The section is perpendicular to the gill's long axis, and the seemingly different thicknesses of the epithelial framework at the right and left trailing edges demonstrated that the opposing filaments were staggered to each other. The trailing edge epithelium together with its associated lymphoid tissue was sharply delineated from the underlying tissue by a prominent basement membrane (Fig. 2C,F). Notable was the single row of oriented epithelial cells with low nuclear density covering the apical basement membrane (Fig. 2C,D,Fand G). At the leading edge and in the interlamellar space, the epithelial layer was thinner and contained far fewer intraepithelial lymphocyte-like cells (Fig. 2D,G). The ILT appeared to be more prominent in mature salmon (Fig. 2A) than in juveniles (Fig. 2H), quite the contrary to the thymus which involutes with age. Sagittal montages of the ILT demonstrated that the large mass of lymphoid cells was confined within the epithelial cell framework (Fig. 2I).

The Van Gieson method stained the basement membrane separating the ILT from underlying tissue red, revealing its collagenous nature (Fig. 3A). The collagenous part of the trailing edge basement membrane was more prominent in adults than in juveniles (data not shown). Periodic acid-methenamine silver staining indicated that only the apical brim of this membrane contained carbohydrate (Fig. 3C). This staining technique also revealed the close association of the secondary vasculature with this membrane and, thus, the distal ILT. The basement membrane at the leading edge was less prominent (Fig. 3B,D). Ovoid mucous cells with large apical secretory granules were prominent in the superficial layers of the epithelium. This mucous cell layer was distinguishable from the deeper epithelial cell layers that contained many lymphocyte-like cells. Strikingly, this mucous cell layer was more extensive at the trailing edge (Fig. 3E), compared with the other regions of the gill

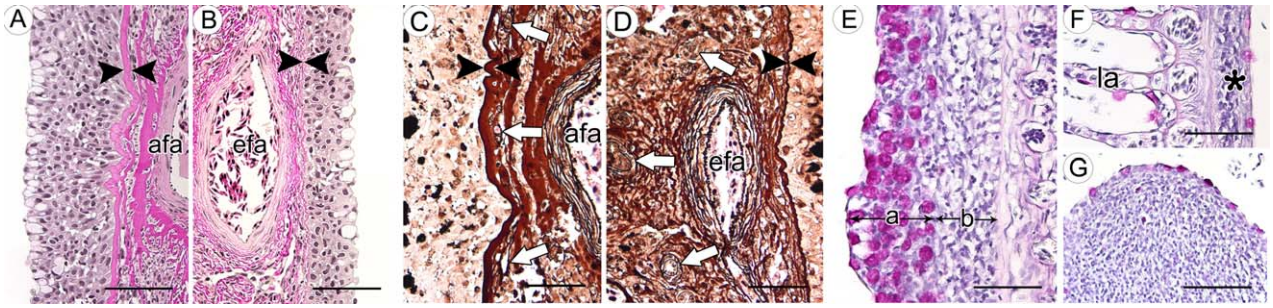

Fig. 3. Properties of the gill lymphoid tissue in mature Atlantic salmon revealed by special staining techniques. (**A**) Van Gieson staining of the proximal-filament trailing edge. Note the prominent basement membrane (bright red, arrowheads). (**B**) Corresponding proximal-filament leading edge, with a less prominent basement membrane (arrowheads). (**C**) Periodic acid-methenamine silver staining of the proximal-filament trailing edge basement membrane, staining the carbohydrate component black. White arrows indicate staining of elastic fibres associated with vessels belonging to the secondary circulation, here seen in close association with the basement membrane. (**D**) Corresponding periodic acid-methenamine silver staining of the proximal-filament leading edge. (**E**) PAS staining of the trailing edge epithelium, displaying a thick apical layer a) containing magenta-coloured mucous cells, covering a basal layer b) of epithelial cells harbouring lymphoid-like cells. (**F**) PAS staining of leading edge (asterisk) and lamellae (la). (**G**) PAS staining of the proximal ILT. Only scarce amounts of mucous cells are seen among the superficial pavement cells. Afferent filamentous artery (afa), efferent filamentous artery (efa), lamellae (la), Periodic acid-Schiff (PAS). (A, B, and E–G) scale bar = 100 μm, (C and D) scale bar = 50 μm.

epithelium, where it consisted of a single, dispersed layer bordered by pavement cells (Fig. 3F,G).

Immunohistochemistry

Labelling with a pan-T-cell marker against CD3ϵ revealed aggregation of T-cells in the proximal ILT (Fig. 4A,B) in agreement with previous investigations (Koppang et al., 2010). However, after making immunohistochemical sections of the gill in the transverse plane, we saw that the lymphoid tissue (indicated by CD3ϵ$^+$ cell staining) of the proximal ILT continued along the free gill filament all the way to its distal end (Fig. 3A). Further, dorsal sections revealed considerable numbers of T-cells both proximally (Fig. 5A,B) and distally (Fig. 6A,B) in the trailing edge filament epithelium. At the leading edge of the filament, the epithelium was thinner and fewer CD3ϵ$^+$ cells were present (Figs. 5C and 6C). At the base of the lamellae's attachment to the filament, that is, in the interlamellar space, there was generally a higher occurrence of CD3ϵ$^+$ cells toward the leading and trailing edges, compared with the middle region. These sites coincide with the outlet and return of the afferent and efferent parts of the respiratory capillary network of the lamellae (Fig. 5A). In one mature salmon with a sporadic occurrence of an epitheliocystis-like formation in the gill filament, accumulations of CD3ϵ$^+$ cells were seen in the draining region toward the leading edge and its collateral vessels, consistent with a tissue response to the upstream lesion (Fig. 4F). While the CD3ϵ$^+$ cells mostly were associated with multilayered mucosal epithelium, only modest numbers of CD3ϵ$^+$ cells were seen in the respiratory epithelium of the lamellae except in a situation associated with pathological changes (Fig. 4F).

By labelling with a pan-keratin marker (Fig. 4C), the aggregates of T-cells were shown to be intraepithelial as described for the ILT (Haugarvoll et al., 2008). Further, the mucosal epithelial tissue was shown to be continuous with the ILT both proximally toward the gill arch (data not shown), and distally through both the proximal (Fig. 5D–F) and the distal (Fig. 6D–F) free filament.

CD8α$^+$ cells also appeared in the regions that were densely populated by CD3ϵ$^+$, but in reduced numbers. CD8α$^+$ cells were present in the ILT (Fig. 4D) and both proximal- (Fig. 5G,H) and distal (Fig. 6G,H) filament trailing edges. Only few CD8α$^+$ cells were seen in the leading edge of the filament, which was also the case with CD3ϵ$^+$ cells (Figs. 5I and 6I). MHC class II$^+$ cells displayed a uniform distribution throughout the epithelium of the ILT (Fig. 4E), the whole free filaments (Figs. 5J–L and 6J–L) and in the respiratory lamellas (Figs. 5J and 6J). Only a few cells stained positive with the immunoglobulin (Ig) marker, and these were observed primarily in the interlamellar region (Fig. 4G). Very few immune-related cells were seen in the tissue beneath the basement membrane with our panel of molecular markers, though occasional CD3ϵ$^+$ cells were identified.

Scanning Electron Microscopy on Gill Vascular Casting

Scanning electron microscopy of a vascular cast from the trailing edge showed that the afferent filament artery (afa) gave rise to large diameter afferent lamellar arterioles (ala) leading to capillaries of the respiratory lamellae (rl) (Fig. 7F). The vascular cast also showed the close association of the secondary circulation of the gill with the trailing edge (Fig. 7F).

Gene Expression

The examined gene transcripts can easily be divided into three main groups covering T-cell,

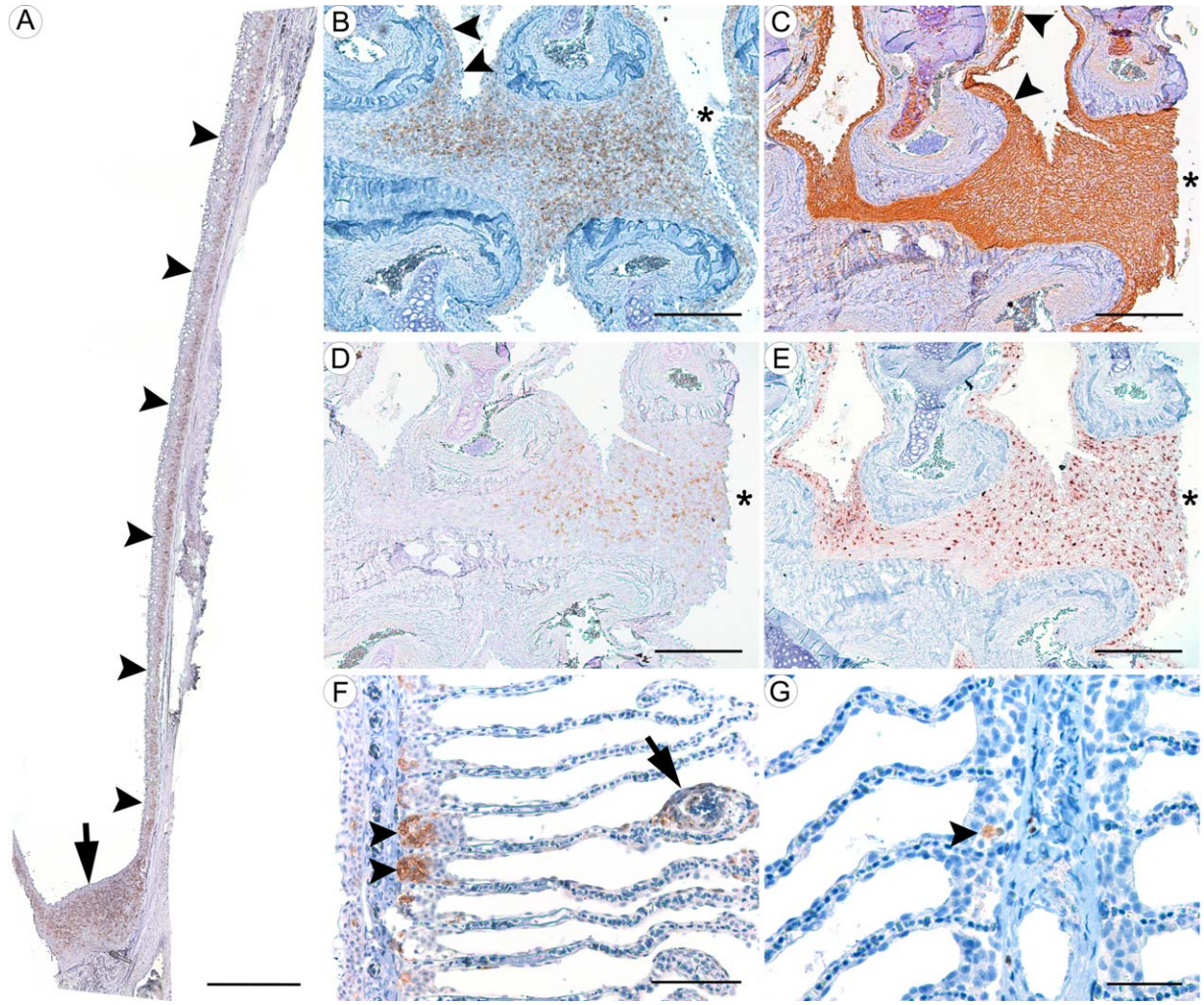

Fig. 4. Immunohistochemistry from the proximal ILT of mature Atlantic salmon. (**A**) Transverse montage of the ILT (arrow) and its continuation throughout the trailing edge (arrowheads), showing aggregation of CD3ϵ^{+}-cells (brown) in the epithelium. (**B–E**) represents sections of the proximal ILT in the dorsal plane (asterisk = apical surface toward the interbranchial cleft) stained against CD3ϵ, cytokeratin, CD8α, and MHC class II, respectively. (**F**) Inflicted damage (arrow) on lamellar tissue resulting in a downstream aggregation of CD3ϵ^{+}-cells (brown, arrowheads) near the efferent lamellar arteriolar- and collateral vessels of the leading edge. The overlying mucosa is displaced by the presence of lymphoid tissue. (**G**) Secretory immunoglobulin-positive cells (brown) were seen in very limited amounts mostly in the interlamellar area (arrowhead). (A) Scale bar = 800 μm, (B–E) scale bars = 400 μm, (F) scale bar = 200 μm, (G) scale bar = 50 μm.

B-cell immunoglobulins, and recombination activation genes (RAG) involved in both T and B cell development (Fig. 8). Using quantitative real time PCR analysis, all T-cell markers except *CD4-2a* displayed generally higher transcript levels in the gills and thymus of juvenile fish than of adult fish. And as expected, this expression was higher in the thymus of the juveniles. The most prominent and significant difference between thymus and the other tissues was observed for *CD8*α ($P < 0.05$) and -β ($P < 0.01$) in the juveniles. In addition, a significant shift in *CD8*α/*CD8*β ratio ($P < 0.05$) from around 0.8 in the gill tissues and head kidney to 0.22 in the thymus was seen in this group (Fig. 9), which suggests the presence of a CD8αα-subset in the former tissues. In the juveniles, there were no significant differences in relative gene expression between the filaments and the region including the proximal ILT for the selected genes. In the adults, the expressions of *CD8*α and –β were significantly higher in the region including the proximal ILT compared with other parts of the filaments ($P < 0.05$). The expression of most T-cell markers in the thymus decreased with maturation, supporting a less prominent role for the thymus with age. The head kidney, which represents a combined primary and secondary lymphoid organ maintained, and for some markers increased, the T-cell expression level with age as opposed to the gill and thymus. Overall for both life stages, the *CD4-2a* expression was generally higher than *CD8*-related genes in the gills and head kidney (juveniles: $P < 0.01$). While

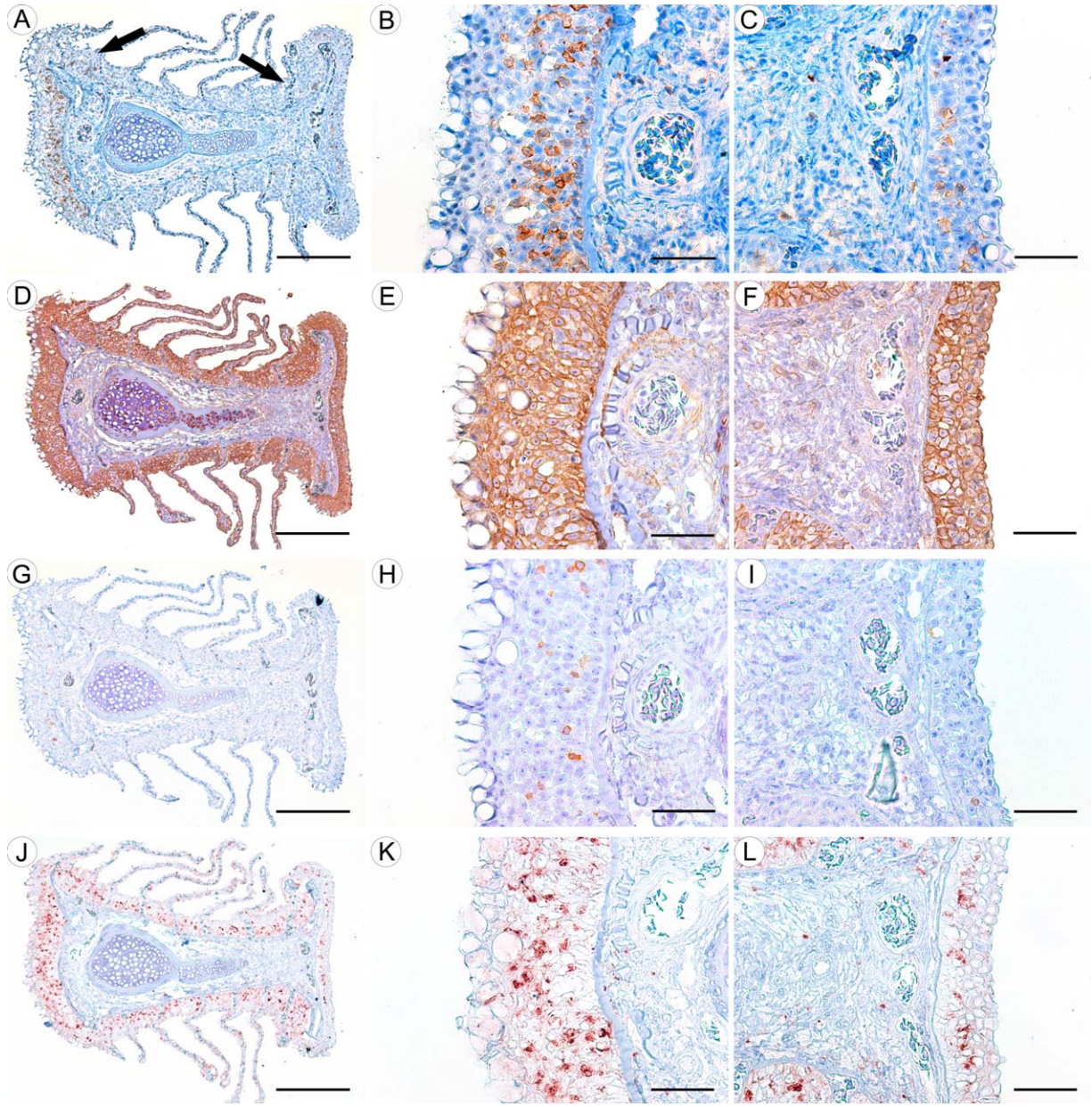

Fig. 5. Immunohistochemistry from the middle part of the free end of the gill filament in mature Atlantic salmon; trailing edge to the left, leading edge to the right. (**A**) Abundant amounts of CD3ε^{+}-cells (brown) predominantly located at the trailing edge of the gill filament, while there are scattered occurrences at the interlamellar space and at the leading edge. In the interlamellar space, highest occurrence is seen close to trailing- and especially leading edge (arrows). (**B**) Higher magnification of trailing edge; the CD3ε^{+}-cells are essentially located at the base of the mucosal epithelium, clearly delineated by the underlying extensive basement membrane. (**C**) Higher magnification of leading edge; thinner mucosal lining with fewer CD3ε^{+}-cells and a less prominent basement membrane. (**D**) Cytokeratin labelling (brown) of epithelial cells forming a framework for the residing lymphoid cells, organised as multilayered tissue at the base of the filament and changing into single layer at the lamellae. (**E**) and (**F**) show higher magnification of the trailing and leading edge, respectively, with trabecular processes surrounding unstained cells of lymphoid morphology. (**G**) Scarce amounts of CD8α^{+}-cells (brown) compared with CD3ε^{+}-cells, implying a heterogenous composition among gill intraepithelial T lymphocytes. (**H**) Most CD8α^{+}-cells are located at the trailing edge, while the leading edge contains few CD8α^{+}-cells (**I**). (**J**) Large quantities of MHC class II^{+}-cells (red) scattered throughout the epithelial tissue of the gills. (**K**) and (**L**) Higher magnification of MHC class II^{+}-cells at the trailing and leading edge, respectively. (A, D, G and J) scale bar = 400 μm. (B, C, E, F, H, I, K, and L) scale bar = 100 μm.

the expression level of *CD4-2a* increased with age, a reduction was seen for *CD8*-related genes.

As expected, the head kidney showed the highest expression levels for *IgM* and *IgT*. There was a higher immunoglobulin expression in the gill tissues of adults than of juveniles and this higher expression was significant for *IgM* ($P < 0.05$) (Fig. 8). In the juveniles, the ratio of *IgM* versus *IgT* was

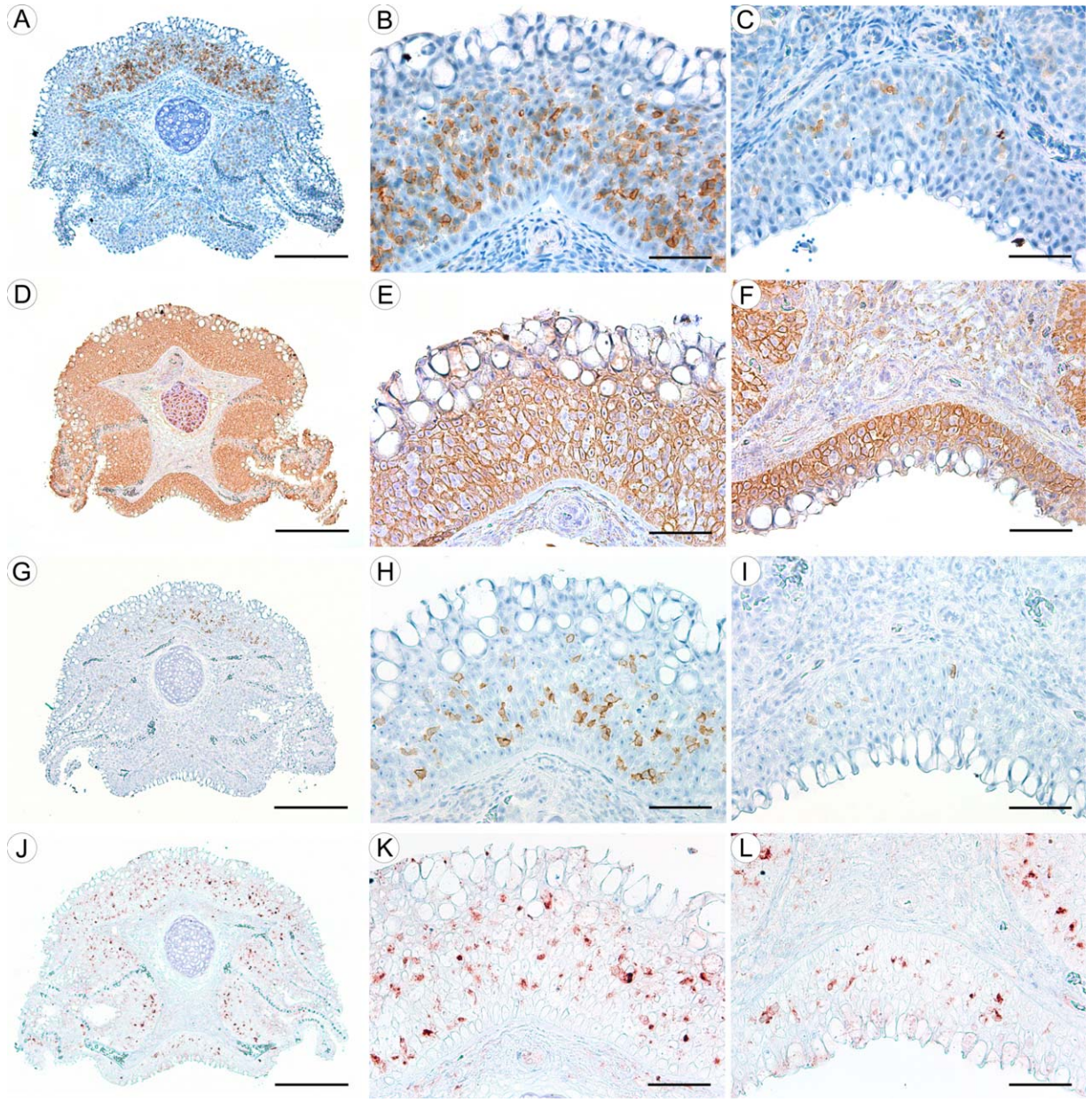

Fig. 6. Immunohistochemistry from the distal part of the free end of the gill filament in mature Atlantic salmon; trailing edge upward, leading edge downward. (**A**) Abundant amounts of CD3ε^{+}-cells (brown) predominantly located at the trailing edge of the gill filament. (**B**) Higher magnification of trailing edge. (**C**) Higher magnification of leading edge; thinner mucosal lining with fewer CD3ε^{+}-cells and a less prominent basement membrane. (**D**) Cytokeratin labelling (brown) of epithelial cells shows the epithelial framework for cells with lymphoid-like morphology. (**E**) and (**F**) show higher magnification of the trailing and leading edge, respectively. (**G**) Scarce amounts of CD8α^{+}-cells (brown) compared with CD3ε^{+}-cells. (**H**) Most CD8α^{+}-cells are located at the trailing edge, while the leading edge contains few CD8α^{+}-cells (**I**). (**J**) MHC class II^{+}-cells (red) scattered throughout the mucosal epithelial tissue of the gills. (**K**) and (**L**) Higher magnification of MHC class II^{+}-cells at the trailing and leading edge, respectively. (A, D, G, and J) scale bar = 400 μm. (B, C, E, F, H, I, K, and L) scale bar = 100 μm.

significantly higher in the head kidney compared with the other organs investigated ($P < 0.001$) (Fig. 9). In the adults this ratio was reduced and became more in line with the rest of the examined organs.

As expected for *RAG-1* and *-2*, strongest expression was observed in the thymus of the juveniles (average Ct-value 27.7 ± 4.6). By defining a threshold of Ct 37, *RAG-2* showed positive values for all tissues examined. In the adults, all tissues investigated were evaluated as *RAG-1* negative. In the juvenile group, a low level of *RAG-1* expressions was detected in the head kidney of all individuals (average Ct-value 30.6 ± 3.7) and in addition, in the gill filaments and ILT-regions of three of six individuals (Ct values ranging from 31.0 to 36.8).

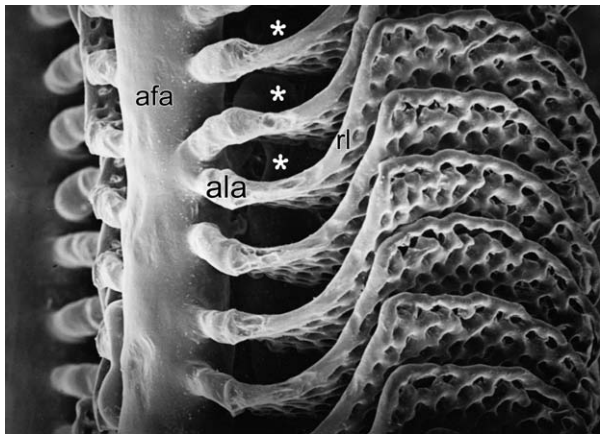

Fig. 7. Scanning electron microscopic image of a vascular cast of the afferent filament artery (afa) giving rise to the large diameter afferent lamellar arterioles (ala) and further the capillaries of the respiratory lamellae (rl), all parts of the arterioarterial circulation of the gills. Note the ruffled surface of the afferent lamellar arterioles. Interlamellar and nutritive vessels, parts of the arteriovenous circulation of the gills, are seen under the respiratory lamellae (asterisks).

DISCUSSION

The fish gill is a major site of physiological interaction between the organism and its surroundings, but the immunological context for this interaction is not well understood. The recent description of the ILT as a lymphoid organ residing in the interbranchial cleft throughout all four paired gill arches has drawn attention to the immune apparatus protecting the gills (Haugarvoll et al., 2008; Koppang et al., 2010). The continuation and elongation of the ILT into the free filaments has not been examined previously. In this article, we show that the intraepithelial lymphoid tissue of the ILT extends to the end of the trailing edge in both axial and abaxial filaments throughout the gill. To distinguish the two parts, the elongation has been named the distal ILT, while the already-described portion located at the very terminal end of the interbranchial septum, is referred to as the proximal ILT. Further, the border between the proximal and distal ILT is suggested to be set as a horizontal line intersecting the elevation of the middle part of the proximal ILT. Both the proximal and distal ILT share the same morphological and immunohistochemical properties, representing a diffuse mucosal lymphoid tissue with no attributes of organized MALT. Given the wide distribution of the newly described lymphoid tissue, this finding demonstrates that gill lymphoid tissue is a more prominent component of the Atlantic salmon immune system than previously considered.

The ILT consists of a continuous network of epithelial cells incorporating a large population of mainly T-cells. This T-cell accumulation is limited basally by a distinct basement membrane and apically by an epithelium containing varying numbers

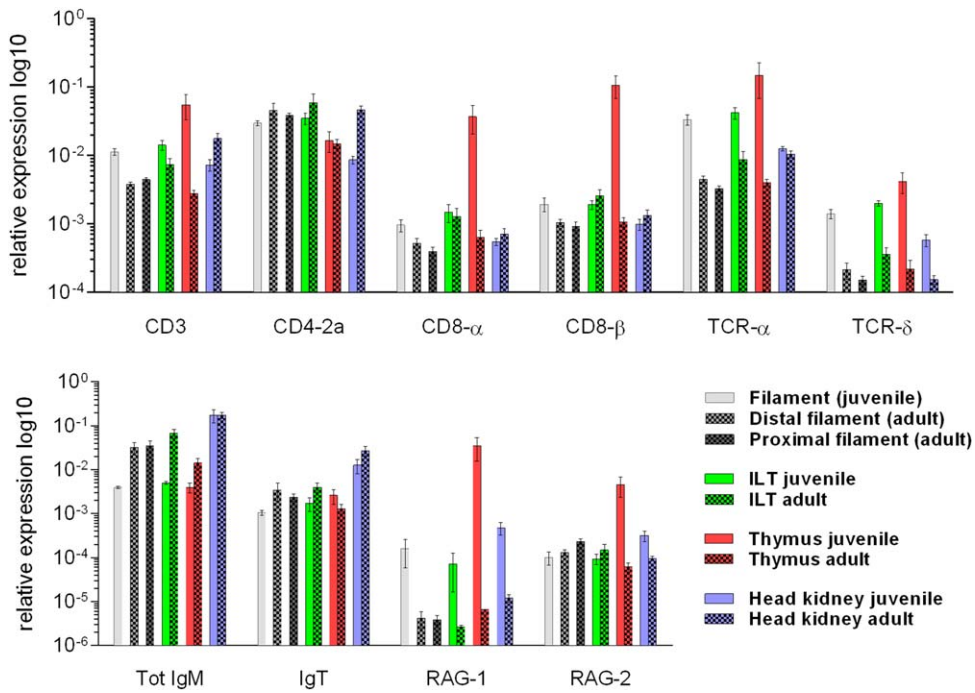

Fig. 8. RT-qPCR results from juvenile and mature fish. In essence, the only statistical difference ($P < 0.05$) in expression between the ILT containing area and the filaments were seen for *CD8α and CD8β* in the mature fish. Cluster of differentiation, CD; T-cell receptor, TCR; immunoglobulin, Ig; recombination activating gene, RAG. Error bars represent standard error of the mean (SEM) and transcript levels are presented relative to $EF1A_B$.

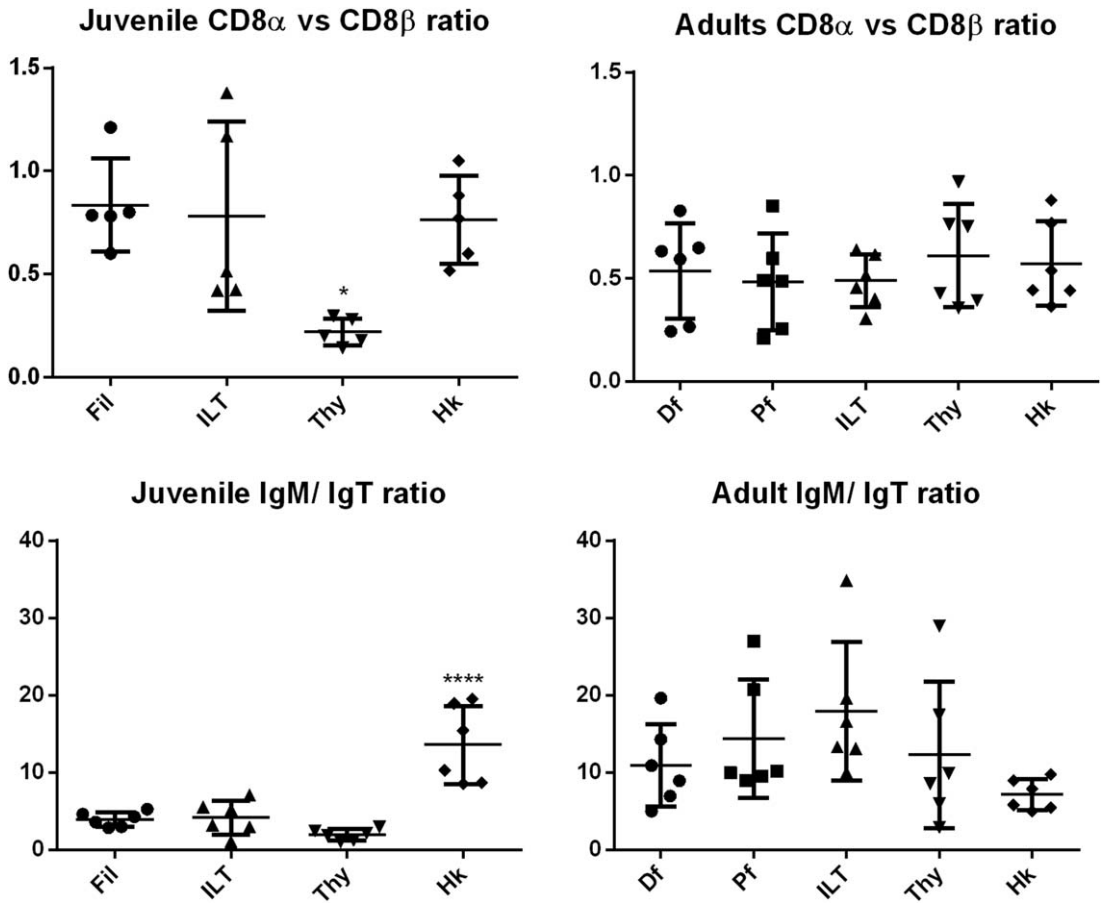

Fig. 9. Comparison of gene expression ratios between selected genes in juvenile and mature Atlantic salmon. The expression ratio *CD8α/CD8β* is significantly ($P < 0.05$) higher in the thymus of juveniles compared with both the gills and the head kidney. The *IgM/IgT* ratio in the head kidney of juvenile fish compared with other tissues is significantly higher ($P < 0.001$). This is, however, not the case in adults. Filament, Fil; distal filament, Df; proximal filament, Pf; interbranchial lymphoid tissue, ILT; thymus, Thy; head kidney, Hk; cluster of differentiation, CD; immunoglobulin, Ig.

of dispersed mucous cells. The immunohistochemical investigation showed that within these boundaries, $CD8^+$- and $CD3^+$ T-cells were distributed throughout the epithelial tissue in both life stages. This qualitative observation was confirmed quantitatively in the juvenile gill by gene expression analysis. In the adult gill there was a significantly higher expression of CD8α and CD8β in the proximal ILT compared with the filament, which may imply that this T-cell subset is more prominent in the former region in adult fish. Taking into account the increased size of the proximal ILT following maturation, this could imply a differentiation and specialization of the ILT-complex with age. It is also worth noting that only nondiseased gills were investigated, and this difference may be altered during immunological stimulation. The slightly lowered gene expression level of the pan T-cell molecule CD3 in mature individuals contradicted the apparent increase in $CD3^+$ cells as inferred from immunohistochemistry. This might be due to accidental imprecision during tissue sampling, in that the macrodissected samples that were used to measure transcript levels could have contained some surrounding tissue. It is also possible that the lack of significant upregulation of CD3ζ-mRNAs, which was surprising considering the positive immunostaining of the CD3ε chain, may be due to the dynamics of transcription and translation of the CD3 molecules.

The plasticity of the proximal ILT has previously been described during both infectious salmon anaemia virus- (ISAV; Hetland et al., 2010; Hetland et al., 2011) and parasitic *Ichthyophthirius multifiliis* theront (Olsen et al., 2011) infection, with depletion of $CD8\alpha^+$ cells from this tissue reported in both cases. In two different challenge experiments, Austbø et al. (2014) and Aas et al. (2014) indicated a size reduction of this part of the tissue during ISAV infection. Interestingly, it was shown that Atlantic salmon surviving an ISAV infection had their ILT repopulated by $CD8\alpha^+$ T-cells (Hetland et al., 2011). Whether the suggested distal ILT show the same plasticity during immunological stimulation remains to be investigated.

Altogether, the ILT's responsiveness during immunological stimulation clearly points toward a tissue of secondary lymphoid character. In this work, the presence of *Rag-1* and *Rag-2* expression was investigated. Together these proteins are decisive for the somatic V(D)J-rearrangement maturation of B- and T-lymphocytes (Oettinger, 1992; Schatz et al., 1992) and may therefore be used as indicators of primary lymphoid tissue (Hansen and Kaattari, 1995; Hansen, 1997). In the adults, all tissues investigated were evaluated as negative for *Rag-1* including the thymus. Lack of *Rag-1* expression in the proximal ILT and free gill filaments is in accordance with previous findings (Aas et al., 2014). However, in addition to the expected expression in the thymus of all juveniles, three individuals were evaluated as weakly positive for both *Rag-1 and -2* expressions in the gills. One could speculate on whether this finding is a remnant of a primary immunological function of the ILT-complex present at an earlier age.

Intraepithelial lymphocytes have been described in numerous tissues in a broad phylogenetic range of animals. These lymphocyte populations, primarily T-cells with potent cytolytic and immune-regulatory capacities, contribute to sustaining epithelial integrity (Hayday et al., 2001). Most mammalian intraepithelial lymphocytes are $CD8^+$ T-cells with the majority belong to the homodimeric CD8αα form expressing γδ TCR (Pabst et al., 2005), although large intraspecies and interspecies variations exist (Cesta, 2006). By calculating the *CD8α/CD8β* –expression ratio, a significantly higher level of *CD8α*- expression was seen in the gills and the head kidney compared with the thymus. This observation indicates the presence of a CD8αα T-cell subset in Atlantic salmon. Using a monoclonal marker against CD8α, which is present in both homodimers (CD8αα) and heterodimers (CD8αβ) of cytotoxic T-cells, we found that $CD8\alpha^+$ cells constituted only a fraction of the $CD3\epsilon^+$ cells seen in the ILT. This is in accordance with Takizawa et al. (2011), who estimated that approximately 25% of the total lymphocyte population in the gill of rainbow trout (*Oncorhynchus mykiss*) belonged to the $CD8\alpha^+$ subset, and that the remaining $CD8\alpha^-$ lymphocytes yielded a high expression of *CD4*-related genes. Just as CD8 defines the cytotoxic T-cell subset, CD4 is a major T-cell marker defining the helper T-cell subset. In Atlantic salmon, *CD4* exists as two homologues, namely *CD4-1* and *CD4-2*, whereof *CD4-2* is further divided into two subtypes, *CD4-2a* and *-2b* (Moore et al., 2009). In our study, the analysis of *CD4-2a* was selected due to its dominant expression level compared with *CD4-2b* and *CD4-1* (Moore et al., 2009). We found that the expression level of *CD4-2a* in general was several times that of both *CD8α* and *–β* in all gill tissues investigated. Thus, presumably the rest of the $CD3\epsilon^+$ population belonged to the CD4 T-cell subset residing in a MHC class II-rich environment. Also, while the expression of the other T-cell markers in general decreased with age, the expression of *CD4-2a* remained relative constant within the gill tissue investigated. Unfortunately, an antibody directed against CD4 positive T-cells in salmon has been difficult to obtain. The occurrence of double-negative T-cells ($CD3^+$-$CD4^-CD8^-$ T-cells), a subset known to contribute to inflammation, immune-regulation and autoimmunity in man, mice, and rats (D'Acquisto and Crompton, 2011), cannot, however, be ruled out.

The intraepithelial lymphoid aggregations were found to be more extensive at the trailing edge of the free filament, compared with the leading edge and the interlamellar space. A reason for this could be that the retention time of water is longer and the mixing more extensive in this region, enabling a more intimate interaction between water and the gill mucosa than in other regions of the filament. This is in agreement with airway-associated lymphoid tissue in mammals, which is predominantly positioned at branching sites (Cesta, 2006). Another interesting feature is the thick layer of stratified mucous cells at the surface of the trailing edge epithelium, and the conspicuous, sharp transition to a single layer of dispersed mucous cells bounded by pavement cells at the surface of the proximal ILT. It has been suggested that the mucous cells are associated with the generation of a protective, laminar water flow, although it might also enable the absorption of pollutants and pathogenic agents (Monteiro et al., 2010). Stratified epithelium, rich in intraepithelial lymphocytes as found in mammalian larynx- and bronchus-associated lymphoid tissue, has fewer goblet cells and a more heterogeneous lymphocyte population than surrounding tissue. While the latter contains mostly CD8 T-lymphocytes, the former consists of both CD4- and CD8 T-lymphocytes together with B-lymphocytes (Gebert and Pabst, 1999). As some of the same pattern is seen in the proximal ILT, this might indicate a role in antigen sampling and immune surveillance.

The lack of vascularisation of the proximal ILT has previously been described (Haugarvoll et al., 2008; Aamelfot et al., 2013), and transverse sections of the gills seemed to show no connection between the ILT and blood vessels. This finding is consistent with the intraepithelial localisation of the organ. However, on examination in the dorsal plane, a close association between the intraepithelial lymphoid cells of the distal ILT and the afferent arterioles leading to the respiratory lamellar capillaries was evident. This close association was present from the level above the proximal ILT and throughout the gill filament, and could represent the site at which T-cells migrate between the ILT and other tissues. Also, the location of a lymphocyte reservoir at the trailing edge is in this regard

very strategic, as recruitment to the exposed and vulnerable respiratory capillaries would be fast and efficient. As viewed on the SEM vascular cast, the ala that connect with the respiratory capillaries of the lamellae have a large luminal diameter with a ruffled endothelium that could facilitate the passage of cells. However, the gill secondary circulatory system, which is a part of the arteriovenous circulation of the gill, has also been proposed as the connection between mucosal-and systemic immunity (Rasmussen et al., 2013). This system is an elaborate, low-flow, large-volume network of thin-walled vessels sharing many anatomical attributes with mammalian lymphatic capillaries. In particular, these vessels have been described as continuing around the afferent border (trailing edge) of the gill filament (Olson, 2002) and to be in close proximity with the exposed epithelium (Olson, 1996) and, thus, the distal ILT. This proximity was clearly demonstrated with the periodic acid-methenamine silver staining. Since these vessels seldom contain erythrocytes, their function is still a matter of debate and the functional connection of the interlamellar vessels with the seemingly well-confined lymphoid intraepithelial tissue remains to be demonstrated. Nevertheless, the continuation of the proximal ILT into the distal ILT along the filaments facilitates a close association with the circulatory system, and this feature might be crucial to understanding the function of the ILT.

In contrast to the thymus, which is a phylogenetic constant site of T-cell differentiation, the location of primary B-cell lymphopoiesis varies greatly among different species and their developmental stages (Boehm and Bleul, 2007). In posthatched teleosts, the head kidney is regarded as the site of primary B-cell lymphopoiesis (Hansen and Zapata, 1998). Under normal conditions, the lymphoid tissue of the gill appears to harbour few Ig^+ positive cells (Koppang et al., 2010). This was also the situation for IgM in this study. Staining for IgT was not conducted due to lack of an appropriate marker, but the gene expression study revealed a higher expression of *IgM* compared with *IgT*, a difference that increased with age as inferred from the *IgM*/*IgT*-ratio. This ratio became more variable with age. Interestingly, during an ISAV infection study conducted by Austbø et al. (2014), the expression of *IgT* was shown to increase during the late disease stage, suggesting a possible clonal expansion and affinity maturation. This is in accordance with IgT being an immunoglobulin class specialized in mucosal immunity (Zhang et al., 2010), and it has been shown that IgT antibodies and IgT^+ B cells have a predominant role in the gut-, skin- (Salinas et al., 2011) and newly discovered nasopharynx-associated lymphoid tissue (Tacchi et al., 2014). However, as noted by Salinas et al. (2011), considerable work remains in describing the distribution and immunological importance of the B-cell population in the gills. Thus, further studies on the distribution of B-cells and in particularly IgT bearing cells with regard to the ILT are, therefore, warranted.

This study presents a detailed morphological characterisation of lymphoid tissue in the free gill filament of the Atlantic salmon. Aggregates of T-cells were found to be present in the thick epithelial lining of the trailing edge of the filament in considerably larger amounts than seen in other parts of the free filament. By demonstrating a continuity of this lymphoid tissue beyond the previously described proximal ILT, we argue that the concept of the ILT must be extended to include the intraepithelial lymphoid tissue of the gill filament, which should be called the distal ILT. Due to its close association with vascular networks, the distal ILT may provide routes of communication with the systemic circulation and, thus, provide clues to the function and dynamics of the ILT. Altogether, the findings of this study provide important and fundamental knowledge of the gill as an essential immune organ of the Atlantic salmon.

ACKNOWLEDGMENTS

The authors are very grateful to the Sport Fishermen's Club at Hellefossen, Drammenselva, Norway, for providing wild salmon. The authors thank Mrs. Elin Valen and Mr. Emil Kristian Westad for invaluable laboratory assistance, both from the Norwegian University of Life Sciences.

LITERATURE CITED

Aamelfot M, Weli SC, Dale OB, Koppang EO, Falk K. 2013. Characterisation of a monoclonal antibody detecting Atlantic salmon endothelial and red blood cells, and its association with the infectious salmon anaemia virus cell receptor. J Anat 222:547–557.

Aas IB, Austbø L, König M, Syed M, Falk K, Hordvik I, Koppang EO. 2014. Transcriptional characterization of the T cell population within the salmonid interbranchial lymphoid tissue. J Immunol 193:3463–3469.

Austbø L, Aas IB, König M, Weli SC, Syed M, Falk K, Koppang EO. 2014. Transcriptional response of immune genes in gills and the interbranchial lymphoid tissue of Atlantic salmon challenged with infectious salmon anaemia virus. Dev Comp Immunol 45:107–114.

Bajoghli B, Guo P, Aghaallaei N, Hirano M, Strohmeier C, McCurley N, Bockman DE, Schorpp M, Cooper MD, Boehm T. 2011. A thymus candidate in lampreys. Nature 470:90–94.

Bancroft JD, Gamble M. 2008. Theory and Practice of Histological Techniques Philadelphia: Churchill Livingstone/Elsevier.

Boehm T, Bleul CC. 2007. The evolutionary history of lymphoid organs. Nat Immunol 8:131–135.

Cesta MF. 2006. Normal structure, function, and histology of mucosa-associated lymphoid tissue. Toxicol Pathol 34:599–608.

D'Acquisto F, Crompton T. 2011. Cd3+CD4-CD8- (double negative) T cells: Saviours or villains of the immune response? Biochem Pharmacol 82:333–340.

Evans DH, Piermarini PM, Choe KP. 2005. The multifunctional fish gill: Dominant site of gas exchange, osmoregulation, acid-base regulation, and excretion of nitrogenous waste. Physiol Rev 85:97–177.

Fischer U, Koppang EO, Nakanishi T. 2013. Teleost T and NK cell immunity. Fish Shellfish Immunol 35:197–206.
Gebert A, Pabst R. 1999. M cells at locations outside the gut. Semin Immunol 11:165–170.
Hansen JD. 1997. Characterization of rainbow trout terminal deoxynucleotidyl transferase structure and expression. TdT and RAG1 co-expression define the trout primary lymphoid tissues. Immunogenetics 46:367–375.
Hansen JD, Kaattari SL. 1995. The recombination activation gene 1 (rag1) of rainbow trout (*Oncorhynchus mykiss*): Cloning, expression, and phylogenetic analysis. Immunogenetics 42:188–195.
Hansen JD, Zapata AG. 1998. Lymphocyte development in fish and amphibians. Immunol Rev 166:199–220.
Haugarvoll E, Bjerkås I, Nowak BF, Hordvik I, Koppang EO. 2008. Identification and characterization of a novel intraepithelial lymphoid tissue in the gills of Atlantic salmon. J Anat 213:202–209.
Hayday A, Theodoridis E, Ramsburg E, Shires J. 2001. Intraepithelial lymphocytes: Exploring the third way in immunology. Nat Immunol 2:997–1003.
Hetland DL, Jørgensen SM, Skjødt K, Dale OB, Falk K, Xu C, Mikalsen AB, Grimholt U, Gjøen T, Press CM. 2010. In situ localisation of major histocompatibility complex class I and class II and CD8 positive cells in infectious salmon anaemia virus (ISAV)-infected Atlantic salmon. Fish Shellfish Immunol 28:30–39.
Hetland DL, Dale OB, Skjødt K, Press CM, Falk K. 2011. Depletion of CD8 alpha cells from tissues of Atlantic salmon during the early stages of infection with high or low virulent strains of infectious salmon anaemia virus (ISAV). Dev Comp Immunol 35:817–826.
Hughes GM. 1984. General anatomy of the gills. In: Hoar WS, Randall DJ, editors. Fish Physiology. New York: Academic Press. pp 1–63.
Kasahara M, Sutoh Y. 2014. Two forms of adaptive immunity in vertebrates: Similarities and differences. Adv Immunol 122:59–90.
Koppang EO, Fischer U, Moore L, Tranulis MA, Dijkstra JM, Köllner B, Aune L, Jirillo E, Hordvik I. 2010. Salmonid T cells assemble in the thymus, spleen and in novel interbranchial lymphoid tissue. J Anat 217:728–739.
Koppang EO, Hordvik I, Bjerkås I, Torvund J, Aune L, Thevarajan J, Endresen C. 2003. Production of rabbit antisera against recombinant MHC class II beta chain and identification of immunoreactive cells in Atlantic salmon (Salmo salar). Fish Shellfish Immunol 14:115–132.
Løkka G, Austbø L, Falk K, Bromage E, Fjelldal PG, Hansen T, Hordvik I, Koppang EO. 2014. Immune parameters in the intestine of wild and reared unvaccinated and vaccinated Atlantic salmon (Salmo salar L.). Dev Comp Immunol 47:6–16.
Matsunaga T, Rahman A. 2001. In search of the origin of the thymus: The thymus and GALT may be evolutionarily related. Scand J Immunol 53:1–6.
Monteiro SM, Oliveira E, Fontainhas-Fernandes A, Sousa M. 2010. Fine structure of the branchial epithelium in the teleost *Oreochromis niloticus*. J Morphol 271:621–633.
Moore LJ, Dijkstra JM, Koppang EO, Hordvik I. 2009. CD4 homologues in Atlantic salmon. Fish Shellfish Immunol 26: 10–18.
Oettinger MA. 1992. Activation of V(D)J recombination by RAG1 and RAG2. Trends Genet 8:413–416.
Olsen MM, Kania PW, Heinecke RD, Skjøedt K, Rasmussen KJ, Buchmann K. 2011. Cellular and humoral factors involved in the response of rainbow trout gills to *Ichthyophthirius multifiliis* infections: Molecular and immunohistochemical studies. Fish Shellfish Immunol 30:859–869.
Olson KR. 1996. Secondary circulation in fish: Anatomical organization and physiological significance. J Exp Zool 275:172–185.
Olson KR. 2002. Vascular anatomy of the fish gill. J Exp Zool 293:214–231.
Olsvik PA, Lie KK, Jordal AE, Nilsen TO, Hordvik I. 2005. Evaluation of potential reference genes in real-time RT-PCR studies of Atlantic salmon. BMC Mol Biol 17:6–21.
Pabst O, Herbrand H, Worbs T, Friedrichsen M, Yan S, Hoffmann MW, Korner H, Bernhardt G, Pabst R, Forster R. 2005. Cryptopatches and isolated lymphoid follicles: Dynamic lymphoid tissues dispensable for the generation of intraepithelial lymphocytes. Eur J Immunol 35:98–107.
Rasmussen KJ, Steffensen JF, Buchmann K. 2013. Differential occurrence of immune cells in the primary and secondary vascular systems in rainbow trout, *Oncorhynchus mykiss* (Walbaum). J Fish Dis 36:675–679.
Rombout JH, Huttenhuis HB, Picchietti S, Scapigliati G. 2005. Phylogeny and ontogeny of fish leucocytes. Fish Shellfish Immunol 19:441–455.
Salinas I, Zhang YA, Sunyer JO. 2011. Mucosal immunoglobulins and B cells of teleost fish. Dev Comp Immunol 35:1346–1365.
Schatz DG, Oettinger MA, Schlissel MS. 1992. V(D)J recombination: Molecular biology and regulation. Annu Rev Immunol 10:359–383.
Tacchi L, Musharrafieh R, Larragoite ET, Crossey K, Erhardt EB, Martin SA, LaPatra SE, Salinas I. 2014. Nasal immunity is an ancient arm of the mucosal immune system of vertebrates. Nature Communications 5:5205.
Takizawa F, Dijkstra JM, Kotterba P, Korytar T, Kock H, Köllner B, Jaureguiberry B, Nakanishi T, Fischer U. 2011. The expression of CD8alpha discriminates distinct T cell subsets in teleost fish. Dev Comp Immunol 35:752–763.
Varga I, Pospíšilová V, Gmitterová K, Gálfiová P, Polák Š, Galbavý Š. 2008. The phylogenesis and ontogenesis of the human pharyngeal region focused on the thymus, parathyroid, and thyroid glands. Neuro Endocrinol Lett 29:837–845.
Wilson JM, Laurent P. 2002. Fish gill morphology: Inside out. J Exp Zool 293:192–213.
Zapata A, Amemiya CT. 2000. Phylogeny of lower vertebrates and their immunological structures. Curr Top Microbiol Immunol 248:67–107.
Zhang YA, Salinas I, Li J, Parra D, Bjork S, Xu Z, LaPatra SE, Bartholomew J, Sunyer JO. 2010. IgT, a primitive immunoglobulin class specialized in mucosal immunity. Nat Immunol 11:827–835.

II

Fish & Shellfish Immunology 58 (2016) 153–164

Contents lists available at ScienceDirect

Fish & Shellfish Immunology

journal homepage: www.elsevier.com/locate/fsi

Full length article

Morphological and functional development of the interbranchial lymphoid tissue (ILT) in Atlantic salmon (*Salmo salar* L)

Alf Seljenes Dalum [a, *], David James Griffiths [a], Elin Christine Valen [a], Karoline Skaar Amthor [b], Lars Austbø [a], Erling Olaf Koppang [a], Charles McLean Press [a], Agnar Kvellestad [a]

[a] Department of Basic Sciences and Aquatic Medicine, Faculty of Veterinary Medicine and Biosciences, Norwegian University of Life Sciences, Oslo, Norway
[b] LetSea Helgeland Havbruksstasjon AS, Sandnessjøen, Norway

ARTICLE INFO

Article history:
Received 26 April 2016
Received in revised form
27 August 2016
Accepted 11 September 2016
Available online 12 September 2016

Keywords:
Ontogeny
Proliferative T-cells
Diffuse MALT
Thymus
Leucocyte trafficking
Gill-associated lymphoid tissue
Stereology

ABSTRACT

The interbranchial lymphoid tissue (ILT) of Atlantic salmon originates from an embryological location that in higher vertebrates gives rise to both primary and secondary lymphoid tissues. Still much is unknown about the morphological and functional development of the ILT. In the present work a standardized method of organ volume determination was established to study its development in relation to its containing gill and the thymus. Based on morphological findings and gene transcription data, the ILT shows no signs of primary lymphoid function. In contrast to the thymus, an ILT-complex first became discernible after the yolk-sac period. After its appearance, the ILT-complex constitutes 3–7% of the total volume of the gill (excluding the gill arch) with the newly described distal ILT constituting a major part, and in adult fish it is approximately 13 times larger than the thymus. Confined regions of T-cell proliferation are present within the ILT. Communication with systemic circulation through the distal ILT is also highly plausible thus offering both internal and external recruitment of immune cells in the growing ILT.

1. Introduction

The interbranchial lymphoid tissue (ILT) of Atlantic salmon (*Salmo salar* L.) is an extensive intraepithelial accumulation of lymphocytes at the end of the interbranchial septum (proximal ILT; pILT) [1,2] extending distally throughout the trailing edges of the free filaments (distal ILT; dILT) [3]. Together, the pILT and the dILT constitute the ILT-complex (or simply the ILT) lining the whole branchial cleft of each gill. The morphological features of this aggregated part of the gill-associated lymphoid tissue (GIALT) have been closely investigated [1–4], but the ontogeny and further development of the tissue as well as its functional role in the immune system of salmon have received less attention. The gills share their embryological origin in the pharyngeal pouches with the thymus, which is a primary lymphoid structure present in all jawed vertebrates [5]. Although the function of the thymus is conserved [6], its location and distribution vary somewhat [7], and in teleosts it is found as an epithelial thickening just beneath the surface of the pharyngeal area [8]. Also, thymus-like tissue was recently discovered at the distal end of the gill filament of the agnathan lamprey [9] indicating a close evolutionary relationship between these two structures. It is therefore of great interest to determine whether the salmonid ILT at any developmental stage can be connected, morphologically or functionally, to the thymus. In the thymus, immature thymocytes are under influence of an array of signalling factors decisive for the production of mature T-lymphocytes [10,11]. The presence of these signalling factors in a tissue may well indicate a site of primary T-lymphocyte development. However, so far no *Rag1* transcript has been detected in the ILT [12] although in the aforementioned study, developmental aspects of ILT's localisation and function were not addressed.

The interaction of the mucosal membrane with the outer environment is complex, both acting as a barrier while being able to secrete and absorb particles from it [13]. This close contact requires

Abbreviations: ILT, interbranchial lymphoid tissue; pILT, proximal ILT; dILT, distal ILT; PCNA, proliferating cell nuclear antigen.

* Corresponding author. Section of Anatomy and Pathology, Department of Basic Sciences and Aquatic Medicine, Faculty of Veterinary Medicine and Biosciences, Norwegian University of Life Sciences, Ullevålsveien 72, P.O. Box 8146 Dep, 0033 Oslo, Norway.
E-mail address: alf.seljenes.dalum@nmbu.no (A.S. Dalum).

http://dx.doi.org/10.1016/j.fsi.2016.09.013
1050-4648/

a finely-tuned immunological system combining both tolerance to innocuous components and reactivity towards potential pathogens. The pharyngeal region is thought to represent the phylogenetical origin of mucosa-associated lymphoid tissues (MALT), driven by the increased antigen exposure as a result of commencing chewing activity with the emerging of jawed vertebrates [14,15]. As such, this region is known to give rise to a range of important lymphoid structures [16]. Thus, study of pharyngeal MALT in lower jawed species might shed new light on the evolution of MALT. In teleosts, GIALT, gut-associated lymphoid tissue (GALT), skin-associated lymphoid tissue (SALT) (reviewed by Ref. [17]), and nasopharyngeal lymphoid tissue (NALT) [18] have been described. Of note, all of these mucosal compartments consist of diffuse lymphoid tissue, in which germinal centres have not been described [5]. Additionally, the respiratory part of the gill epithelium displays the extraordinary feature of separating blood circulation from external environment by only two-three cell layers thick boundary, an architecture that leaves the gills particularly vulnerable [19,20].

The general ability of gills to adapt to the surroundings and to the physiological needs of the fish is well recognized [21–23]. Whether the ILT shares this adaptability is still unclear. In order to investigate such adaptability, a standardized and systematic approach for studying its size during development-, environmental- and immunological influences is warranted. The size of a lymphoid tissue during aging and immunological stimulation is a non-specific but fundamental property and its mapping provides a better understanding of the nature of the tissue. Infectious diseases have been demonstrated to affect the size [12,24] and the immune cell composition [12,25–27] of the proximal ILT. Depletion and replenishment of CD8α^+ cells was noted in the pILT of Atlantic salmon undergoing experimental infection with infectious salmon anaemia-virus (ISAV) [26], a finding which may indicate lymphocyte-trafficking between the ILT and circulation. In higher vertebrates, such trafficking of lymphocytes takes place through high endothelial venules, which morphologically are characterized by their plump endothelial cells [28]. Interaction of ILT with the inner environment has so far not been described.

The aim of the present study was to investigate the development of the ILT during different life stages of Atlantic salmon both in relation to its position in the gills and to its neighbouring organ, the thymus. A procedure for stereological estimation of gill volume and its component tissues was developed, and the role of T-cell proliferation in the volume increase of ILT was investigated. The morphological association of the ILT with the gill vascular system was examined. Finally, evidence for a morphological and functional relationship between the thymus and ILT was investigated, through morphology and testing for presence of thymus-specific transcription factors in the gills.

2. Material and methods

2.1. Fish sampling

The four investigated life stages (yolk-sac larvae, juveniles, adults and sexually-mature) and methods of investigation are presented in Table 1. Before sampling, each fish was anaesthetised in accordance with regulations of the Norwegian Animal Research Authority (NARA). The larvae, after removing parts of the operculum, were transferred to RNAlater (incubated at 4 °C overnight and then stored at −20 °C) or stored in 10% phosphate-buffered formalin for 72 h until processing. From the juveniles, adults and mature fish, the whole left gill basket, the ipsilateral thymus, parts of the head kidney, skin and posterior gut were sampled and stored in formalin. Samples from the right gills, right thymus, head kidney, posterior gut and skin were collected into RNAlater. In addition, samples from the gills of wild, mature salmon were stored in 3%

Table 1
Overview of sampled research material and examination methods used.

Life stage: Numbers (n) Weight (mean, *SD*) Length (mean, *SD*)	Site, date(s) and water temperature(s):	Examination methods:
Yolk-sac larvae (cultivated):	Freshwater:	Histology (HE) whole larvae ($n = 8$)
$n = 16$	Hellefossen in the river Drammenselva, Norway. March	IHC staining of CD3ε on whole larvae ($n = 8$)
0.22 g, 0.05 g	2015 (7 °C)	IF double staining CD3ε and PCNA whole larvae ($n = 8$)
23 mm, 0.5 mm		Whole gill for RT-qPCR ($n = 6$)
Juvenile (fingerling, cultivated):	Freshwater:	Histology (HE) ($n = 8$) and morphometrically volume estimation ($n = 6$) of ILT and thymus
$n = 8$	Hellefossen in the river Drammenselva, Norway.	IHC staining of CD3ε and PCNA in gills and thymus ($n = 8$)
36.3 g, 8.7 g	December 2014 (5 °C)	IF double staining of CD3ε and PCNA in different regions of gill and thymus ($n = 8$)
135 mm, 11 mm		Pooled samples of dILT and pILT for RT-qPCR ($n = 6$)
Adults (before sexual maturation, cultivated):	Sea water:	Histology (HE) ($n = 9$) and morphometrically volume estimation ($n = 6$) of ILT and thymus
$n = 9$	LetSea Helgeland Havbruksstasjon, Mosjøen, Norway.	IHC staining of CD3ε and PCNA in gills and thymus ($n = 9$)
3660 g, 742 g	November 2015 (7 °C) and January 2016 (3 °C)	IF double staining of CD3ε and PCNA in different regions of gill and thymus ($n = 9$)
64.0 cm, 4.2 cm		Pooled samples of dILT and pILT for RT-qPCR ($n = 6$)
Sexually-mature (fully developed gonads, wild):	Freshwater:	Histology (HE) ($n = 8$) and morphometrically volume estimation ($n = 6$; 3 ♀ and 3 ♂) of ILT and thymus
$n = 8$ (3 ♀, 5 ♂)	Hellefossen in the river Drammenselva, Norway.	IHC staining of CD3ε and PCNA in gills and thymus ($n = 8$)
	December 2014 (3 °C) and November 2015 (3 °C)	Scanning electron microscopy.
5065 g, 2600 g		IF double staining CD3ε and PCNA in different regions of gill and thymus ($n = 8$)
80.0 cm, 15.0 cm		Ultrastructural study (TEM) of connection between dILT and blood vessels ($n = 3$)
		Pooled samples of dILT and pILT for RT-qPCR ($n = 6$)

Gene transcription was investigated in gills, thymus, head kidney, posterior gut segment and skin. In post-larvae stage, regions from the gills were selected in order to target the T-cell proliferative zones. n; number of individuals investigated, HE; haematoxylin and eosin, IHC; immunohistochemistry, CD; complementary determining region, IF; immunofluorescence, PCNA; proliferating cell nuclear antigen, ILT; interbranchial lymphoid tissue, dILT; distal ILT, TEM; transmission electron microscopy.

glutaraldehyde (GAH, electron microscopy grade, Merck KGaA, Damstadt, Germany) in 0.1 M cacodylate buffer, pH 7.2. No disease outbreak had been recorded at the sampling sites in the recent past. All fish were sampled during the winter at similar water temperatures (Table 1).

2.2. Histology

Formalin-fixed samples were paraffin-embedded and processed for histological analysis using standard procedures [29]. Orientations and nomenclature are presented in Fig. 1. In larvae, transverse and sagittal sectioning of the gill region was performed on properly-aligned, whole fish. Gills of the other stages were sectioned in the transverse and dorsal planes [3] for best visualization of the ILT. The same orientations were used for immunostainings.

2.3. Morphometric evaluation of gills, ILT and thymus in juveniles and older fish

It was assumed that neither the ILT-complexes nor the thymus differed systematically between the right and left side of the fish, and all investigations were undertaken on the left side. The volumetric density of ILT, total gill and thymus was estimated stereologically by point-counting [30]. To ensure that the HE-stained tissue examined was in fact ILT and thymus, immunohistochemistry was performed on at least 2 sections from each organ using an antibody against CD3ε.

2.3.1. Volume estimation

The volumes of each of the gills of the left gill complex and the ipsilateral thymus from six individuals from each of the groups were estimated according to the method of Scherle (1970), which uses the principle of Archimedes' law on buoyancy forces [31,32]. This method was chosen over the Cavalier method because it retains the continuity between the free filaments and the rest of the gill during segmentation described below. For each gill or thymus, as much formalin as possible was blotted off with absorbent paper before weighing. The organ was then suspended from a thin string of negligible weight (Frog Hair™ tippet 0.127 mm, Gamma Technologies, PA, USA) and submerged in a volume of formalin placed on an electronic scale (GR-120-EC, A&D Instruments LTD, CA, USA). Great care was taken to avoid contact between the organ and the walls of the container. The increase in weight during submersion corresponded to the volume of the gill (V_t) or thymus after correcting for the specific gravity of formalin. Average volume was calculated from three replicate measurements of each organ.

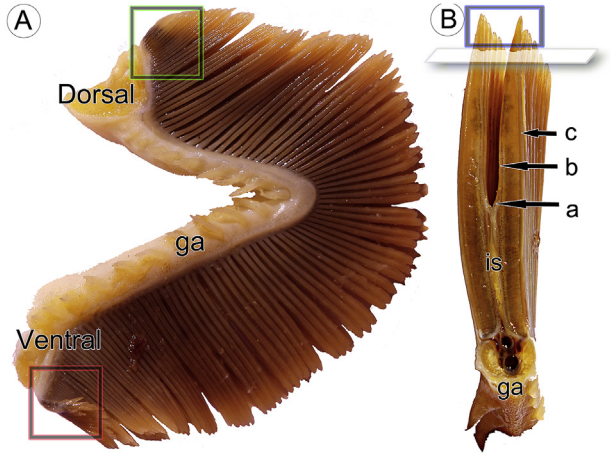

Fig. 1. Orientations and nomenclature. (A) Second gill from adult in medio-lateral projection. Green and red squares depict the regions of the dorsal and ventral ends, respectively, of the proximal interbranchial lymphoid tissue (pILT). Both regions were targeted for RT-qPCR. (B) An excised gill segment in transversal projection. Dorsal plane indicated by semi-transparent rectangle. Blue rectangle indicates distal part of distal ILT (dILT) targeted for RT-qPCR. a; region of the pILT, b; region of the dILT at the trailing edge (water outlet-region with reference to the direction of water flow), c; leading edge (water inlet-region). ga; gill arch, is; interbranchial septum. (For interpretation of the references to colour in this figure legend, the reader is referred to the web version of this article.)

2.3.2. Segmentation and sectioning

The organs were embedded in paraffin, and a ruler was placed at the ends of the gill arches, extending 100 mm outside in one direction (Fig. 2A). For the thymus, the ruler was placed along its long axis. A random number between 0 and 100 mm was chosen (using the RANDBETWEEN(0,100)-function in Microsoft Excel 2010) and used as the starting point outside the organ [30,33]. From this point, parallel slices oriented perpendicular to the ruler were cut at fixed intervals across the entire gill or thymus (Fig. 2A). At most, nine segments were needed for estimation of both the pILT and dILT separately, to get a standard error of the mean (SEM) less than 10% of the mean. Six segments of each thymus were needed. These segments were excised from the paraffin block and reoriented in a transverse plane to the gill arch or the long axis of the thymus. From each segment, one 2.5 μm histological section was cut and stained with haematoxylin and eosin (HE).

2.3.3. Point counting

The histological slides were examined at a total magnification of x100 for juveniles or x25 for adults and mature fish. A microscope equipped with a digital camera (Leica DFC295 digital microscope colour camera, Leica Microsystems Ltd. Heerbrugg, Switzerland) was used. A random number between 0 and 180 was generated for each slide and the microscope stage rotated accordingly to achieve unbiased probing [33]. The resulting image from the camera was shown on a monitor, upon which was mounted a transparent overlay with a coherent grid of coarse and fine points (16 fine points per 1 coarse point) [30,34] (Fig. 2B). For each slide, the number of points hitting pILT, dILT, filaments (including lamellas and gill rays), septum and gill arch was recorded and the volume density (hits on target tissue/total hits; Section 2.3.4 below) of pILT and dILT calculated. All counts were made using the coarse point grid, with the exception of ILT, which, due to its scarcity, was counted using the fine point grid to increase accuracy. Internal vascular and skeletal structures were included in the total count, while points hitting interlamellar spaces were omitted. The border between gill arch and gill filament was set at the proximal part of the filament (Fig. 2C), and the border between gill arch and septum was set at the distal border of the afferent branchial artery (Fig. 2C). The transition between the pILT and dILT was set either at the horizontal level of the highest point of the pILT (Fig. 2E), or, when this was not applicable, at the deflection between the broader pILT and narrower dILT (Fig. 2F). The border between dILT and neighbouring tissue was set either at the basement membrane or at the border towards the closest afferent lamellar arteriole (Fig. 2G). The mucosal surface covering the ILT was counted as ILT because of its possible importance for antigen sampling. For the thymus, the volume density of thymic and non-thymic tissue was calculated.

2.3.4. Calculations

Due to the different behaviour of bone or cartilage and soft tissue during processing, the gill arch was excluded from the calculation of gill volume. An adjusted gill volume (V_a) including filaments and septum was calculated as the total volume of gill (V_t)

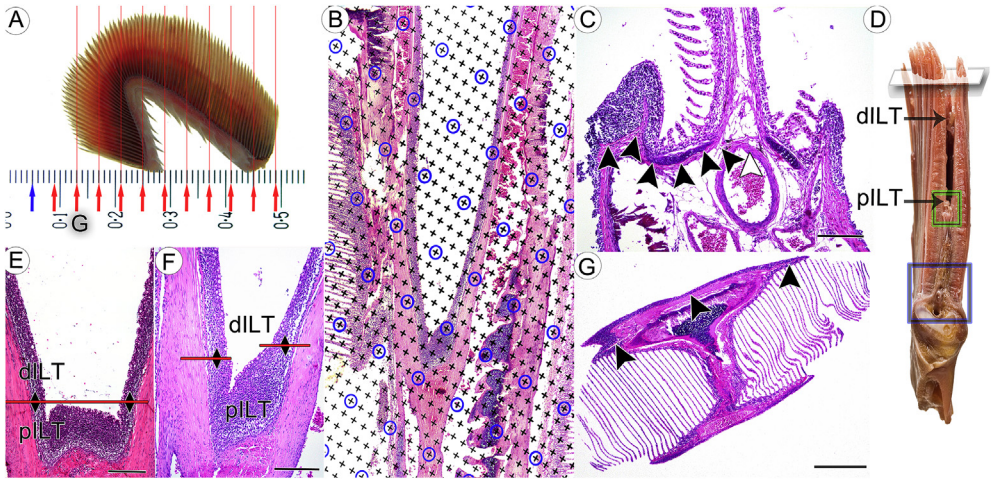

Fig. 2. Volume estimation of the ILT. (A) Model for unbiased sampling of gill; the blue arrow points at a randomly generated starting point, the red arrows point to equally-spaced intervals and red lines depict the planes of segmentation and sectioning (original image courtesy of Trygve T. Poppe). The segment shown in D was obtained by cutting transversely to the medial plane and in parallel with the red lines. (B) Transverse section (HE, mature fish) as depicted by green square in D. A transparent lattice test grid of 1/16 fine to coarse (the latter encircled crosses) points was used to quantify the volume of ILT and thymus (not shown). Note the arbitrary orientation of the test grid relative to the section. (C) Defined transition between gill arch and filament (filled arrowheads) or septum (open arrowhead) (HE, juvenile) in a transverse section as indicated by the blue square in D. (D) Transverse cut gill with orientation perpendicular to A. (E) Defined boundary between dILT and pILT based on the highest point of the pILT (HE, adult; region indicated by green square in D). (F) Defined boundary between dILT and pILT based on the deflection between these two regions (HE, adult; region indicated by green square in D). (G) Defined boundary between dILT and sub-epithelial gill tissue (black arrowheads) (HE, adult). Section cut in the dorsal plane collected from a site indicated by the letter G in A. Scale bars: (C, E and F); 200 μm, (G); 600 μm. (For interpretation of the references to colour in this figure legend, the reader is referred to the web version of this article.)

minus volume of the gill arch (V_{ga}):

$$V_a = V_t - V_{ga} \tag{1}$$

where:

$$V_{ga} = \frac{\text{points hitting gill arch } (P_{ga})}{\text{points hitting the whole gill } (P_t)} \times V_t \tag{2}$$

The absolute volume of ILT (V_{ILT}) was calculated by (taking the coherent factor of the grid into account dividing point hitting ILT by 16):

$$V_{ILT} = \frac{\text{fine points hitting ILT } (P_{ILT})/16}{\text{total points excluding gill arch } (P_a)} \times V_a \tag{3}$$

The percentage of the ILT within the gill (excluding gill arch) was calculated as follows:

$$\%_{ILT} = \frac{\text{points hitting ILT } (P_{ILT})/16}{\text{total points excluding gill arch } (P_a)} \times 100 \tag{4}$$

The percentage of the dILT ($\%_{dILT}$) (and correspondingly for pILT) was calculated as:

$$\%_{dILT} = \frac{\text{points hitting the pILT}(P_{dILT})}{\text{points hitting the ILT } (P_{ILT})} \times 100 \tag{5}$$

The volume of the thymus (V_{thy}) was calculated as the ratio of points hitting thymic tissue to total points multiplied by the total estimated volume of the excised tissue ($V_{t\text{-}thy}$) containing the whole thymus:

$$V_{thy} = \frac{\text{points hitting thymic tissue } \left(P_{thy}\right)}{\text{total points hitting all excised tissue } \left(P_{t-thy}\right)} \times V_{t-thy} \tag{6}$$

Finally, the volume ratio between ILT- and thymic tissue was calculated as:

$$R_{ILT\ thy} = \frac{V_{ILT}}{V_{thy}} \tag{7}$$

2.4. Immunohistochemistry and immunofluorescence

If not otherwise stated, incubations were performed at room temperature. Formalin-fixed, paraffin-embedded thymus and gill tissues were sectioned at 4 μm thickness and mounted on poly-L-lysine-coated slides (Superfrost Plus, Thermo scientific, Braunschweig, Germany). The slides were incubated at 37 °C for 24 h, followed by 58 °C for another 24 h, before deparaffinization in xylene and hydration in graded ethanol dilutions to distilled water. Heat-induced epitope retrieval was performed at 121 °C for 10 min in 0.01 M citrate buffer, pH 6. The slides were subsequently washed in 0.01 M phosphate-buffered saline (PBS, pH 7.3). Inhibition of endogenous peroxidase activity was obtained by incubation for 40 min at 37 °C in preheated PBS with 0.05% phenylhydrazine (Aldrich Chemistry, MO, USA), followed by washing with PBS and blocking for 20 min in 0.05 M tris-buffered saline (TBS, pH 7.6) with 0.2% goat normal serum and 5% bovine serum albumin (BSA) (immunohistochemistry; IHC) or 10% goat normal serum in PBS with 0.5% Tween 80 (immunofluorescence; IF). Primary antibodies of appropriate concentrations were diluted in TBS with 1% BSA (IHC) or PBS with 10% goat normal serum and 0.5% Tween 80 (IF) before application, and the slides were incubated overnight at 4 °C.

For IHC, the monoclonal antibody anti-PCNA (Clone PC10, Dako, Glostrup, Denmark) was labelled with polymer-HRP anti-mouse (Dako EnVison + System-HRP, Dako, Glostrup, Denmark) and developed with 3-amino-9-ethyl carbazol (AEC) as substrate, producing a red reaction product. The polyclonal antibody anti-CD3ε [2] was labelled with polymer-HRP anti-rabbit (Dako EnVison + System-HRP) and developed with 3,3′-diaminobenzidine (DAB) as substrate, producing a brown reaction product. Between each step, the slides were rinsed in TBS. Counterstaining was performed with haematoxylin followed by washing

Table 2
Primers and probes used for RT-qPCR assay. Primers or probes were designed to span internal exon-exon junctions if possible.

Gene	Sequence (5′–3′)	Description
Ef1Ab	F – TGCCCCTCCAGGATGTCTAC R – CACGGCCCACAGGTACTG P – FAM-AAATCGGCGGTATTGG- MGB	With identified role in enzymatic delivery of aminoacyl-tRNA ribosomes among others, the transcription of EF1Ab has been found to be the most stable among a range of potential reference genes in Atlantic salmon and thus most suitable for RT-qPCR studies [36]
Foxn1	F – AGTGCCTCTCCACTCCAAC R – CCCTGTCTTACTGTTCCTCAG P – FAM-AAGGACTGCATGCTACTGTCCTGATG-BHQ1	Foxn1 is regarded as the ontogenetically earliest thymus specific marker required for proliferation and differentiation of thymic epithelial cells [7]
Psmb11	F – CTGGCCTTCATGTTCCAG R – GTGGACAGGCAGGATCTTC P – FAM-GTGTGTCTGCTGCAGCTATCACTCC-BHQ1	Psmb11, or beta-5t (β5t), is a catalytic subunit transcribed exclusively in cortical thymic epithelial cells, thus regarded as one of the most specific markers of cortical thymic epithelial cells [47]
Rag1	F – GAGGCCATGATGCAAGGC R – CTTGACGGTGCGGTACATCT P – FAM-ATCCTGCTGTGTGTCTGGCCATC- BHQ1	Rag1, transcribed in primary lymphoid tissues, is an essential component in the V (J) D recombinase creating the primary diversity in T-cell receptors and immunoglobulins [48]
Rag2	F – GTTCTTCGAGACGTTCAAACAG R – TTCACTGCAGTCAGTGGTTG P – FAM-ACGTTAGCTACTTGAGCAGGAGCCAC- BHQ1	Just as Rag-1 is Rag-2 a vital part of the V (J) D recombinase primarily transcribed in primary lymphoid tissues [49]

Primers (400 nM each) and probes (100 nM) used for RT-qPCR assay on genes specific for primary lymphoid tissues. Elongation factor (EF), forkhead box N1 (Foxn1),proteasome subunit beta type 11 (Psmb11), recombination activating gene (Rag), 6-carboxyfluorescein (FAM), Black Hole Quencher®(BHQ), Minor groove binding (MGB).

in distilled water and mounted with polyvinyl alcohol (PVA) (Apotekproduksjon, Oslo, Norway).

For IF, slides co-incubated with primary antibodies were rinsed in PBS before co-incubation with fluorochromes for 60 min; Alexa 488 rabbit anti-mouse IgG (H + L) secondary antibody (Thermo Fisher, IL, USA) was used for the monoclonal PCNA-antibody, and Alexa 594 goat anti-rabbit IgG (H + L) secondary antibody (Thermo Fisher, IL, USA) was used for the polyclonal CD3ε-antibody. After incubation the slides were rinsed three times in PBS before mounting with PVA adjusted to pH 8.2. Since the antibodies used for double labelling target different cell regions (CD3ε is a cell membrane-associated T-cell receptor, while PCNA labels proliferative cell nuclei), double-labelled cells were evaluated as cells with a labelled nucleus surrounded by a brim of labelled cell membrane.

Pre-immune sera were included as a negative control in both IHC and IF. For double labelling combining PCNA and CD3ε, thymus was used as a positive control.

2.5. Electron microscopy study of ILT-containing regions

For transmission electron microscopy (TEM), the samples were post-fixed in 2% OsO_4 in cacodylate buffer for 2 h, dehydrated in ascending concentrations of ethanol before orientation in the dorsal plane and embedding in LR White resin (London Resin Company, EMS, England). Semi-thin (1 μm) sections were cut, collected on glass slides and stained with Stevenels blue. Ultra-thin sections were collected on uncoated copper grids, counterstained with an aqueous solution of 4% uranyl acetate and 1% potassium permanganate for 10 min and examined with a FEI MORGAGNI 268 transmission electron microscope (FEI Electron Optics, Eindhoven, The Netherlands) operated at 80 kV. Samples for scanning electron microscopy (SEM) were processed as previously described [35].

2.6. Transcription of thymus-specific transcription factors

Total RNA was extracted from macro dissected thymus, head kidney, gills, posterior gut and skin of six individuals in each group. Whole gills of larvae were examined, while in post-larvae, samples from regions expected to contain proliferative T-cells (tips of filaments with dILT and dorsal and ventral ends of pILT; see Fig. 1) were pooled for each individual before extraction. Total RNA-extraction, cleaning and quality control, cDNA synthesis and TaqMan assay was performed as previously described [3]. In short, cDNA was prepared from 1 μg extracted total RNA in a reaction volume of 20 μl using M-MLV Reverse Transcriptase RNase H Minus, PointMutation kit (Promega Corporation, WI) with Oligo dT15 and random hexamer primers. The resulting product was diluted 1:10 such as to give cDNA corresponding to 15 ng of total RNA in each reaction volume of 13 μl. Each sample was amplified in triplicate, and the transcription levels were evaluated relative to elongation factor 1Ab (EF1Ab) as the reference gene [36]. Primers and hydrolysis probes used are listed in Table 2. For the two genes Foxn1 and Psmb11b, no salmon transcript sequences were available in the NCBI database (http://blast.ncbi.nlm.nih.gov). However, genomic sequences

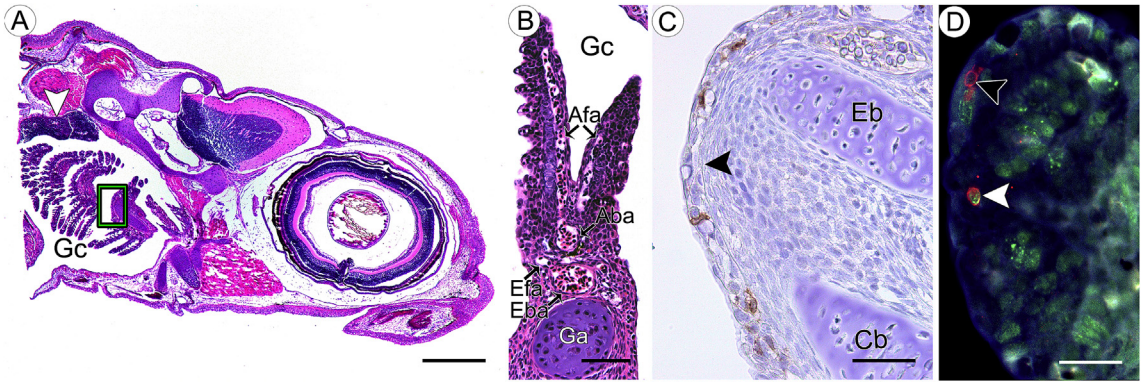

Fig. 3. The primordial ILT of the Atlantic salmon yolk-sac larva. (A) HE stain of a sagittal-sectioned larva with all four gill arches visible. Note the well-developed thymus residing dorso-laterally in the gill cavity (white arrowhead). The region targeted in C and D is marked by the rectangle in A. (B) HE-stained transversal section of the second gill. No discernible ILT is observed, while the arterio-arterial vasculature is present. (C) Low numbers of dispersed CD3ε$^+$ cells (DAB; brown) were seen within the low epithelium of the primordial pILT sectioned sagitally. (D) Sagittal section with both proliferative (CD3ε$^+$ (red)-PCNA$^+$ (green); white arrowhead) and non-proliferative (CD3ε$^+$-PCNA$^-$; black arrowhead) T-cells in the primordial ILT. Gc; gill cavity, Aba; Afferent branchial artery, Afa; Afferent filament artery, Efa; Efferent filament artery, Eba; Efferent branchial artery, Ga; Gill arch, Cb; ceratobranchial cartilage, Eb; epibranchial cartilage. Scale bars: (A); 800 μm, (B); 100 μm, (C) and (D); 50 μm. (For interpretation of the references to colour in this figure legend, the reader is referred to the web version of this article.)

containing the expected numbers of coding exons (8 and 1, respectively) were identified by tblastx using the zebrafish homologues (Foxn1: NP_997738 and Psmb11b: NP_001268731). Primers and probe for Foxn1 were designed to match salmon genome contig AGKD04000101 (2707 kbp-2665kbp) spanning the coding exons 4 and 5. For Psmb11, primers and probe had to be designed within the only exon located in salmon genome contig AGKD04000063 (703 kbp-701kbp). For all RT-qPCR assays, in-house transcriptome sequences were used for sequence verification and exon intron boundaries. Controls, including no reverse transcriptase and non-template controls, were included in the study.

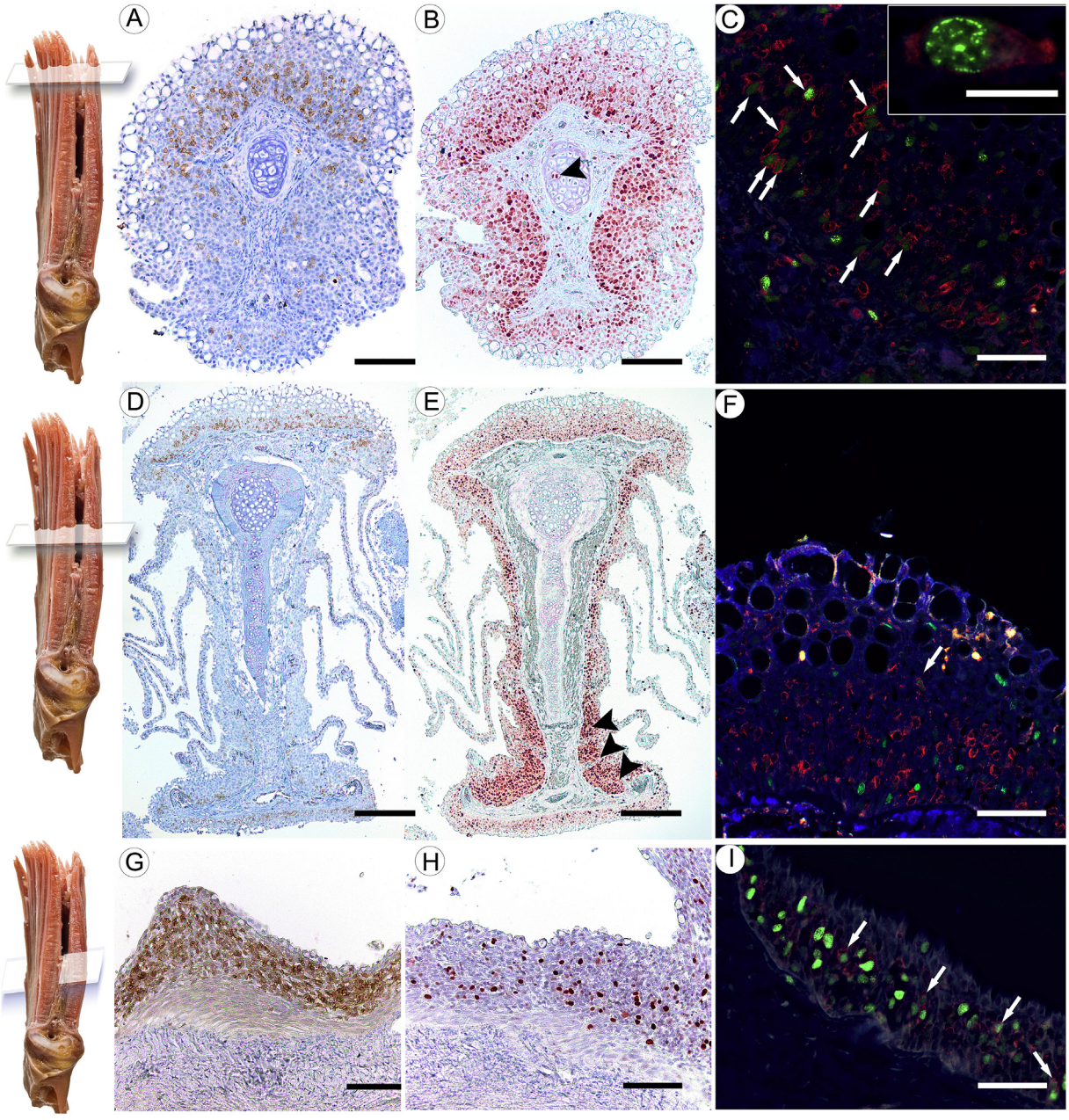

Fig. 4. The presumptive proliferative zones of the Atlantic salmon ILT (mature fish). Transversely cut gill segments at left depict levels and planes of the sections. In (A–F) the trailing edge of the free filament face upwards and is sectioned in the dorsal plane. In (G–H), sections were cut in the medial plane at the dorsal end of the gill. (A) CD3ε+ cells (DAB; brown) in the distal region of the free filament dILT. (B) High numbers of PCNA + cells (AEC; red) both in the trailing edge- and the interlamellar epithelium, while low numbers are seen at the leading edge (arrowhead; proliferative cartilaginous cell). (C) Higher magnification of the dILT in the distal part of the free filament. High proportion of the CD3ε + cells (red) identified as proliferative cells (white arrows, PCNA + cell nuclei green) at the end of the trailing edge, indicating an extensive T-cell proliferation in the distal part of the dILT. Inset: Higher magnification of an elongated, double positive cell. (D) CD3ε+ cells in the trailing edge epithelium of the middle part free filament dILT. (E) High numbers of PCNA+ in the interlamellar epithelium, and in particular towards the leading edge (black arrowheads), and moderate numbers at the leading and trailing (dILT) edges. (F) Higher magnification of the dILT in the middle part of the free filament. Double-positive cells were identified only occasionally in the mid free filament dILT (white arrow). (G) CD3ε+ cells within the pILT at the dorsal end of the gill. (H) Same as G, but labelled for PCNA. (I) Same as G, indicating a high degree of T-cell proliferation in this region. Scale bars: (A and B); 200 μm, (C); 30 μm, (D and E); 400 μm, (F and I); 50 μm, inset in (C); 10 μm, (G, H); 100 μm. (For interpretation of the references to colour in this figure legend, the reader is referred to the web version of this article.)

2.7. Statistical analysis

Statistical analysis of data was performed using a 1-way ANOVA followed by Tukey's multiple comparison (Prism Version 6.02, GraphPad Software, CA, USA). Data from volume measurements and gene transcription study all passed the Kolmogrov-Smirnov normality test. For the gene transcription study, log10-transformed data were used.

3. Results

3.1. Morphology of the ILT in larvae

The presented results for histology and immunostainings apply to all investigated individuals (Table 1). No discernible ILT was observed in transverse sections of the larvae gills (Fig. 3A and B). In sagittal sections of the region expected to hold the pILT, a one to three cell-layer-high epithelium was seen (Fig. 3C) delimited from the underlying connective tissue by a thin basement membrane. Immunohistochemical labelling for the pan-T-cell marker CD3ε indicated the presence of low numbers of dispersed CD3ε$^+$ cells within the epithelium (Fig. 3C). Double immunofluorescence labelling for CD3ε and PCNA identified the presence of both proliferative and non-proliferative CD3ε$^+$ cells (Fig. 3D). These few labelled cells were more elongated and irregular than the more rounded lymphocytes seen in older animals (Fig. 3C). In contrast, thymus had high levels of proliferative cells (data not shown).

3.2. Morphology of the ILT in juvenile, adult and mature fish

Results of histology and immunostainings were similar in all the individuals (Table 1). Accumulations of CD3ε$^+$ lymphocytes were evident in the ILT-complex (Fig. 4A, D and G). Particularly, the height of the lymphocyte-containing epithelium and the population density of CD3ε$^+$ cells increased toward the distal end of the dILT. PCNA$^+$ cells were seen in high numbers in the same region (Fig. 4B) as well as in the pILT at both the dorsal and ventral ends of the gills (Fig. 4H), while far less were seen in other regions of the ILT-complex (such as the middle free filament dILT, Fig. 4E). High numbers of proliferating T-cells were demonstrated by the presence of CD3ε$^+$ and PCNA$^+$ double labelled cells in aforementioned regions of the dILT (Fig. 4C) and the pILT (Fig. 4I). Only low numbers were observed in other parts of the ILT-complex (such as the middle free filament dILT, Fig. 4F). No double labelled cells were noted in the epithelium of gills outside the ILT-complex. The thymus of juveniles and adults was well-developed and served as a positive control, contained high numbers of double labelled cells (data not shown).

3.3. Morphometry of gills, ILT-complex and thymus in juveniles, adults and mature fish

In sharp contrast to the primordial ILT in larvae, the ILT was well developed in the older stages. In juveniles and adults, the ILT-complex constituted on average (SEM) 7.0 (±0.2) % and 6.8 (±0.3)

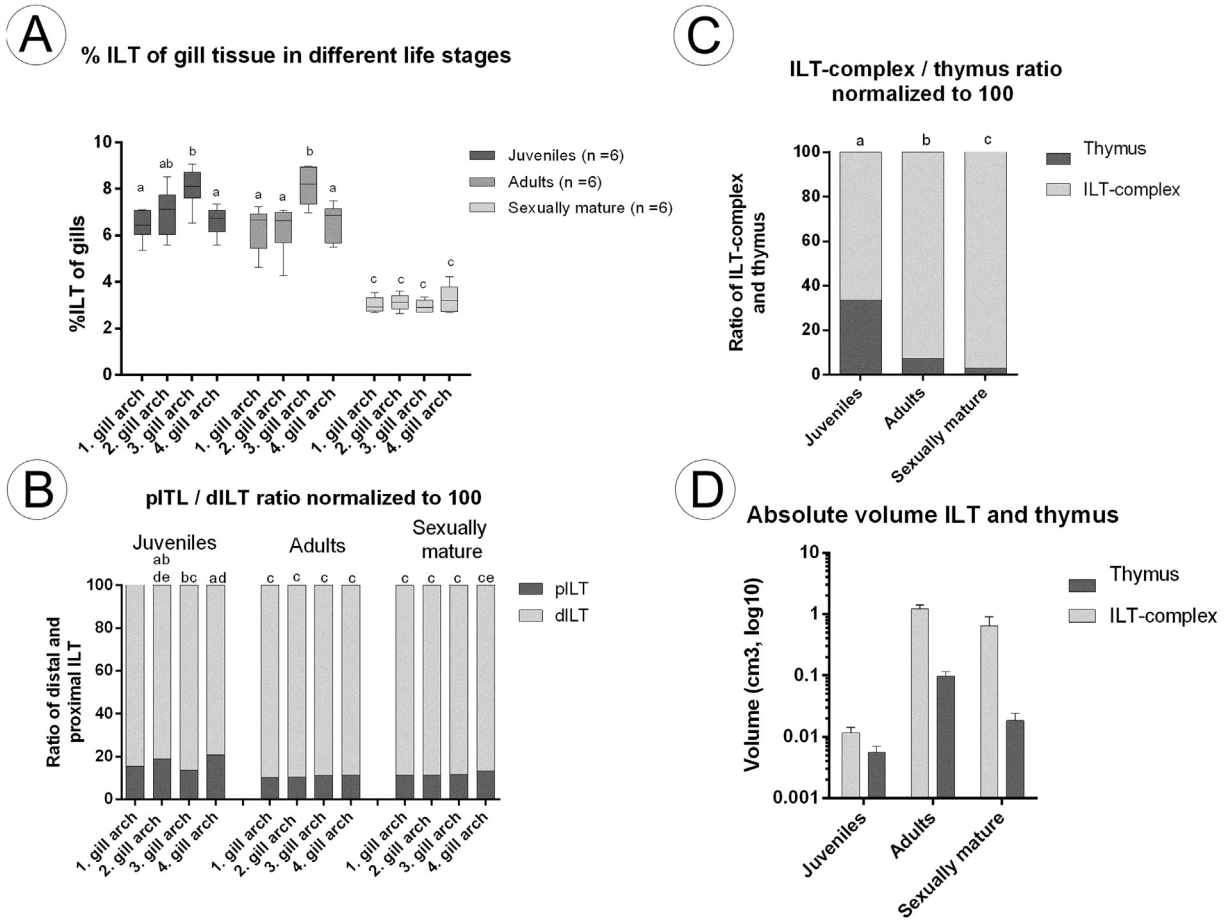

Fig. 5. Relative volumes of the left ILT and ipsilateral thymus at the different developmental stages. Statistically significant difference are indicated by different letters (A and B; $P \leq 0.05$, C; $P \leq 0.001$). (A) Percentage of ILT-complex of each gill (excluding gill arch) (box and whisker plot). (B) Proportions of dILT and pILT, normalised to 100. (C) Volume ratio of the ILT-complex related to the thymus, normalised to 100. (D) Absolute values of volume of the ILT-complex and the thymus (mean with SEM).

%, respectively, of the total volume of gills of all four left gills (excluding the gill arch) (Fig. 5A). After sexual maturation, the proportion of ILT-complex decreased to 3.1 (±0.2) %. When the ILT-complex of each gill was considered separately, the third gill contained a higher volume percentage of ILT-tissue than most other gills in juveniles and adults ($P \leq 0.05$, see also Table 3). Interestingly, the recently discovered dILT constituted a major part of the ILT-complex (Fig. 5B), and the ratio between the dILT and pILT did not vary significantly between the different gills or between the adult and mature groups ($P > 0.05$), while slight differences were seen between the gills in the juvenile group. The absolute volume of the thymus increased from the juvenile to adult stage and was reduced to an intermediate level at the mature stage (Fig. 5D). The ratio between the volumes of the left ILT-complex and the ipsilateral thymus was lowest in juveniles but significantly increased from each stage to the next (Fig. 5C and D; $P \leq 0.001$).

3.4. Ultrastructure of the ILT regions in mature fish

Due to the previously-described proximity of the dILT and the gill secondary vascular system (SVS) [3], and the observation of CD3ε^+ cells associated with these vessels (Fig. 6C), this region was selected for ultrastructural study together with the rest of the dorsal cut filament and transversal cut pILT for comparison. A conspicuous high endothelium was noted in all the narrow bore SVS vessels bordering the basal lamina of the dILT (Fig. 6D and E), and in these vessels mononuclear leucocytes, some seemingly associated with the vessel endothelium, were a regular finding (Fig. 6E). Similar architecture in the SVS vessel walls was not observed in other regions of the filament (Fig. 6F). In addition, mononuclear leucocytes were often seen within the epithelium of the dILT close to the basal lamina (Fig. 6G and H) or in direct contact with the basal lamina of the dILT (Fig. 6E). Very seldom, and only in mature individuals, vessels were seen in direct contact with the basal lamina of the pILT, which mostly associated with the underlying musculature.

3.5. Investigation of morphological and functional connection between ILT and the thymus of the different life stages

Immunohistochemical labelling for CD3ε revealed the close anatomical proximity of the thymus and the gills, with a presence of CD3ε^+ cells between the thymus and the gills in larvae and juveniles (Fig. 7A–C). However, this zone could not be traced all the way to the ILT-complex. A branch of thymus-like tissue extended between the third and fourth gills in juveniles and larvae.

Table 3
Morphometrical evaluation of gills, ILT-complex and thymus in juveniles, adults and mature fish.

		Juvenile (n = 6)	Adult (n = 6)	Mature (n = 6)
1. gill	Volume of gill and gill arch (cm^3):	0.047 ± 0.004	5.002 ± 0.286	5.603 ± 0.743
	Volume of ILT-complex (cm^3):	0.003 ± 0.0001	0.311 ± 0.014	0.171 ± 0.028
	% ILT of the gill	6.5 ± 0.3	6.3 ± 0.4	3.0 ± 0.1
	% dILT:	84.0 ± 1.2	89.9 ± 1.2	88.7 ±0.5
2. gill	Volume of gill and gill arch (cm^3):	0.046 ± 0.004	4.843 ± 0.510	5.756 ± 0.838
	Volume of ILT-complex (cm^3):	0.003 ± 0.0002	0.297 ± 0.023	0.182 ± 0.031
	% ILT of the gill	7.0 ± 0.4	6.3 ± 0.4	3.1 ± 0.1
	% dILT:	81.3 ± 1.2	89.8 ± 2.2	88.7 ± 1.9
3. gill	Volume of gill and gill arch (cm^3):	0.048 ± 0.004	4.549 ± 0.396	5.322 ± 0.753
	Volume of ILT-complex (cm^3):	0.004 ± 0.0003	0.364 ± 0.022	0.159 ± 0.026
	% ILT of the gill	8.1 ± 0.4	8.1 ± 0.3	3.0 ± 0.1
	% dILT:	86.4 ± 1.7	89.6 ± 1.6	88.3 ± 0.5
4. gill	Volume of gill and gill arch (cm^3):	0.027 ± 0.002	3.433 ± 0.381	3.948 ± 0.611
	Volume of ILT-complex (cm^3):	0.002 ± 0.0001	0.224 ± 0.0256	0.129 ± 0.021
	% ILT of the gill	6.6 ± 0.3	6.6 ± 0.3	3.3 ± 0.2
	% dILT:	79.6 ± 1.8	88.1 ± 1.3	86.7 ± 1.2
Volume ILT-complex (V_{ILT}) of all four gills, left side (cm^3):		0.011 ± 0.001	1.228 ± 0.067	0.641 ± 0.104
Volume thymus, left side (cm^3):		0.005 ± 0.001	0.097 ± 0.007	0.018 ± 0.002
Volume ratio ILT-complex / thymus:		2.25 ± 0.37	12.8 ± 0.75	34.40 ± 1.39

Here, gill refers to the filament and septum but excluding the gill arch (boundaries defined in Fig. 1). Values are given as average ± standard error of means (SEM). ILT; interbranchial lymphoid tissue, pILT; proximal ILT, dILT; distal ILT.

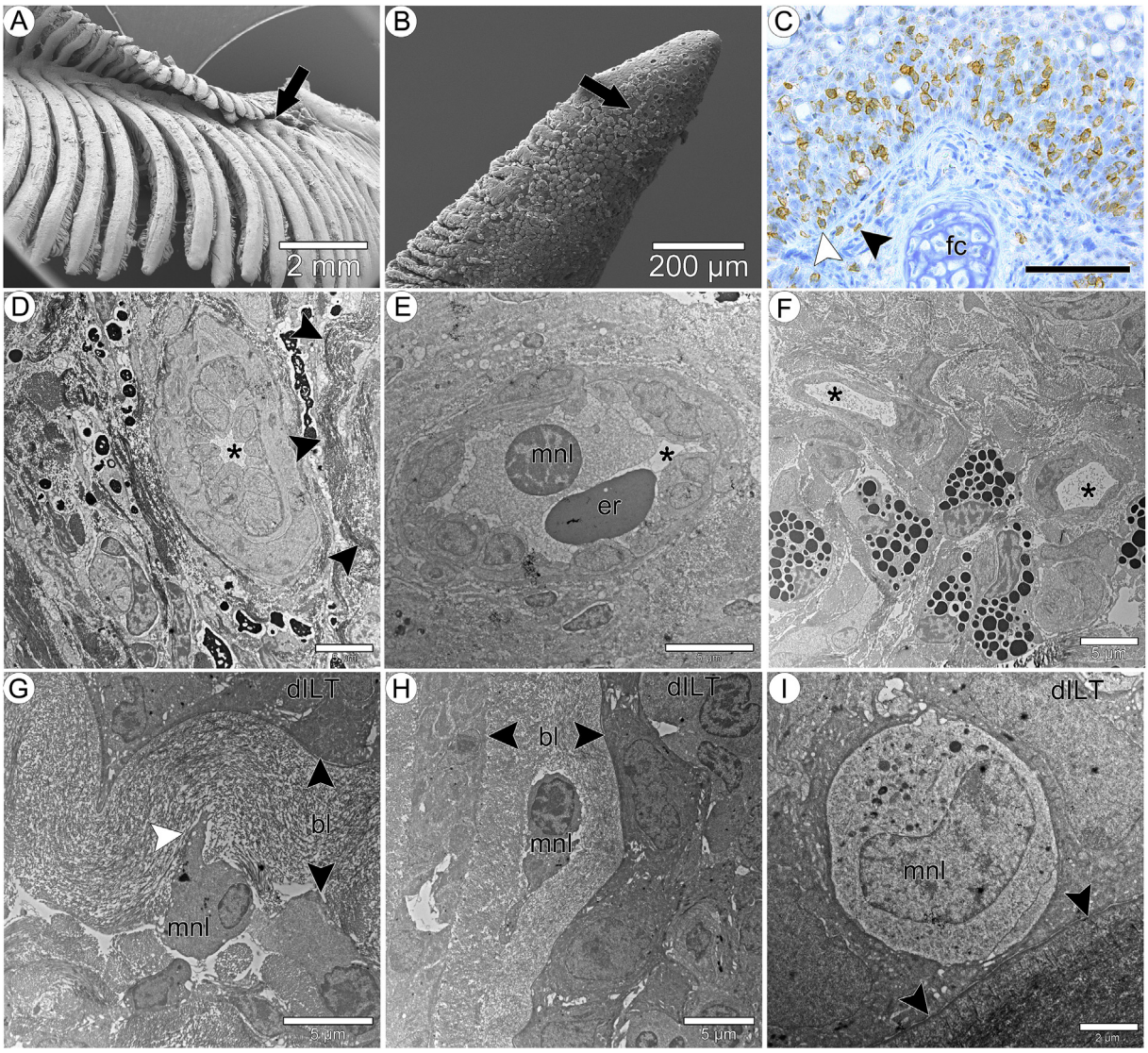

Fig. 6. The proximal- and distal ILT and the latter's vascular tributary in mature Atlantic salmon. (A–B) Scanning electron microscopy. (C) Immunohistochemistry. (D–I) Transmission electron microscopy. In (D–F), vascular lumina are indicated by asterisks. (A) Dorsal end of the 4th gill, containing one of the two identified T-cell proliferative zones of the pILT (arrow). (B) Surface of the distal free filament trailing edge where the dILT T-cell proliferative zone is situated alongside the growth zone of the filament (arrow). (C) CD3ε^{+} cells (DAB; brown) of the dILT both interspersed between basal epithelial cells (white arrowhead) and also below the basement membrane in the connective tissue containing the gill secondary vascular system (SVS; black arrowhead). (D) Ultrastructure of a secondary circulation vessel bordering the basal lamina of the epithelium with dILT; lamina reticularis indicated with arrowheads. Several endothelial cells of conspicuous height bulge into the narrow vascular lumen. (E) Vessel of same location as (D); a mononuclear leucocyte (mnl) is seen associated with the endothelium. (F) Morphology of SVS close to the (filament) leading edge. Note the low height and low numbers of endothelial cell in each vessel wall. (G) Mnl bordering the basal lamina (◂ bl ▸) of epithelium with dILT, seemingly sending out a cell projection (white arrow) into the lamina. (H) Mnl seen inside the basal lamina. (I) Intraepithelial Mnl close to the lamina lucida (arrowheads) of the basal lamina in the region depicted in (A). Fc; filamentous cartilage, er; erythrocyte. Scale bars: (A); 2 mm; (B); 200 µm, (C); 100 µm, (D–H); 5 µm, (I); 2 µm. (For interpretation of the references to colour in this figure legend, the reader is referred to the web version of this article.)

Presence of thymus- and primary lymphoid tissue-specific transcription factors were investigated in ILT (including zones of T-cell proliferation), head kidney, posterior gut and skin, and compared to that of thymus (Fig. 7). In general, levels of the thymus-specific transcription factors remained fairly high in thymus of juveniles and adults, and then fell sharply in mature fish. This finding coincides well with the marked thymus-atrophy in adult fish as evaluated from morphology and morphometry. Transcription levels above a Ct-value of 37 were considered negative, and for juveniles, adults and mature fish, all other tissues than the thymus were negative for both the thymus-specific genes *Foxn1*- and *Psmb11*. Although significantly lower than in the thymus, low levels of transcripts were detected for *Foxn1* in gills and posterior gut of larvae, while in head kidney and skin the transcript levels were not significantly different from that of the thymus. Transcription of *Foxn1* in larvae skin might parallel that of higher vertebrates [37], and is probably of non-immunological relation and therefore not further discussed. Low transcription levels of *Psmb11* were also detected in the head kidney of larvae. Transcription levels of *Rag1* and *Rag2* were significantly higher in thymus compared with the other tissues investigated.

4. Discussion

Variation in size during development, maturation and disease is a fundamental property of any lymphoid tissue. The present study

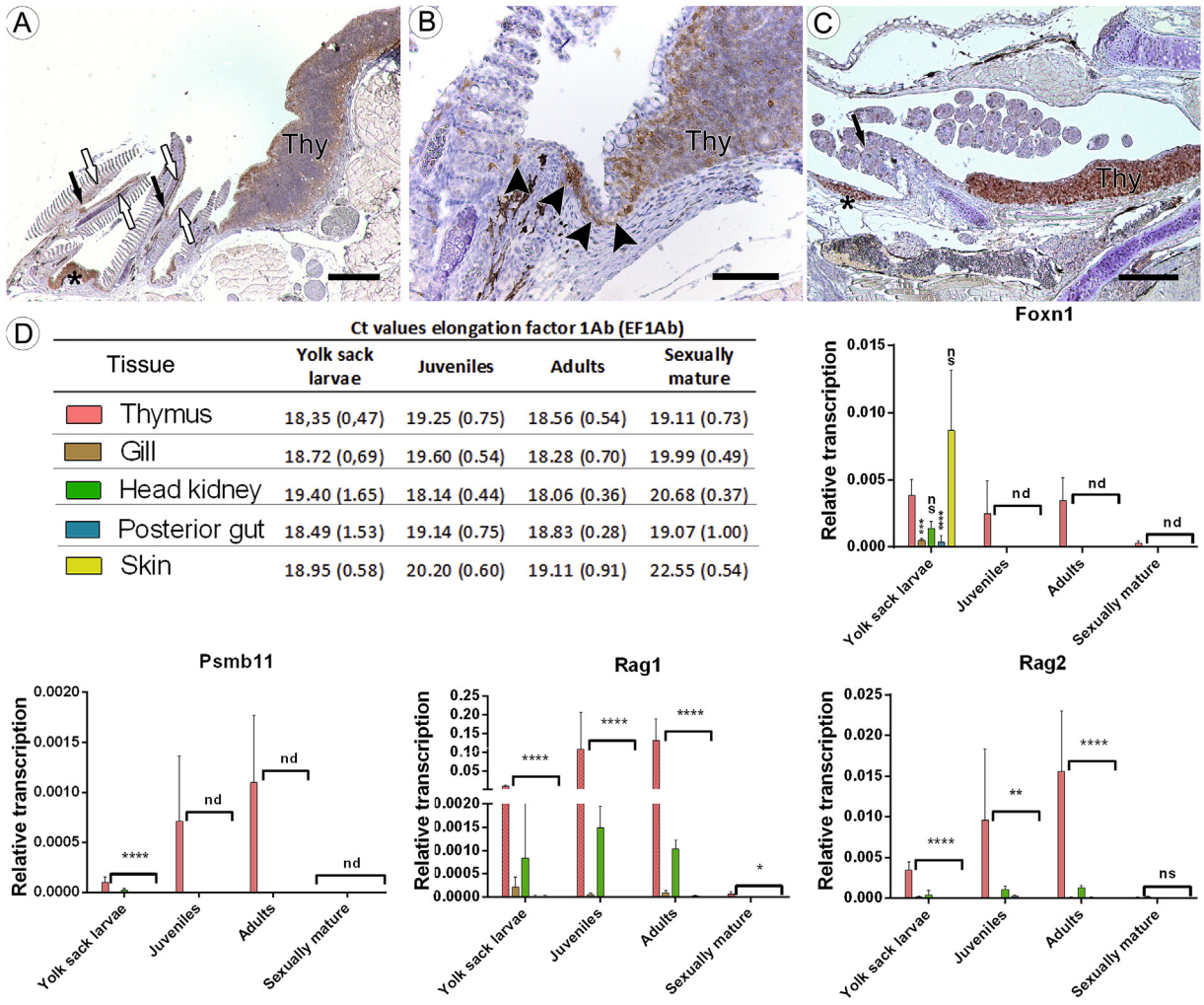

Fig. 7. Morphological and functional relationships between the thymus and the ILT. (A) Dorsal section through the thymus (Thy) and gill of a juvenile with CD3ε^{+} cells (DAB; brown), indicating the morphological closeness. Also seen is the elongation of the thymus between the third and fourth gill (asterisk), pILT and dILT indicated by black and white arrows, respectively. (B) Magnification of A, showing a bridge of CD3ε^{+} cells between the thymus and the gills (arrowheads). (C) Same as A, but in yolk-sac larva; elongation of thymus indicated by asterisk, region expected to harbour pILT (not present) indicated by arrow. (D) Results from RT-qPCR assay of thymus-associated factors relative to elongation factor 1Ab (EF1Ab; Ct values (mean and standard deviation) given in table), indicating no direct functional relation between the thymus and the gill ILT. nd; not detected (Ct above 37), ns; not significant ($P > 0.05$), *; $P \leq 0.05$, **; $P \leq 0.01$, ***; $P \leq 0.001$, ****; $P \leq 0.0001$. Thy; thymus, Foxn1; forkhead box N1, Psmb11; proteasome subunit beta type 11; Rag; recombination activating gene. Scale bars: (A); 1000 μm, (B); 100 μm, (C); 300 μm. (For interpretation of the references to colour in this figure legend, the reader is referred to the web version of this article.)

established a standardized method to estimate ILT's volume, which was more closely related to development and growth of the gills with age than to the thymus.

The morphological investigations of the larvae stage provided insight into the possible developmental role of the ILT. In sharp contrast to the neighbouring thymus, only a few dispersed T-cells were discernible at the distal end of the interbranchial septum of the larvae stage. Transition from larvae to juvenile includes several morphological and physiological transformations, as well as presumed increased antigen exposure subsequent to the transition from cutaneous to branchial respiration implying ventilation of gills [38,39], and to the transition from endogenous to exogenous feeding. It has been proposed that the emergence of MALT is a result of the increase in antigen exposure to the pharynx due to mastication, a behaviour common of all gnathostomes [14,40]. In this context, it is tempting to compare the ILT with the tonsils of Waldeyer's ring found in higher vertebrates including man. Common to both is the embryological origin in the pharyngeal region close to the thymus, ontogenetic emergence after the thymus and an anatomical location of high antigen load during respiration and feeding. However, the ILT appears to lack certain features consistent with a conventional secondary lymphoid tissue of higher vertebrates. We found the volume ratio of ILT versus that of the gills to remain fairly constant in juveniles and adults, indicating similar growth rates of the ILT and the gill. However, in mature fish the relative volume of ILT-tissue was decreased. The weight of the fish and gill volumes of the adult and mature group were comparable, but the volume ratio of the ILT was significantly lower in the mature group. In salmonids, endocrine changes during maturation include an increased level of cortisol, which results in lymphopenia and increasing the susceptibility to disease [41,42]. The hormonal changes accompanying maturation could thus be responsible for the reduction of the relative volume of the ILT. However, it should be kept in mind that the ILT volumes might have been influenced also by other factors associated with the different stages, such as different water qualities, e.g. salinity, differences in fish density, and

starvation during sexual maturation.

The demonstration of increased ILT volume with age raises a fundamental question: where do the T-cells come from? In the gills of post-larvae stages, a predominance of proliferative T-cells was found in what could be regarded as the growth zones of the ILT, that is, the dorsal and ventral ends of the pILT, and at the distal ends of the free filament dILT. Interestingly, this was even the case in mature fish. Despite a slight decrease in the volume ratio of the ILT in this life stage, we were not qualitatively able to claim lower density of proliferating T-cells. On the other hand, the recently-described association between the gill SVS and the dILT [3], together with its known depletion of CD8α^+ T-cells during various infectious states [27,43], may indicate a communication of this lymphoid tissue with the systemic circulation. Supporting this argument is the lack of detection of primary lymphoid tissue-associated transcripts in the ILT, meaning that fully rearranged T-cells must at least at a certain time point come from extrabranchial sites. Interestingly, ultrastructural study of the gill SVS bordering the dILT's basal lamina revealed that its vessels contains conspicuously high numbers of endothelial cells of remarkable height, which sets them apart morphologically from those of the SVS in other parts of the filament. The functional significance of this finding was not further investigated here, and as far as we know, equivalents of high endothelial venules have so far not been described in fishes. However, mononuclear leucocytes were often seen in these vessels, alongside mononuclear leucocytes in close association with the basal lamina, a feature not observed for the pILT. This is in agreement with Rasmussen et al. [44], who found a significantly higher number of both CD8α^+- and IgT$^+$ lymphocytes in the SVS compared with the arterio-arterial circulation of rainbow trout (*Onchorhyncus mykiss*). These authors suggested that the SVS might be the link between the mucosal immune system of the gill and skin and other parts of the immune system [44]. All these findings points to the ILT as a dynamic lymphoid structure throughout the life of Atlantic salmon.

From the juveniles and onwards, the lymphoid tissue of the ILT assumed an increasing presence in comparison with the thymus. In mature fish, the well-developed thymus of juvenile and adult fish appeared atrophic as is typical for mature teleosts [45]. The ILT also showed some decline in volume in the mature group but remained approximately 34 times larger than the thymus, indicating a continued capacity as a lymphoid tissue with aging. Other observations in the present study reinforced the morphological and the observed gene transcriptional differences between the ILT and the thymus. While the proliferation of T-cells seemingly ceased in thymus, the proliferation was still apparent even in the ILT of mature fish. Significant levels of thymus-specific transcription factors were not detected in the gills at any stage of development. These observations would preclude a thymus-like primary lymphoid function for the ILT during the examined stages in Atlantic salmon.

The establishment of a method for volume estimation will benefit further research on lymphoid tissue and immunological responses in fishes, both of which are particularly relevant in evaluating gill health and the effect of potential mucosal-delivered vaccines. The method used for volume estimation in the present study of Atlantic salmon is reproducible, measures the whole gill and can easily be adapted to study the ILT in other teleost species. A fundamental strength of the present method of estimation, apart from easy use and no need for expensive instruments, is that it allows for determination of the whole ILT-complex. Amongst others, it revealed that the recently described dILT constitutes a major proportion of the ILT-complex. Evaluating the size of the ILT in terms of area or height would require a much more rigid sampling scheme ensuring isotropy in three dimensions [30]. Paraffin was selected as embedding medium in order to retain the possibility for immunohistochemistry although this embedding-medium is not optimal regarding tissue distortion [33,46]. Therefore, great care was taken to treat every section equally, ensuring a valid result in the evaluation of different volume ratios.

4.1. Concluding remarks

No support for a functional relationship between the ILT and the thymus was found, evaluated from deviation in volume during growth, degree of T-cell proliferation and differences between levels of transcripts. This study represents the first estimation of the total volume of the ILT-complex, and it has shown that the ILT outgrew the thymus in orders of magnitude with age. Also, the recently discovered dILT was shown to be a vital part of the ILT-complex evaluated both from its volume but also possible functional properties. We speculate that the initial appearance of the ILT is stimulated by external antigen exposure through feeding and branchial respiration. Evidence for both external and internal recruitment of immune cells to the ILT was found. As a dominant lymphoid structure on an exposed surface of the fish, the ILT emerges as an obvious target for mucosal delivered vaccines.

Acknowledgments

This work was supported by the Research Council of Norway (FRIMEDBIO-222207/F20) and Torsteds legat. The authors acknowledge the Sport Fishermen's Club at Hellefossen, river Drammenselva, Norway, for providing wild salmon, Steinar Stølen, Department of Oral Biology, Faculty of Dentistry, University of Oslo, Norway, for excellent technical support on scanning electron microscopy, and Lene Cecilie Hermansen and Hilde Kolstad, Imaging Centre, Norwegian University of Life Sciences, Ås, Norway, for excellent technical support on transmission electron microscopy. Helene Seljenes Dalum is deeply thanked for helpful discussions on project planning and improvement of the manuscript.

References

[1] E. Haugarvoll, et al., Identification and characterization of a novel intra-epithelial lymphoid tissue in the gills of Atlantic salmon, J. Anat. 213 (2) (2008) 202–209.
[2] E.O. Koppang, et al., Salmonid T cells assemble in the thymus, spleen and in novel interbranchial lymphoid tissue, J. Anat. 217 (6) (2010) 728–739.
[3] A.S. Dalum, et al., The interbranchial lymphoid tissue of Atlantic salmon (Salmo salar L) extends as a diffuse mucosal lymphoid tissue throughout the trailing edge of the gill filament, J. Morphol. 276 (9) (2015) 1075–1088.
[4] M. Aamelfot, et al., Characterisation of a monoclonal antibody detecting Atlantic salmon endothelial and red blood cells, and its association with the infectious salmon anaemia virus cell receptor, J. Anat. 222 (5) (2013) 547–557.
[5] A. Zapata, C.T. Amemiya, Phylogeny of lower vertebrates and their immunological structures, Curr. Top. Microbiol. Immunol. 248 (1) (2000) 67–107.
[6] T. Boehm, I. Hess, J.B. Swann, Evolution of lymphoid tissues, Trends Immunol. 33 (6) (2012) 315–321.
[7] Q. Ge, Y. Zhao, Evolution of thymus organogenesis, Dev. Comp. Immunol. 39 (1–2) (2013) 85–90.
[8] T.J. Bowden, P. Cook, J.H.W.M. Rombout, Development and function of the thymus in teleosts, Fish. Shellfish Immunol. 19 (5) (2005) 413–427.
[9] B. Bajoghli, et al., A thymus candidate in lampreys, Nature 470 (7332) (2011) 90–94.
[10] G. Anderson, Y. Takahama, Thymic epithelial cells: working class heroes for T cell development and repertoire selection, Trends Immunol. 33 (6) (2012) 256–263.
[11] L. Calderón, T. Boehm, Synergistic, context-dependent, and hierarchical functions of epithelial components in thymic microenvironments, Cell 149 (1) (2012) 159–172.
[12] I.B. Aas, et al., Transcriptional characterization of the T cell population within the salmonid interbranchial lymphoid tissue, J. Immunol. 193 (7) (2014) 3463–3469.
[13] E.O. Koppang, A. Kvellestad, U. Fischer, Fish mucosal immunity: gill, in: B.H. Beck, E. Peatman (Eds.), Mucosal Health in Aquaculture, Elsevier Academic Press, Amsterdam, 2015, pp. 93–133.
[14] T. Matsunaga, A. Rahman, In search of the origin of the thymus: the thymus

and GALT may be evolutionarily related, Scand. J. Immunol. 53 (1) (2001) 1–6.
[15] T. Matsunaga, A. Rahman, What brought the adaptive immune system to vertebrates? The jaw hypothesis and the seahorse, Immunol. Rev. 166 (1998) 177–186.
[16] I. Varga, et al., The phylogenesis and ontogenesis of the human pharyngeal region focused on the thymus, parathyroid, and thyroid glands, Neuro Endocrinol. Lett. 29 (6) (2008) 837–845.
[17] I. Salinas, Y.A. Zhang, J.O. Sunyer, Mucosal immunoglobulins and B cells of teleost fish, Dev. Comp. Immunol. 35 (12) (2011) 1346–1365.
[18] L. Tacchi, et al., Nasal immunity is an ancient arm of the mucosal immune system of vertebrates, Nat. Commun. 5 (2014) 5205.
[19] G.M. Hughes, General anatomy of the gills, in: W.S. Hoar, D.J. Randall (Eds.), Fish Physiology. Volume X. Gills. Part a. Anatomy, Gas Transfer, and Acid-base RegulationAcademic Press Inc, New York, 1984, pp. 1–63.
[20] P. Laurent, Gill internal morphology, in: W.S. Hoar, D.J. Randall (Eds.), Fish Physiology. Volume X. Gills. Part a. Anatomy, Gas Transfer, and Acid-base RegulationAcademic Press Inc, New York, 1984, pp. 73–183.
[21] C.J. Brauner, P.J. Rombough, Ontogeny and paleophysiology of the gill: new insights from larval and air-breathing fish, Respir. Physiol. Neurobiol. 184 (3) (2012) 293–300.
[22] J. Sollid, G.E. Nilsson, Plasticity of respiratory structures–adaptive remodeling of fish gills induced by ambient oxygen and temperature, Respir. Physiol. Neurobiol. 154 (1–2) (2006) 241–251.
[23] K. Park, W. Kim, H.Y. Kim, Optimal lamellar arrangement in fish gills, Proc. Natl. Acad. Sci. U. S. A. 111 (22) (2014) 8067–8070.
[24] C.C. Norte dos Santos, et al., Changes in the interbranchial lymphoid tissue of Atlantic salmon (Salmo salar) affected by amoebic gill disease, Fish. Shellfish Immunol. 41 (2) (2014) 600–607.
[25] L. Austbø, et al., Transcriptional response of immune genes in gills and the interbranchial lymphoid tissue of Atlantic salmon challenged with infectious salmon anaemia virus, Dev. Comp. Immunol. 45 (1) (2014) 107–114.
[26] D.L. Hetland, et al., In situ localisation of major histocompatibility complex class I and class II and CD8 positive cells in infectious salmon anaemia virus (ISAV)-infected Atlantic salmon, Fish. Shellfish Immunol. 28 (1) (2010) 30–39.
[27] M.M. Olsen, et al., Cellular and humoral factors involved in the response of rainbow trout gills to Ichthyophthirius multifiliis infections: molecular and immunohistochemical studies, Fish. Shellfish Immunol. 30 (3) (2011) 859–869.
[28] H. Hayasaka, et al., Neogenesis and development of the high endothelial venules that mediate lymphocyte trafficking, Cancer Sci. 101 (11) (2010) 2302–2308.
[29] J.D. Bancroft, M. Gamble, Theory and Practice of Histological Techniques, sixth ed., Churchill Livingstone/Elsevier, , Philadelphia, 2008.
[30] C. Mühlfeld, Quantitative morphology of the vascularisation of organs: a stereological approach illustrated using the cardiac circulation, Ann. Anat. 196 (1) (2014) 12–19.
[31] W. Scherle, A simple method for volumetry of organs in quantitative stereology, Mikroskopie 26 (1) (1970) 57–60.
[32] S.W. Hughes, Archimedes revisited: a faster, better, cheaper method of accurately measuring the volume of small objects, Phys. Educ. 40 (5) (2005) 468–474.
[33] S. Tschanz, J.P. Schneider, L. Knudsen, Design-based stereology: planning, volumetry and sampling are crucial steps for a successful study, Ann. Anat. 196 (1) (2014) 3–11.
[34] P.A. Luciw, et al., Stereological analysis of bacterial load and lung lesions in nonhuman primates (Rhesus macaques) experimentally infected with Mycobacterium tuberculosis, Am. J. Physiol. Lung Cell Mol. Physiol. 301 (5) (2011) L731–L738.
[35] A. Dalum, et al., Coronary changes in the Atlantic salmon Salmo salar L: characterization and impact of dietary fatty acid compositions, J. Fish. Dis. 39 (1) (2014) 41–54.
[36] P.A. Olsvik, et al., Evaluation of potential reference genes in real-time RT-PCR studies of Atlantic salmon, BMC Mol. Biol. 6 (21) (2005).
[37] M. Schorpp, et al., Characterization of mouse and human nude genes, Immunogenetics 46 (6) (1997) 509–515.
[38] W.W. Burggren, A.W. Pinder, Ontogeny of cardiovascular and respiratory physiology in lower vertebrates, Annu. Rev. Physiol. 53 (1991) 107–135.
[39] P.J. Rombough, Respiratory gas exchange, aerobic metabolism, and effects of hypoxia during early life, in: W.S. Hoar, D.J. Randall (Eds.), Fish Physiology. Volume 11. The Physiology of Developing Fish. Part a. Eggs and LarvaeAcademic Press Inc, New York, 1988, pp. 59–161.
[40] T. Matsunaga, E. Andersson, Evolution of vertebrate antibody genes, Fish. Shellfish Immunol. 4 (6) (1994) 413–419.
[41] A.D. Pickering, T.G. Pottinger, Lymphocytopenia and interrenal activity during sexual maturation in the brown trout, Salmo trutta L, J. Fish. Biol. 30 (1) (1987) 41–50.
[42] A.D. Pickering, Factors affecting the susceptibility of salmonid fish to disease, in: Fifty-seventh Annual Report for the Year Ended 31st March 1989 Freshwater Biological Association Ambleside, UK, 1989, pp. 61–80.
[43] D.L. Hetland, et al., Depletion of CD8 alpha cells from tissues of Atlantic salmon during the early stages of infection with high or low virulent strains of infectious salmon anaemia virus (ISAV), Dev. Comp. Immunol. 35 (8) (2011) 817–826.
[44] K.J. Rasmussen, J.F. Steffensen, K. Buchmann, Differential occurrence of immune cells in the primary and secondary vascular systems in rainbow trout, Oncorhynchus mykiss (Walbaum), J. Fish. Dis. 36 (7) (2013) 675–679.
[45] S. Chilmonczyk, The thymus in fish: development and possible function in the immune response, Annu. Rev. Fish. Dis. 2 (1992) 181–200.
[46] K.A. Dorph-Petersen, J.R. Nyengaard, H.J. Gundersen, Tissue shrinkage and unbiased stereological estimation of particle number and size, J. Microsc. 204 (3) (2001) 232–246.
[47] Y. Takahama, et al., β5t-containing thymoproteasome: specific expression in thymic cortical epithelial cells and role in positive selection of CD8+ T cells, Curr. Opin. Immunol. 24 (1) (2012) 92–98.
[48] J.D. Hansen, S.L. Kaattari, The recombination activation gene 1 (RAG1) of rainbow trout (Oncorhynchus mykiss): cloning, expression, and phylogenetic analysis, Immunogenetics 42 (3) (1995) 188–195.
[49] J.D. Hansen, S.L. Kaattari, The recombination activating gene 2 (RAG2) of the rainbow trout Oncorhynchus mykiss, Immunogenetics 44 (3) (1996) 203–211.

III

Description of interbranchial lymphoid tissue in the gills of common carp (*Cyprinus carpio* L.): a layered and vascularized lymphoid aggregate

AUTHORS' NAMES AND AFFILIATIONS:

AS Dalum[1], A Kvellestad[1], C Embregts[2], M Forlenza[2], DJ Griffiths[1], J Petit[2], M Scheer[2], CMcL Press[1], EO Koppang[1], GF Wiegertjes[2]

[1] Department of Basic Sciences and Aquatic Medicine, Faculty of Veterinary Medicine and Biosciences, Norwegian University of Life Sciences, Oslo, Norway.

[2] Cell Biology and Immunology Group, Department of Animal Sciences, Wageningen University & Research, Wageningen, the Netherlands.

ABSTRACT

The gills of fish constitute a significant proportion of the total mucosal surface, and their immunological potential has been highlighted by the discovery of the ILT in salmonids. It was hypothesised that other fish species would possess similar lymphoid aggregations. Employing different morphological techniques ILT in common carp was identified and characterized. As in salmonids carp ILT consists of proximal and distal regions of intraepithelial lymphocyte aggregations lining the branchial cleft. However, the carp proximal ILT could be divided into three morphologically distinct compartments. The basal compartment contained high numbers of ZAP-70^+ T-cells, moderate numbers of IgT-1^+ B-cells and was traversed by blood vessels. The intermediate and uppermost compartments contained moderate numbers of T-cells, low numbers of IgT-1^+ B-cells and appeared devoid of blood vessels. Furthermore, the intermediate compartment was distinctive due to the presence of WCL38^+ putative mucosal T-cells and high numbers of eosinophilic granule cells (EGCs). The morphology of the intermediate and uppermost compartments extended into the distal ILT. These findings show that the ILT of the more recently-evolved common carp has a higher degree of organization than the ILT of salmonids.

ABBREVIATIONS

ILT; interbranchial lymphoid tissue, dILT; distal ILT, pILT; proximal ILT, EGC; eosinophilic granule cell, ZAP-70; Zeta-chain-associated protein kinase 70, MALT; mucosa-associated lymphoid tissue, O-MALT; organized MALT.

1. INTRODUCTION

The respiratory surface of the piscine gills is exvaginated and directly exposed to its surroundings, in contrast to the invaginated and relatively protected respiratory surface of the mammalian lung (1). Furthermore, water is a favorable medium for microorganism-growth compared to air thus posing an additional challenge to the respiratory mucosal immune system of gill-breathers (2). The gills' location in the pharynx also exposes the organ to diverse antigens from feeding. Given that the gill respiratory surface represents a thin, semi-permeable membrane of extensive proportions, the piscine gills would be expected to be equipped with an effective immune system in addition to its respiratory and supporting tissue. Indeed, the importance of gill immune functions has been recognized (3) and its potential further substantiated by the discovery of the interbranchial lymphoid tissue (ILT) in the gills of Atlantic salmon *(Salmo salar* L.) and rainbow trout (*Oncorhynchus mykiss* Walbaum) (4, 5). This structure has been described as an intraepithelial aggregation of T-cells (5), which was later shown to be divided into a minor proximal part lining the distal end of the interbranchial septum (proximal ILT; pILT) and a major distal part lining the free filament trailing edges (distal ILT; dILT) in Atlantic salmon (6, 7). Together, the pILT and dILT constitute the ILT, and as such, the ILT lines the whole branchial cleft (i.e. the cleft between two hemibranchs).

It has so far not been possible to relate the salmon ILT to any previously-described lymphoid tissues (5, 8, 9), even though it has been suggested to represent an evolutionary forerunner of mammalian mucosa-associated lymphoid tissue (MALT) (10). In particular, lymphoid structures such as lymph nodes and organized mucosa associated lymphoid tissue (O-MALT) have not been reported in teleosts (11, 12). Yet teleosts possess most of the principal innate and adaptive immune molecules including the adaptive molecules of the immunoglobulin- superfamily as found in higher vertebrates (13).

To our knowledge, the presence of ILT-like structures has not been described in any non-salmonid species, although it has been suggested to exist in European eel (*Anguilla anguilla* L.) (14). We therefore searched for a similar structure in the common carp (*Cyprinus carpio* L.), an important species in both aquaculture (15) and research (16). Carp have adapted to aquatic environments characterized by low oxygen concentration, high variation in temperatures and high content of organic matter (17, 18). We found that common carp possess mucosal lymphoid aggregates in the gills that are far more organized than previously recognized in the other examined fish species, and we here present a morphological study on this novel mucosa-associated lymphoid tissue.

2. MATERIAL AND METHODS

2.1 Fish

European common carp ranging in size from 300 g to 2,000 g (see Table 1) were raised in tanks of recirculating, UV-treated water (23 °C ±1 °C, 12:12 light: dark photoperiod) at the aquatic research facility of Wageningen University & Research, the Netherlands. No disease had been observed in the fish in the recent past. Prior to sampling, the fish were anesthetized with an overdose of FINQUEL® MS-222Tricaine Methanesulfonate (Argent Chemical Laboratories Inc., WA, USA), after which the spinal cord was severed at the level of the brain. For histology, immunohistochemical labelling and scanning electron microscopy (SEM), all four gills and thymus from the left side were transferred to and stored in 10 % phosphate-buffered formalin until further processing. For transmission electron microscopy (TEM), a transverse slice containing one pair of opposing filaments including associated interbranchial septum and gill arch was transferred to 6.25 % glutaraldehyde (electron microscopy grade, Merck KGaA, Damstadt, Germany) in Sorensen`s 0.2 M sodium solution (19). During anesthesia, each fish intended for preparation of vascular casts received an injection via the caudal vein with heparin (5,000 IE/ml, LEO pharma, Lysaker, Norway), at a dose rate of 150 mg/kg (20). At 2 min post-injection, the tail was transected for bleed-out. After severing the spinal cord, the gills' vessels were flushed via the ventral aorta with 9 mg/ml sodium chloride (Fresenius Kabi Norge AS, Halden, Norway). Either the whole head with intact gill basket or free-dissected gills were kept on ice for immediate infusion of resin.

2.2 Histology

Formalin- fixed tissue was paraffin-embedded and processed for histological analysis using standard procedures (21). Sagittally-, transversely- and dorsally-oriented gill sections (Fig. 1) (6) of thickness 2.5 µm were stained with hematoxylin and eosin (HE) (n = 26), Toluidine blue (TB) (n = 13) and Martius scarlet blue (MSB) (n = 13).

2.3 Immunohistochemistry and immunofluorescence

A protocol adapted from Dalum et al. 2016 (7) was employed on formalin-fixed, paraffin-embedded thymus and gill tissues including ILT sectioned at 4 µm thickness and mounted on poly-L-lysine-coated slides (Superfrost Plus, Thermo scientific, Braunschweig, Germany) (n = 26 for both immunohistochemistry and immunofluorescence). Information about antibodies used is summarized in Table 2. Pre-immune sera and omissions of primary antibodies were included as a negative control in both IHC and IF.

2.4 Transmission electron microscopy

Relevant regions (pILT and filament including dILT) from the glutaraldehyde-fixed gill samples (n = 6) were dissected out and post-fixed in 2 % OsO_4 in 0.1 M cacodylate buffer, pH 7.2 for 2 h, dehydrated in ascending concentrations of ethanol before orientation for sectioning in the dorsal plane and embedding in LR White resin (London Resin Company, EMS, England). Semi-thin (1 µm) sections were mounted on glass slides and stained with Stevenel's blue. Ultra-thin sections were mounted on uncoated copper grids, counterstained with 4 % aqueous uranyl acetate and 1 % potassium permanganate for 10 min and examined with a FEI MORGAGNI 268 transmission electron microscope (FEI Electron Optics, Eindhoven, The Netherlands) operated at 80 kV.

2.5 Vascular casts and scanning electron microscopy

Vascular casts (n = 6) were made by infusing red-pigmented PU4ii-L-resin (VasQtec, Zurich, Switzerland; prepared according to manufacturer's protocol) at controlled pressure (6.2 kPa) through a 0.9 mm vascular catheter. The catheter was either placed in the afferent- (normograde to blood flow) or efferent (retrograde to blood flow) branchial artery of free-dissected (separate) gills, or in the ventral- (normograde) or dorsal (retrograde) aorta targeting the whole gill basket. Infusion was continued until the resin was clearly visible in the filaments and emerged from the opposite side of the vascular system. After hardening of the resin for a day in water at room temperature, the casts were transferred to a 3 % aqueous solution of potassium hydroxide at room temperature and agitated twice daily for 3 days until all tissues were dissolved.

Casts and formalin-fixed gills were examined with SEM. The formalin-fixed gill tissues were dehydrated in ascending concentrations of ethanol and critical point dried (Polaron E3100 Critical Point Dryer, Polaron Equipment Ltd, Watford, UK) using carbon dioxide as the transitional fluid; this procedure was omitted for vascular casts. Tissues and casts were subsequently mounted on platforms and coated with 30 nm-thick layer of palladium in a Polaron E5100 sputter coater before examination in a Philips XL30 Environmental Scanning Electron Microscope (Philips, Eindhoven, The Netherlands).

3. RESULTS

Reticular epithelial tissue rich in lymphocytes was found along the distal end of the interbranchial septum corresponding to the pILT, and the filament trailing edges corresponding to dILT (see Fig. 1 B and C). The pILT could be divided into basal, intermediate and uppermost compartments, of which the first contained numerous blood vessels, all detailed in the following text. The dILT consisted of layers corresponding to the intermediate and uppermost layers of the pILT. No obvious morphological differences were observed between the four gill pairs of individual fish, nor between different-sized fish (Table 1).

3.1 Morphology of vessels in conjunction to the basal compartment of the pILT

The paths of all afferent filament arteries (AFAs) of each hemibranch were interrupted by an interconnecting vascular ampulla running dorso-ventrally in the distal end of the interbranchial septum (Fig. 2A) (22). No communication between the ampullae of the two hemibranchs was found in any of the four gill pairs (Fig. 3D and H). We therefore chose to differentiate between a proximal- and distal part of each AFA (pAFA and dAFA, respectively) with reference to the ampulla (Fig. 2 and 3A). While the pAFAs drained into the ampulla, two different and parallel outlets from the ampulla were discovered: *i)* cisternae giving of basal pILT-associated vessels, and *ii)* dAFA. The basal pILT-associated vessels merged with the dAFA at the level of the proximal free filaments after traversing the basal pILT.

3.1.1 Ampulla and cisternae

The luminae of the ampullae and their cisternae were irregular in outline and limited by a low, continuous endothelium resting on a continuous basal lamina and surrounding thick layers of connective tissue (Fig. 4B). In general, the walls of the ampullae has previously been described as devoid of smooth musculature (23), which also seemed to be the case for the cisternae. The distal delimiting connective tissue covering the vascular cisternae appeared as bands projecting into the basal part of the pILT (Fig. 3J and K), with one interconnecting band for the cisternae of each hemibranch. Within these bands, the basal pILT-associated vessels originated at apparently regular intervals (Fig. 3J-L).

3.1.2 Basal pILT-associated vessels

The blood-supply of the basal pILT was derived from clusters of small vessels, termed basal pILT-associated vessels, originating from the cisternae (Fig. 2 C and 3). As these clusters approached the epithelial tissue of the pILT, the vessels became surrounded by the epithelial basal lamina to form vascular cords traversing the basal pILT (Fig. 4C-F and Fig. 5F). In cross-sections of these cords, perivascular tissue was seen between the outer epithelial basal lamina and the basal pILT-associated vessels within the cord (Fig. 4C-E). This perivascular tissue was dominated by EGCs, pericytes and lymphocytes-like (Fig. 4C and D), as inferred from morphology in TEM. Lymphocytes were also regularly seen in direct contact with the epithelial basal lamina surrounding the cords. In the basal pILT-associated vessels, a continuous layer of endothelial cells on a continuous basal lamina was the predominant pattern, although in a few places, a fenestrated endothelium was noted (Fig. 4E). At the border between the basal and intermediate compartments of the pILT, these cords formed arches before connecting with the dAFAs. Most of the basal pILT-associated vessels were of capillary size (Fig. 4C-E), with a narrow lumen usually containing a single, or occasionally two blood cells. However, some larger diameter vessels were also seen. High numbers of leukocytes were noted within the basal pILT-associated vessels.

Immunohistochemical labelling for cytokeratin showed that the vascular cords of the basal pILT were surrounded by epithelium (Fig. 6F and G). Communication between the blood vessels associated with the basal pILT and secondary vascular system of the gill (nutritive- and interlamellar system (24)) or bypassing the lamellar microcirculation to the efferent side (as it has been described in some other fish species (25)) was not found. Thus, all these vessels appeared to empty into the dAFA. No vessels were seen within the intermediate or uppermost compartments of the ILT.

No morphological difference was noted between the vascular casts produced by infusion through the afferent - or efferent branchial artery, or ventral or dorsal aorta.

3.1.3 Proximal dAFA

The most proximal segment of dAFA running in parallel with the basal pILT-associated vessels apparently differed from the other segments of AFA by having a thicker vessel wall, with endothelial cells protruding more clearly into the lumina, suggesting the presence of contractile elements in the wall (Fig. 4A).

3.2 Morphology of the ILT epithelium and associated cells

The pILT could be divided into basal, intermediate and uppermost compartments (with reference to levels above the basement membrane) based on HE- and immunohistochemical labelling (Table 3). In all compartments, high numbers of cytokeratin-positive reticular epithelial cells were identified. No labelling with the WCL9-antibody targeting cortical, immature thymocytes (26) was seen within the gills.

3.2.1 The basal pILT compartment

The basal pILT compartment was delineated from underlying tissue, including the vascularized cords, by a prominent basal lamina (Fig. 4G). High numbers of lymphocytes were seen within this compartment, many of which were organized into rows between epithelial cells parallel to the epithelial surface (Fig. 4H and 5D). Lymphocytes were also seen in low numbers in the connective tissue beneath the basement membrane. Most of the lymphocytes within the basal compartment were ZAP-70$^+$, a protein normally expected to be part of the T-cell receptor complex (Fig. 6A, Fig. 7C and G), although moderate numbers of IgT-1$^+$ cells and low numbers of IgM$^+$ cells were also seen (Fig. 6C and E). Moreover, high numbers of proliferating, PCNA$^+$ cells were seen within this compartment (Fig. 6D).

3.2.2 The intermediate pILT compartment

The height of the intermediate compartment decreased towards the median plane of the pILT (Fig. 6B). It was characterized by high numbers of EGCs (Fig. 4I, 5A-E, 7). ZAP-70$^+$, IgT-1$^+$ and PCNA$^+$ cells were seen in lower numbers than in the basal compartment, while

IgM^+ cells were observed in similar numbers. The putative mucosal T-cell antibody WCL38, which is also known to react with epithelial cells within carp mucosal lymphoid tissues (27), labelled cells exclusively and extensively in this compartment (Fig. 6B, Fig. 7B, E and H). Furthermore, WCL38 was also seen to label cells within the epithelium of the trailing- and leading edges of the filaments (Fig. 6H). Putative mucosal T-cells appeared both as a few, small lymphocyte-like cells with dense nuclei, but mostly as larger epithelial-like cells with extended cellular processes and less-dense nuclei. Immunofluorescence labelling combining cytokeratin and WCL38 revealed some co-localization (Fig. 7F). Only few instances of co-localization between WCL38 and ZAP-70 were detected (Fig. 7I), indicating that most of the $WCL38^+$ cells were epithelial cells and not cells with T-cell receptors.

3.2.3 The uppermost pILT compartment

The uppermost compartment was low in height and contained goblet cells amid pavement cells. We did not observe any essential modification of surface epithelium morphology covering the ILT-complex when compared with other regions of the gills (Fig. 8). Moderate numbers of $ZAP\text{-}70^+$ and low numbers of $IgT\text{-}1^+$and $PCNA^+$-cells were present, whereas no EGCs $WCL38^+$ or IgM^+ cells were seen (Fig. 6A-E). However, slight IgT-1-labelling was noted within mucus of goblet cells (Fig. 6C).

3.2.4 The dILT

Along the entire filament trailing edge, the dILT appeared as a continuation of the intermediate and uppermost compartments as described for the pILT. The epithelium in the trailing edge labelled with the putative mucosal T-cell marker (corresponding to the intermediate compartment), except in the outer surface (corresponding to the uppermost compartment) (Fig. 6H). The only difference noted between the dILT and the intermediate and uppermost compartments of the pILT was the higher numbers of IgM^+-cells in the dILT (Fig. 6E and I). Extensive IgM labelling of serum in blood vessels was noted (Fig. 6E and I). In addition, labelling with the putative mucosal T-cell marker was seen in the leading edge of the filaments (Fig. 6H). As judged from HE-staining, the height of the epithelium and the density of lymphocytes were higher in the trailing- compared to the leading edges.

4. DISCUSSION

The common carp possesses an ILT similar to the structure previously described in the Atlantic salmon and rainbow trout (5-7), consisting of a lymphocyte-rich epithelial framework suggested to be an evolutionary forerunner of mammalian MALT (10). However, the level of organization seen in common carp surpasses that described for salmonids, with the carp pILT consisting of three readily-distinguishable compartments that differ in the distribution of cell types and association with blood vessels. The pILT basal compartment

contained high numbers of lymphocytes and was intimately associated with an elaborate network of blood vessels. The intermediate and uppermost compartments, and their continuation throughout the trailing edge dILT, were characterized by EGCs and goblet cells, respectively, in addition to moderate numbers of lymphocytes.

The basal pILT-associated blood vessels were organized in vascular cords surrounded by the pILT epithelium and were remarkable in their intimate relationship with the epithelium. A striking similarity was noted between the ultrastructure of these vascularized cords and those of the thymus of common carp (28), rainbow trout (29) and sharpsnout seabream (*Diplodus puntazzo* Walbaum) (30) as well as in higher vertebrates (31). In both the thymus and the basal pILT, the vascular cords were completely surrounded by epithelial cells and associated basement membrane forming the outer delineation of the perivascular tissue. Similarly, the inner delineation of the perivascular tissue was formed by the endothelial basement membrane of each vessel within the cords. While the thymus-associated blood vessels are important for trafficking of lymphocytes to and from the reticulo-epithelial thymic framework (32), the extent of such trafficking between the basal pILT and its vessels needs further investigation. Although there have been few investigations of leukocyte trafficking involving mucosal compartments in teleosts, both functional and morphological indications of such have been suggested for the gills of salmonids (7, 33). Based on our morphological findings in the carp basal pILT, further investigation of the functional association between the ILT and its blood vessels is warranted.

Blood perfusion through the basal pILT-associated vessels is possibly regulated by the paralleling dAFA. Morphologically, this part of the dAFA was shown to contain a thicker tunica media with seemingly more contractile elements than other parts of the dAFA, as well as the pAFA. Altogether, the strategic placement of this vascular organization immediately before the respiratory lamellae, probably the most vulnerable part of the whole fish, would enable rapid recruitment of leukocytes in the event of contact with harmful foreign organisms. However, a putative role of basal pILT-associated vessels in lymphocyte trafficking and immune cell recruitment needs further investigation.

Low and moderate numbers of IgM^+ B-cells were observed in all the compartments of the pILT and dILT, respectively. The ILT-complex of healthy Atlantic salmon is also known to hold low numbers of IgM^+ B-cells (5, 6). However, in comparison to IgM, $IgT\text{-}1^+$ cells appeared in relatively higher numbers and in a compartmentalized manner, predominantly in the basal pILT. The importance of IgT in gill immunity in rainbow trout has recently been noted, where pathogen-specific IgT^+ B-cell proliferation upon microbial exposure was shown to take place (34). The spatial distribution of this response, and in particularly whether the ILT was involved, was not reported. In common carp and zebrafish, two subclasses (IgT-1 (IgZ-1) and IgT-2 (IgZ-2)) have been described (35, 36). The presence of high numbers of IgT^+ cells in the vessel-associated basal compartment is consistent with the reported abundance of the IgT-1- subset at systemic sites of common carp (spleen, head kidney and peripheral

blood leukocytes) (37). The IgT-2 subset, however, has been described as preferentially localized at mucosal sites (37). The distribution pattern of IgT-2 was not investigated in this study due to lack of a specific antibody. However, the lack of labelling for the putative mucosal T-cell antibody WCL38 may suggest that the basal pILT is not primarily involved in mucosal immunity. It will be an important issue for the future to determine how the immune responsive cells of the ILT are influenced during both systemic and mucosal immuno-stimulation.

The intermediate compartment differed from the other compartments in housing high numbers of EGCs and possessing cells that labelled with the putative mucosal T-cell marker WCL38. The comparison of EGCs to mammalian mast cells is a matter of debate, partly fuelled by the variable staining properties of the cells depending on species, fixation- and staining methods (38, 39). Like mammalian mast cells, teleost EGCs have been shown to degranulate when exposed to various degranulation agents (40), but among teleosts, histamine content of the granules has so far only been claimed for gilthead seabream (41). Even though EGCs are found throughout the body in teleosts, they are reported to occur commonly in association with blood vessels and nerves, and in proximity to external surfaces including the digestive tract and gills (2). As for amphibians and reptiles, a great diversity in histological appearance and species-specific distribution of teleost EGCs has been described (42), and high numbers are often associated with chronic inflammation (38). The ILT of Atlantic salmon is commonly devoid of EGCs, and this apparent species difference may underline the importance of habitat in developing different innate strategies as has been described for skin (43). We thus speculate whether the EGCs of the intermediate pILT of carp represent an additional layer of innate immunity after the mucus- and epithelial barriers. EGCs were also noted within the perivascular tissue of the basal pILT and may play a role in regulation of vascular tone (44). The WCL38 antibody targets putative gut mucosal T-cells (27) and labelling with this antibody was found exclusively in the intermediate pILT and in the trailing- and leading edge epithelium. However, double labelling indicated a prevalence of co-localization with epithelial cells in the ILT. As the exact epitope recognized by the WCL38 antibody is so far unknown, further characterization is needed before conclusions can be drawn based on this marker. Nevertheless, the distribution of EGCs in concert with WCL38-positive cells – epithelial cells and putative mucosal T-cells - clearly demonstrates the compartmentalization of the carp ILT.

The uppermost compartment of pILT consisting of goblet cells amid epithelial cells and moderate numbers of ZAP-70^{+} T-cells, contained no EGCs or staining against putative mucosal T-cells. In Atlantic salmon, pavement-like cells of the gills have been shown to sample antigens and to translocate them to underlying macrophage-like cells (45). Whether this process takes place in the ILT of salmonids and common carp still remains an interesting and important question, particularly with regard to development of new strategies for mucosal vaccines.

The water in which these fish were reared was treated with UV-light, which might have reduced pathogen loads to a level influencing the morphology of ILT. Therefore, the ILT in wild and farmed carp living in different water qualities, as well as fish with mucosal infection and inflammation, should be investigated in the future.

Here, we described a lymphoid tissue within the gills of common carp with certain resemblances to O-MALT of higher vertebrates, that is, organization into distinct compartments and in close association with blood vessels. Vertebrate evolution is characterized by an increasing complexity of secondary rather than primary lymphoid tissues (46). While O-MALT, according to present knowledge, first appears in anurans (47), nasal-associated- and gut-associated lymphoid tissues with certain similarities have recently been reported in African lungfishes (*Protopterus dolloi* and *P. annectend*) (48). These tissues, termed primitive O-MALT, consisted of extensive aggregations of T- and B-cells in an apparently non-organized fashion, covered by a modified epithelium (48). We were not able to identify a modified epithelium of the ILT with the methods applied. However, a separation into distinct compartments within the intraepithelial lymphoid tissue and an intimate relationship to blood vessels were found, which could represent a step towards O-MALT.

Conclusion

We have shown that the gills of common carp contain aggregates of MALT that can be divided into three distinct epithelial compartments based on tissue morphology and cell composition. Such lymphoid compartmentalization within a mucosal epithelium has to the best of our knowledge not been described before for in fish. The intimate association of this lymphoid tissue with the vascular system makes a functional interaction with the systemic immune system highly probable. A superficial mucosal tissue of such size and complexity would be expected to be important in the defence against infectious agents, and could be a potential target for mucosa-delivered vaccines. These findings challenge the view that teleosts lack mucosa-associated lymphoid tissues of organized character, and emphasize the importance of the pharyngeal region as an evolutionary source of lymphoid tissue diversity (49).

ACKNOWLEDGEMENT

The authors thank Lene Cecilie Hermansen and Hilde Kolstad, Imaging Centre, Norwegian University of Life Sciences, Ås, Norway, for excellent technical support with transmission- and scanning electron microscopy.

REFERENCES

1. Maina JN. Structure, function and evolution of the gas exchangers: comparative perspectives. Journal of anatomy. 2002;201(4):281-304.
2. Gomez D, Sunyer JO, Salinas I. The mucosal immune system of fish: the evolution of tolerating commensals while fighting pathogens. Fish & shellfish immunology. 2013;35(6):1729-39.
3. dos Santos NMS, Taverne-Thiele JJ, Barnes AC, Van Muiswinkel WB, Ellis AE, Rombout JHWM. The gill is a major organ for antibody secreting cell production following direct immersion of sea bass (*Dicentrarchus labrax*, L.) in a *Photobacterium damselae* ssp *piscicida* bacterin: an ontogenetic study. Fish & shellfish immunology. 2001;11(1):65-74.
4. Haugarvoll E, Bjerkås I, Nowak BF, Hordvik I, Koppang EO. Identification and characterization of a novel intraepithelial lymphoid tissue in the gills of Atlantic salmon. Journal of anatomy. 2008;213(2):202-9.
5. Koppang EO, Fischer U, Moore L, Tranulis MA, Dijkstra JM, Köllner B, et al. Salmonid T cells assemble in the thymus, spleen and in novel interbranchial lymphoid tissue. Journal of anatomy. 2010;217(6):728-39.
6. Dalum AS, Austbø L, Bjørgen H, Skjødt K, Hordvik I, Hansen T, et al. The interbranchial lymphoid tissue of Atlantic salmon (*Salmo salar* L) extends as a diffuse mucosal lymphoid tissue throughout the trailing edge of the gill filament. Journal of morphology. 2015;276(9):1075-88.
7. Dalum AS, Griffiths DJ, Valen EC, Amthor KS, Austbø L, Koppang EO, et al. Morphological and functional development of the interbranchial lymphoid tissue (ILT) in Atlantic salmon (*Salmo salar* L). Fish & shellfish immunology. 2016;58:153-64.
8. Koppang EO, Kvellestad A, Fischer U. Fish mucosal immunity: gill. In: Beck BH, Peatman E, editors. Mucosal Health in Aquaculture. Amsterdam: Elsevier Academic Press; 2015. p. 93-133.
9. Austbø L, Aas IB, König M, Weli SC, Syed M, Falk K, et al. Transcriptional response of immune genes in gills and the interbranchial lymphoid tissue of Atlantic salmon challenged with infectious salmon anaemia virus. Developmental and comparative immunology. 2014;45(1):107-14.
10. Aas IB, Austbø L, König M, Syed M, Falk K, Hordvik I, et al. Transcriptional characterization of the T cell population within the salmonid interbranchial lymphoid tissue. Journal of immunology (Baltimore, Md : 1950). 2014;193(7):3463-9.
11. Zapata A, Amemiya CT. Phylogeny of lower vertebrates and their immunological structures. Current topics in microbiology and immunology. 2000;248(1):67-107.
12. Rombout JHWM, Abelli L, Picchietti S, Scapigliati G, Kiron V. Teleost intestinal immunology. Fish & shellfish immunology. 2010;31(5):616-26.
13. Flajnik MF, Kasahara M. Origin and evolution of the adaptive immune system: genetic events and selective pressures. Nature reviews Genetics. 2010;11(1):47-59.
14. Callol A, Reyes-Lopez FE, Roig FJ, Goetz G, Goetz FW, Amaro C, et al. An enriched european eel transcriptome sheds light upon host-pathogen interactions with *Vibrio vulnificus*. PloS one. 2015;10(7):e0133328.
15. Food and Agriculture Organization of the United Nations (FAO). Fishery and Aquaculture Statistics, FAO yearbook 2012 Rome: FAO Fisheries and Aquaculture Department; 2014.
16. Bongers AB, Sukkel M, Gort G, Komen J, Richter CJ. Development and use of genetically uniform strains of common carp in experimental animal research. Laboratory animals. 1998;32(4):349-63.
17. Pethon P. Aschehougs store fiskebok: alle norske fisker i farger. 3 ed. Oslo: Aschehoug; 1994.

18. Gracey AY, Fraser EJ, Li W, Fang Y, Taylor RR, Rogers J, et al. Coping with cold: An integrative, multitissue analysis of the transcriptome of a poikilothermic vertebrate. Proceedings of the National Academy of Sciences of the United States of America. 2004;101(48):16970-5.
19. Mascorro JA, Bozzola JJ. Processing biological tissues for ultrastructural study. In: Kuo J, editor. Electron microscopy: Methods and protocols. Methods in molecular biology. 2 ed. Totowa, New Jersy: Humana Press Inc.; 2007. p. 19-34.
20. Hattingh J. Heparin and ethylenediamine tetra-acetate as anticoagulants for fish blood. Pflügers archiv. 1975;355(4):347-52.
21. Bancroft JD, Gamble M. Theory and practice of histological techniques. 6 ed. Philadelphia: Churchill Livingstone/Elsevier; 2008.
22. Endo M, Uchida S. Study on vascular system in the gills of some teleosts by the resin-replica method. Japanese journal of ichthyology. 1986;33(2):168-73.
23. Olson KR. Respiratory System. In: Ostrander GK, editor. The Laboratory fish. The handbook of experimental animals. San Diego: Academic Press; 2000. p. 151-9.
24. Olson KR. Vascular anatomy of the fish gill. Journal of experimental zoology. 2002;293(3):214-31.
25. Hughes GM. General anatomy of the gills. In: Hoar WS, Randall DJ, editors. Fish physiology Volume X Gills Part A Anatomy, gas transfer, and acid-base regulation. 10. New York: Academic Press; 1984. p. 1-63.
26. Rombout JH, van de Wal JW, Companjen A, Taverne N, Taverne-Thiele JJ. Characterization of a T cell lineage marker in carp (*Cyprinus carpio* L.). Developmental and comparative immunology. 1997;21(1):35-46.
27. Rombout JH, Joosten PH, Engelsma MY, Vos AP, Taverne N, Taverne-Thiele JJ. Indications for a distinct putative T cell population in mucosal tissue of carp (*Cyprinus carpio* L.). Developmental and comparative immunology. 1998;22(1):63-77.
28. Romano N, Taverne-Thiele AJ, Fanelli M, Baldassini MR, Abelli L, Mastrolia L, et al. Ontogeny of the thymus in a teleost fish, *Cyprinus carpio* L.: developing thymocytes in the epithelial microenvironment. Developmental and comparative immunology. 1999;23(2):123-37.
29. Chilmonczyk S. The thymus of the rainbow trout (*Salmo gairdneri*) - light and electron microscopic study. Developmental and comparative immunology. 1983;7(1):59-68.
30. Romano N, Fanelli M, Maria Del Papa G, Scapigliati G, Mastrolia L. Histological and cytological studies on the developing thymus of sharpsnout seabream, *Diplodus puntazzo*. Journal of anatomy. 1999;194 (Pt 1):39-50.
31. Kato S. Thymic microvascular system. Microscopy research and technique. 1997;38(3):287-99.
32. Langenau DM, Ferrando AA, Traver D, Kutok JL, Hezel JP, Kanki JP, et al. In vivo tracking of T cell development, ablation, and engraftment in transgenic zebrafish. Proceedings of the National Academy of Sciences of the United States of America. 2004;101(19):7369-74.
33. Castro R, Bromage E, Abos B, Pignatelli J, Gonzalez Granja A, Luque A, et al. CCR7 is mainly expressed in teleost gills, where it defines an IgD+IgM- B lymphocyte subset. Journal of immunology (Baltimore, Md : 1950). 2014;192(3):1257-66.
34. Xu Z, Takizawa F, Parra D, Gomez D, von Gersdorff Jørgensen L, LaPatra SE, et al. Mucosal immunoglobulins at respiratory surfaces mark an ancient association that predates the emergence of tetrapods. Nature communications. 2016;7:10728.

35. Hansen JD, Landis ED, Phillips RB. Discovery of a unique Ig heavy-chain isotype (IgT) in rainbow trout: Implications for a distinctive B cell developmental pathway in teleost fish. Proceedings of the National Academy of Sciences of the United States of America. 2005;102(19):6919-24.
36. Danilova N, Bussmann J, Jekosch K, Steiner LA. The immunoglobulin heavy-chain locus in zebrafish: identification and expression of a previously unknown isotype, immunoglobulin Z. Nature immunology. 2005;6(3):295-302.
37. Ryo S, Wijdeven RH, Tyagi A, Hermsen T, Kono T, Karunasagar I, et al. Common carp have two subclasses of bonyfish specific antibody IgZ showing differential expression in response to infection. Developmental and comparative immunology. 2010;34(11):1183-90.
38. Reite OB, Evensen O. Inflammatory cells of teleostean fish: a review focusing on mast cells/eosinophilic granule cells and rodlet cells. Fish & shellfish immunology. 2006;20(2):192-208.
39. Reite OB. The mast cell nature of granule cells in the digestive tract of the pike *Esox lucius*: similarity to mammalian mucosa mast cells and globule leucocytes. Fish & shellfish immunology. 1996;6:363-9.
40. Vallejo AN, Jr., Ellis AE. Ultrastructural study of the response of eosinophil granule cells to *Aeromonas salmonicida* extracellular products and histamine liberators in rainbow trout *Salmo gairdneri* Richardson. Developmental and comparative immunology. 1989;13(2):133-48.
41. Mulero I, Sepulcre MP, Meseguer J, García-Ayala A, Mulero V. Histamine is stored in mast cells of most evolutionarily advanced fish and regulates the fish inflammatory response. Proceedings of the National Academy of Sciences of the United States of America. 2007;104(49):19434-9.
42. Baccari GC, Pinelli C, Santillo A, Minucci S, Rastogi RK. Mast cells in nonmammalian vertebrates: an overview. International review of cell and molecular biology,. 2011;290:1-53.
43. Nigam AK, Kumari U, Mittal S, Mittal AK. Comparative analysis of innate immune parameters of the skin mucous secretions from certain freshwater teleosts, inhabiting different ecological niches. Fish physiology and biochemistry. 2012;38(5):1245-56.
44. Reite OB. Mast cells/eosinophilic granule cells of salmonids: staining properties and responses to noxious agents. Fish & shellfish immunology. 1997;7:567-84.
45. Zapata AG, Torroba M, Alvarez F, Anderson DP, Dixon OW, Wisniewski M. Electron microscopic examination of antigen uptake by salmonid gill cells after bath immunization with a bacterin. Journal of fish biology. 1987;31:209-17.
46. Boehm T, Hess I, Swann JB. Evolution of lymphoid tissues. Trends in immunology. 2012;33(6):315-21.
47. Goldstine SN, Manickavel V, Cohen N. Phylogeny of gut-associated lymphoid tissue. American Zoologist. 1975;15(1):107-18.
48. Tacchi L, Larragoite ET, Muñoz P, Amemiya CT, Salinas I. African lungfish reveal the evolutionary origins of organized mucosal lymphoid tissue in vertebrates. Current biology : CB. 2015;25(18):2417-24.
49. Varga I, Pospíšilová V, Gmitterová K, Gálfiová P, Polák Š, Galbavý Š. The phylogenesis and ontogenesis of the human pharyngeal region focused on the thymus, parathyroid, and thyroid glands. Neuro endocrinology letters. 2008;29(6):837-45.
50. Forlenza M. Immune responses of carp - A molecular and cellular approach to infections. Wageningen: Wageningen University; 2009.

51. Yoon S, Mitra S, Wyse C, Alnabulsi A, Zou J, Weerdenburg EM, et al. First Demonstration of Antigen Induced Cytokine Expression by CD4-1+ Lymphocytes in a Poikilotherm: Studies in Zebrafish (*Danio rerio*). PloS one. 2015;10(6):e0126378.
52. Embregts C, Boudinot P, Parra D, Wiegertjes G, Forlenza M. Characterization of IgT1 and IgT2 B lymphocyte population in common carp and their roles during infection and vaccination. In prep. 2016.
53. Gu J, Krogdahl A, Sissener NH, Kortner TM, Gelencser E, Hemre GI, et al. Effects of oral Bt-maize (MON810) exposure on growth and health parameters in normal and sensitised Atlantic salmon, Salmo salar L. The British journal of nutrition. 2013;109(8):1408-23.
54. Secombes CJ, van Groningen JJ, Egberts E. Separation of lymphocyte subpopulations in carp *Cyprinus carpio* L. by monoclonal antibodies: immunohistochemical studies. Immunology. 1983;48(1):165-75.
55. Koumans-van Diepen JC, Egberts E, Peixoto BR, Taverne N, Rombout JH. B cell and immunoglobulin heterogeneity in carp (*Cyprinus carpio* L.); an immuno(cyto)chemical study. Developmental and comparative immunology. 1995;19(1):97-108.

FIGURE LEGENDS

Table 1: Research material and examination methods.

Date of sampling:	**Fish sampled:** **- Numbers (n)** **- Weight (mean, SD)**	**Examination methods and number of individuals investigated (n):**
November 5th, 2014	n = 10 459 g, 133 g	Histology (HE and special staining) (n = 8) IHC labelling (n = 8) IF double labelling (n = 8) Vascular casts (n = 2)
December 10th, 2014	n = 9 783 g, 160 g	Histology (HE and special staining) (n = 5) IHC labelling (n = 5) IF double labelling (n = 5) Vascular casts (n = 4)
December 2 th, 2015	n = 6 1621 g , 379 g	Histology (HE) (n = 6) IHC labelling (n = 6) IF double labelling (n = 6) TEM (n = 6)
March 3 th, 2016	n = 7 3172 g, 544 g	Histology (HE) (n = 7) IHC labelling (n = 7) IF double labelling (n = 7)

HE; hematoxylin and eosin, IHC; immunohistochemistry, IF; immunofluorescence, TEM; transmission electron microscopy.

Table 2: Primary antibodies used for immunohistochemical and immunofluorescence studies.

Primary antibody - Substrate used for IHC - Fluorochrome (if applicable)	Description	Reference and producer
ZAP-70 clone 99F2 (rabbit IgG anti-human, monoclonal) - DAB - Alexa 594 goat anti-rabbit IgG (H+L)	In mammalians, the protein tyrosin kinase ZAP-70 belongs to the Syk family and, expressed in T-cells and NK-cells, plays a critical role in propagating intracellular cell signalling after activation of the membrane bound T-cell receptor. Cross-reactivity has been confirmed in common carp and zebrafish.	Cell signalling Technology Inc, 32 Tozer Road, Beverly, MA, 01915, USA, Forlenza 2009 (50), Yoon et al. 2015 (51)
WCL38 (mouse IgM anti-carp, monoclonal) - DAB - Alexa 488 goat anti-mouse IgM (H+L)	Mucosal lymphoid tissue antibody, labelling both putative mucosal T-cells but also associated epithelial cells	Rombout et al. 1998 (27)
IgT-1 (rabbit IgG anti-carp, polyclonal) - AEC	Binds to IgT1, which is one of two subclasses (the other is IgT2) identified in common carp. In general, the isotype IgT has been suggested in mucosal immunity of teleost fishes.	Embregts et al. 2016 (in prep) (52)
PCNA clone PC10 (mouse IgG2a-κ anti-rat, monoclonal) - AEC	The antibody reacts with cells in proliferative phase in late G1- or early S- phase, where PCNA constitutes an essential factor during DNA replication,- recombination and -repair	Dako, DK-2600 Glostrup, Denmark, Gu et al. 2013 (53)
WCI12 (mouse IgG1 anti-carp, monoclonal) - AEC	Binds to the heavy chain of carp IgM and was used to identify B-cells	Secombes et al. 1983 (54), Koumans-van Diepen. 1995 (55)
Cytokeratin (Pan) clone AE1/AE3 (mouse IgG1-κ anti-human, monoclonal) - DAB - Alexa 594 goat anti-mouse IgG (H+L)	Mix of monoclonal antibody reacting with a broad range of keratins visualizing normal simple epithelial cells; AE1 recognizes keratins 10, 14, 15, 16, and 19 in the acidic subfamily, and AE3 recognizes the entire basic subfamily of keratins	Invitrogen Corporation 1600 Faraday avenue Carlsbad, CA 92008, USA, Haugarvoll et al. 2008 (4)
WCL9 (mouse IgG1 anti-carp) - DAB	Binds to cortical, immature thymocytes	Rombout et al. 1997 (26)

Fluorochromes used for immunofluorescent study were produced by Thermo Fisher, IL, USA. AEC; 3- amino- 9- ethyl carbazol, CD; cluster of differentiation, DAB; 3,3`- diaminobenzidine, Ig; immunoglobulin, MHC; major histocompatibility complex, NK; natural-killer cell, PCNA; proliferating cell nuclear antigen, ZAP-70; Zeta-chain-associated protein kinase 70.

Table 3: Summary of morphological findings in the carp gill proximal interbranchial lymphoid tissue (pILT).

Compartment	Bv [1, 2]	EGC [1, 3]	Zap-70 [2, 3]	WCL38 [2, 3]	IgT-1 [2]	PCNA [2]	IgM [2]	Cytok [2, 3]	Cytok - WCL38[4]	ZAP-70-WCL38[4]
Basal	+++	(+) [5]	+++	0	++	+++	+	+++	0	0
Intermediate	0	+++	++	+++	+	++	+	+++	+	+
Uppermost	0	0	++	0	+	+	0	+++	0	0

The intraepithelial compartments are defined with reference to levels above the basement membrane. Semi-quantitative grading: 0; not detected, +; low numbers, ++; moderate numbers, +++; high numbers. Bv; blood vessels, EGC; eosinophilic granule cells, ZAP-70; zeta-chain-associated protein kinase 70 (T-cell and NK-cell), WCL38; carp putative mucosal T-cell, IgT-1; carp immunoglobulin T-1, PCNA; proliferative cell nuclear antigen, WCL12; carp immunoglobulin M, Cytok; cytokeratin. 1; histology, 2; immunohistochemistry, 3; immunofluorescence, 4; immunofluorescent double labelling. 5; only found within vascular cords.

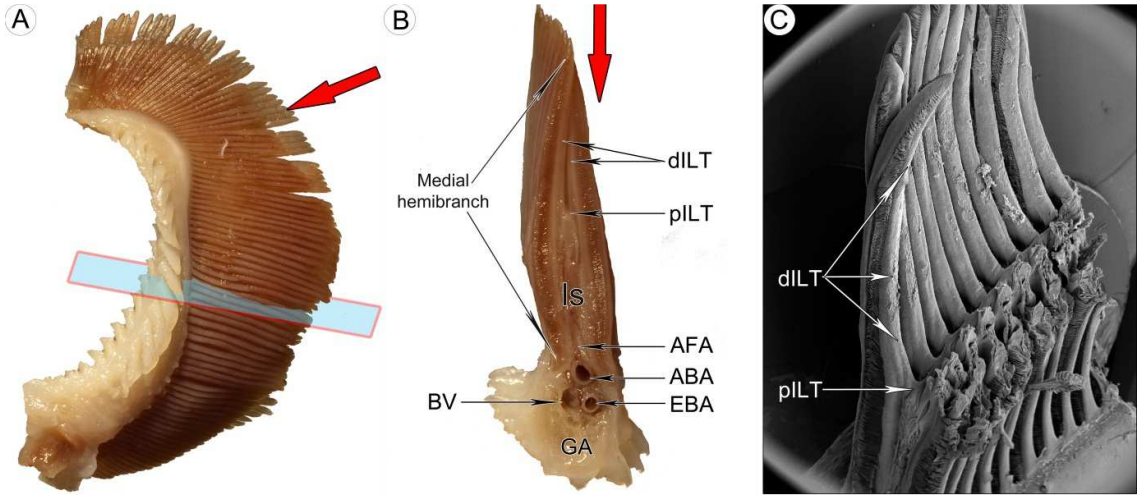

Figure 1: Overview of the common carp gills and interbranchial lymphoid tissue (ILT). (A) The second left gill in medio-lateral projection. (B) Segment obtained by transversal sections (as depicted by section plane in A) and oriented in transversal projection. Regions for the proximal- and distal ILT (pILT and dILT) depicted. (C) Scanning electron microscopic image (second right gill) visualizing extension of the pILT along the distal edge of the interbranchial septum and the dILT along the trailing edge of each filament (medial row; lateral row of free filaments removed just above the level of the pILT). BV; branchial vein, AFA; afferent filament artery, ABA; afferent branchial artery, EBA; efferent branchial artery, GA; gill arch, Is; interbranchial septum. Red arrows depicts the dorsal disto-proximal projection.

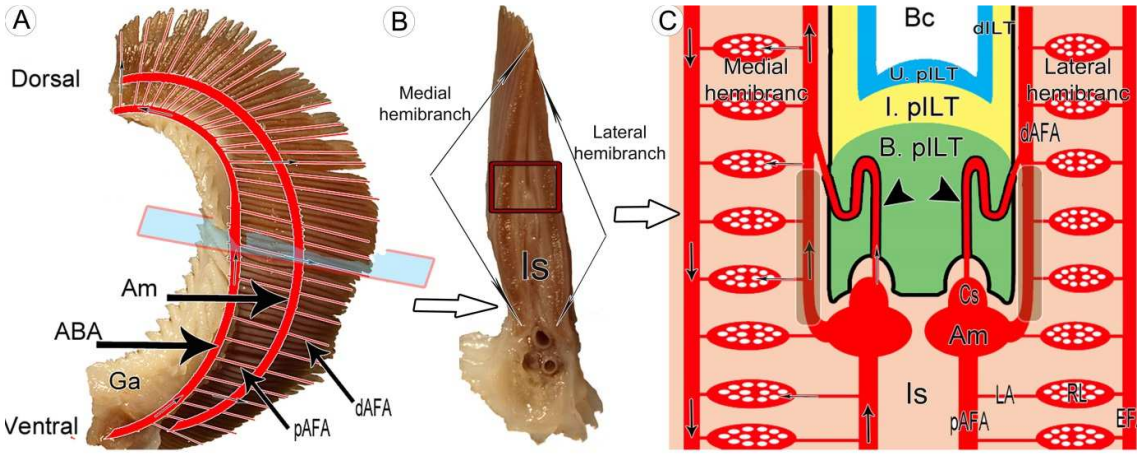

Figure 2: Schematic drawings of the gill proximal interbranchial lymphoid tissue (pILT) and associated vascular structures of common carp. (A) The second left gill in medio-lateral projection, with the afferent arteries of the medial hemibranch including afferent branchial artery (ABA), proximal afferent filament artery (pAFA), common ampulla (Am) and distal afferent filament artery (dAFA) accentuated. Every pAFA enters the ampulla, from which originate dAFAs and cisternae with downstream basal ILT-associated vessels. (B) Segment obtained by transversal sections (as depicted by section plane in A) and viewed in transversal projection. (C) Principal drawing of primary blood vessels and ILT in the area depicted by the square in B. The directions of blood flow are depicted by arrows in the medial hemibranch, i.e. in mentioned order pAFAs - ampullae - cisternae - basal pILT-associated vessels (black arrowheads) or dAFAs. The pILT-associated vessels empty into dAFA. Note the thickening of the proximal-most segment of the dAFA vascular wall (grey shade) before it receives blood from the basal pILT-associated vessels. The basement membrane of the ILT-epithelium is outlined in black, forming boundaries to underlying connective tissue. The vascular systems of each hemibranch appear separate. Each ampulla runs along the distal interbranchial septum of each hemibranch in the dorso-ventral direction. LA; lamellar arterioles, RL; respiratory lamella, EFA; efferent filament artery, B. pILT; basal compartment of the pILT, I. pILT; intermediate compartment of the pILT, U. pILT; uppermost compartment of the pILT, dILT; distal interbranchial lymphoid tissue, Bc; branchial cleft, Is; interbranchial septum.

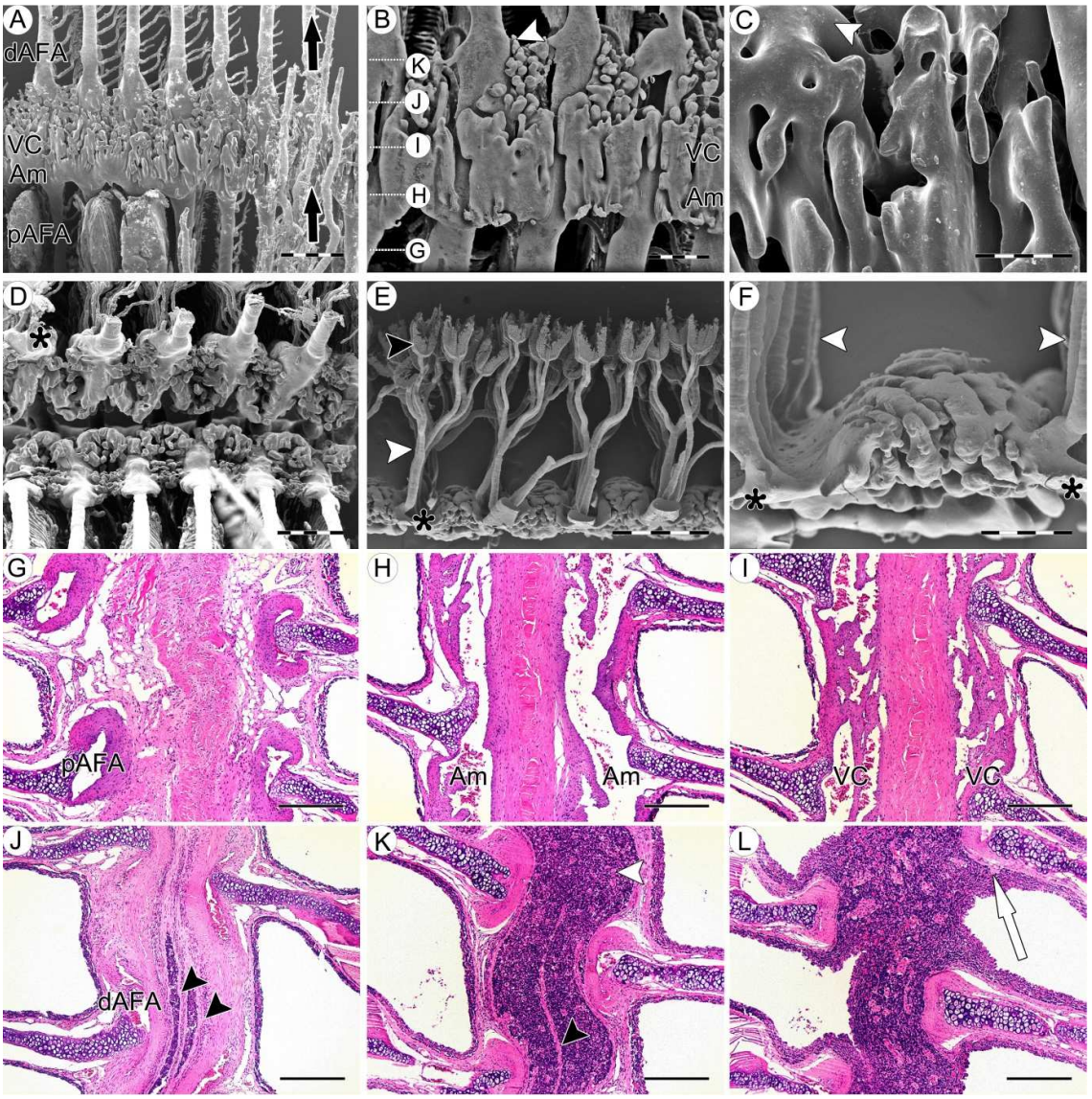

Figure 3: Morphology of the gill vascular structures in conjunction with the basal compartment of the proximal interbranchial lymphoid tissue (pILT) of common carp.

(A-C) Scanning electron microscopy (SEM) images of a hemibranch vascular cast, medio-lateral projection, in the region of the distal end of the interbranchial septum. The direction of blood flow in the afferent filament arteries (AFAs) is depicted by the black arrows in A. Fig. 1A shows the corresponding orientation of a whole gill. (A) Proximal AFAs (pAFAs) enter each hemibranch's common ampulla (Am), from which originate the distal AFAs (dAFAs) and vascular cisternae (VC). (B) VC, from which arise basal pILT-associated vessels that distally connects with the dAFAs (white arrowhead) after traversing the basal pILT. (C) Higher magnification of B, showing connection between the basal pILT-associated vessels and dAFA (white arrowhead).

(D-F) SEM in disto-proximal projection from the distal part of the filaments towards distal margin of the interbranchial septum (orientation depicted by red arrows in Fig. 1A and B). Asterisks depict dAFAs' cut-ends located adjacent to the ILT, white arrowheads depict lamellar afferent arterioles and black arrowhead lamellar capillary networks. (D) No communication is seen between the ampullae of the two hemibranchs. (E) Basal pILT-associated vessels appear as nests between each dAFA. (F) Higher magnification of E, showing the nested structures of the cords and their distal connections to the dAFA. *(G-L)* Hematoxylin and eosin- stained serial sections through the pILT at various levels (from proximal to distal in relation to the filaments) in the dorsal plane supporting findings from SEM (tissue level in the sagittal orientation is indicated in B). (G) pAFAs before joining the ampulla. (H) The ampulla with an irregular lumen. (I) Irregular vascular cisternae projecting in distal direction from the ampulla. (J) dAFA originating from the ampulla. (J-L). The basal pILT-associated vessels emerge from wide-stretching bands of connective tissue at the distal end of the cisternae (black arrowheads), before clusters of basal pILT-associated vessels get surrounded by the basal pILT epithelial basement membrane by way of vascular cords traversing the basal pILT (white arrowhead in K). Toward the upper part of the basal pILT, these vessels run in close proximity to the dAFA (white arrow). Scale bars: (A and D); 1 mm, (B and F); 400 µm, (C, G-L); 200 µm, (E); 800 µm.

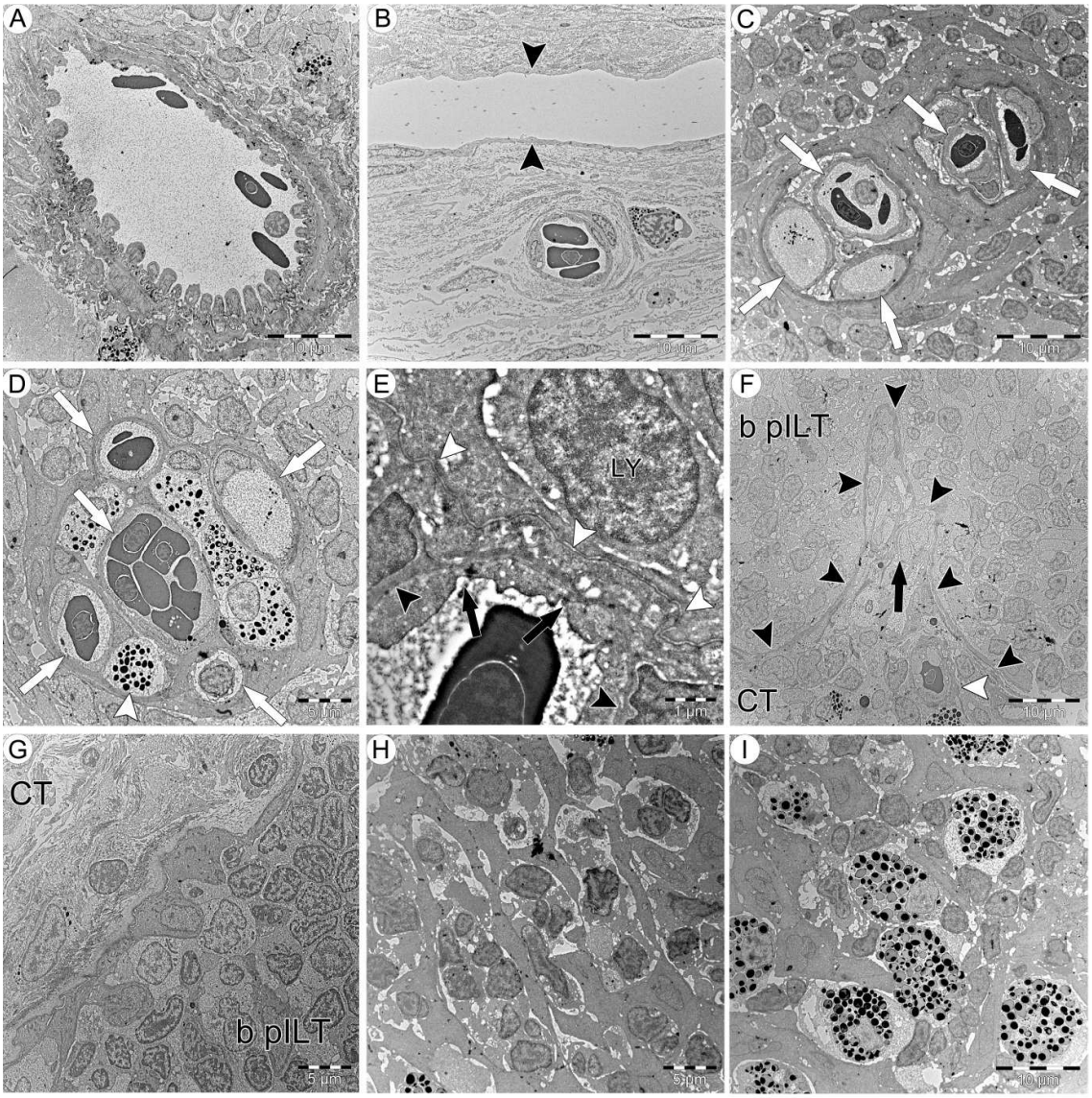

Figure 4: Ultrastructure of the proximal interbranchial lymphoid tissue (pILT) and subepithelial structures in the gills of common carp.

(A) Folded endothelium of a distal afferent filament artery (dAFA) at the level of the pILT, indicating a contractible vascular wall (dorsal plane). (B) Low and wide-stretched endothelium of the cisternae (black arrowheads) resting on a thick layer of connective tissue (dorsal plane). (C) Vascular cords surrounded by epithelium and its basal lamina forming the outer limitation of the perivascular tissue. The inner limitation of the perivascular tissue is formed by the basal pILT-associated vessels' endothelium and its basal lamina, and each cord could hold several vessels (white arrows for each vessel). High numbers of lymphocytes were found in the epithelium surrounding the vascular cords (dorsal plane). (D) A vascular cord at higher magnification, with eosinophilic granule cells (EGCs; white arrowhead) in the perivascular tissue (dorsal plane). (E) The basal laminae of the surrounding epithelium (white arrowheads) and the endothelium (black arrowheads) were closely associated,

although separate. Some vessels apparently had fenestrated endothelium (black arrows). The associated basal lamina appeared continuous in all basal pILT-associated vessels. A lymphocyte (LY) is seen in the epithelium close to the vascular cord (dorsal plane). (F) Section through an initial segment of a vascular cord, showing an upward subepithelial orientation (black arrow) covered by epithelial basal lamina (black arrowheads). An entering blood capillary containing an erythrocyte is seen within the subepithelial connective tissue (CT) (white arrowhead) (medial plane). (G) A thick basal lamina between basal pILT (b pILT) and underlying connective tissue (transversal plane). (H) Lymphocytes and reticular epithelial cells' perikarya were to a large extent oriented in alternating parallel rows (dorsal plane). (I) High numbers of EGCs in the intermediate compartment of the pILT (dorsal plane).

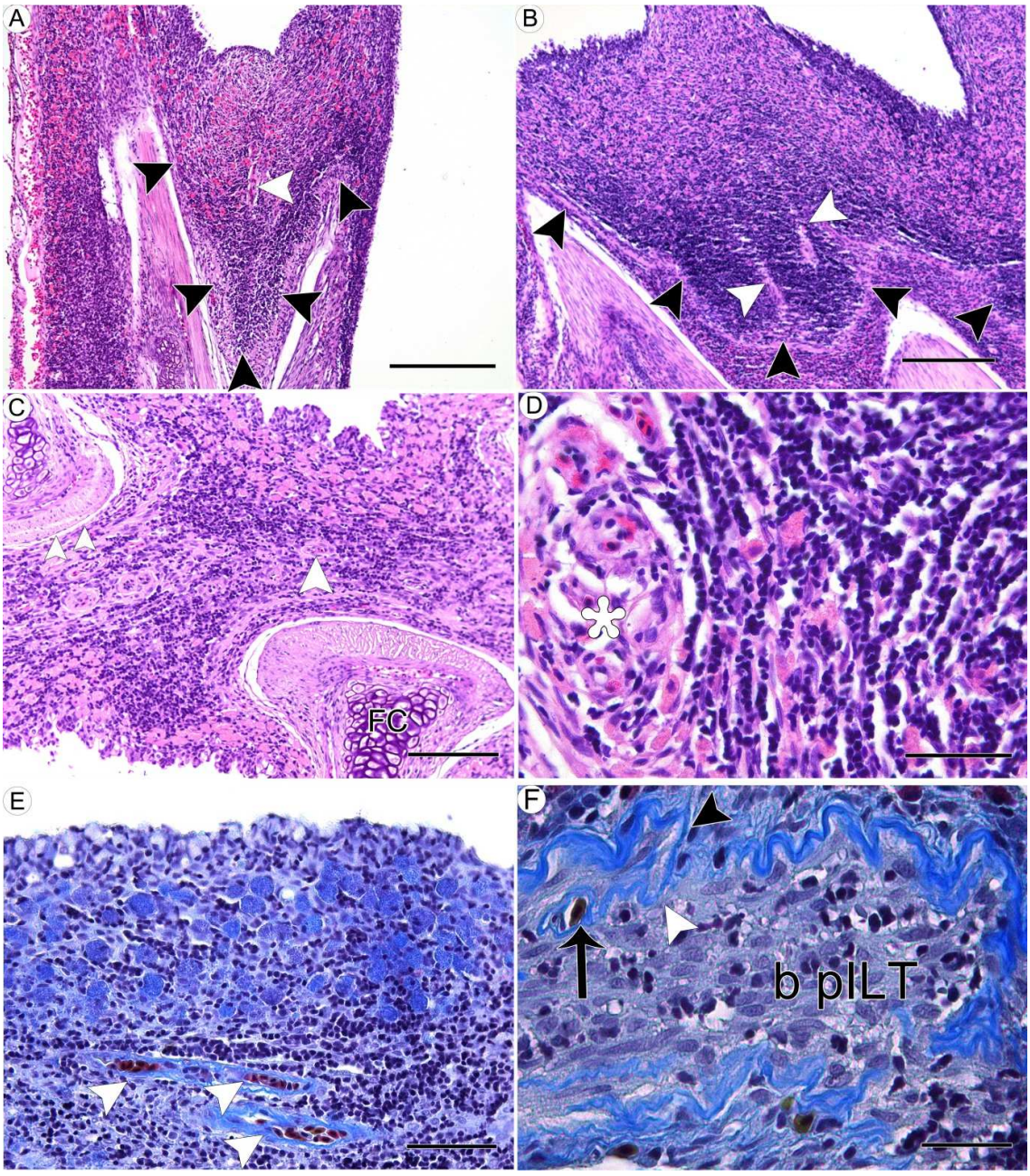

Figure 5: Morphology of the gill proximal interbranchial lymphoid tissue (pILT) of common carp.

(A) Transversal, (B) sagittal and (C) dorsal sections of gill (hematoxylin and eosin; HE). Lymphocytes and eosinophilic granule cells (EGCs) dominate the basal and the intermediate compartments of the pILT, respectively. Blood vessels (white arrowheads) are seen within pILT. (D) Higher magnification of a cluster of basal pILT-associated vessels within a vascular cord (asterisk), and a surrounding reticular epithelium with high numbers of lymphocytes situated in rows (HE, dorsal plane). (E) Prominent basement membrane of collagenous nature of the vascular cords (arrowheads). Martius Scarlet Blue (MSB) staining, sagittal plane. Erythrocytes stain yellow. (F) Upward deflection of the pILT epithelial basement

membrane (white arrowhead) is seen surrounding a vascular cord (holding the basal pILT-associated vessels, black arrow) as the cord traverses the basal pILT (b pILT, middle region). The surrounding ILT epithelial basement membrane is marked by black arrowhead (MSB, dorsal plane). Scale bars: A and B; 200 μm, C; 100 μm, D and F; 40 μm, E; 50 μm.

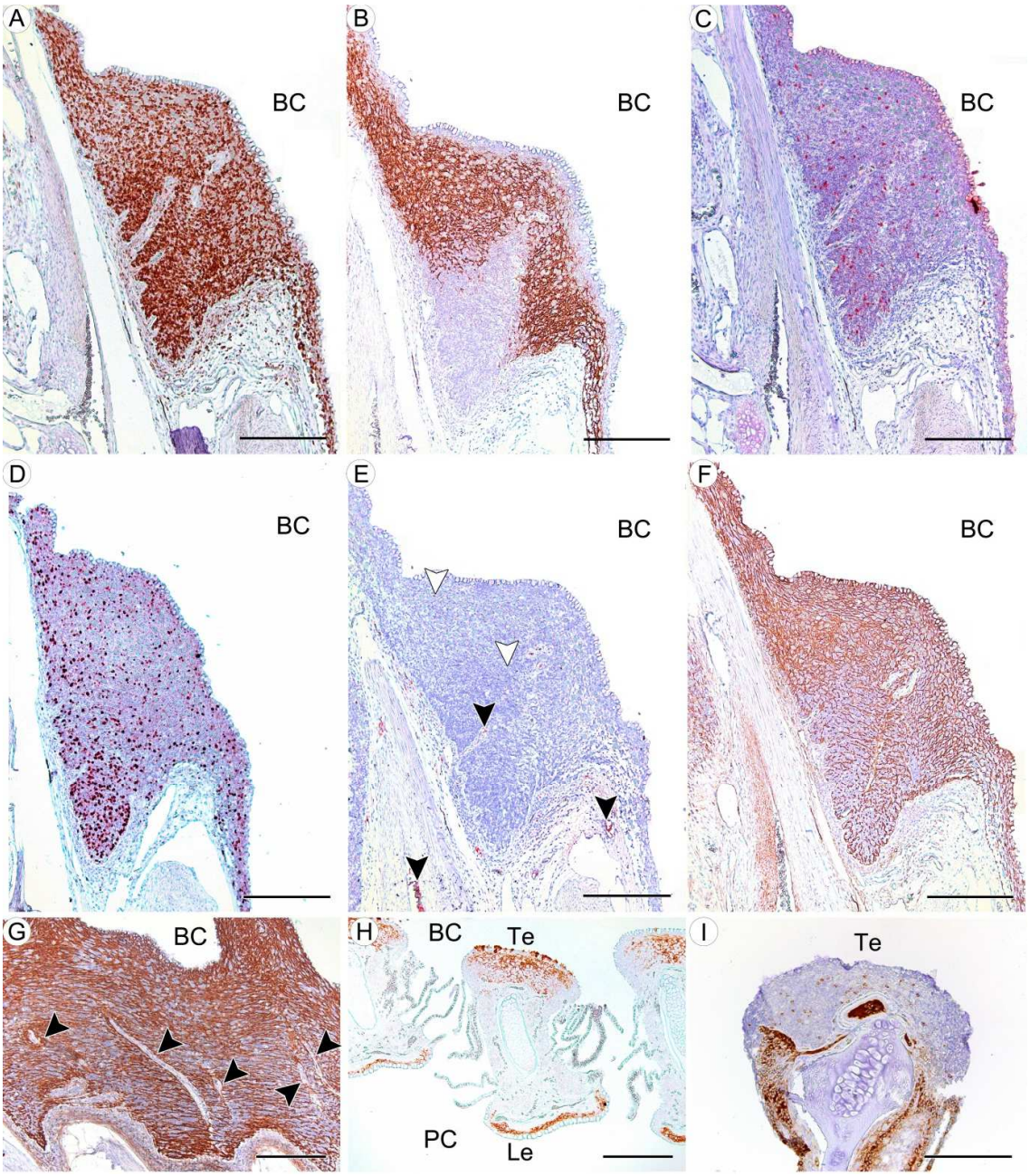

Figure 6: Immunohistochemical labelling of the gill interbranchial lymphoid tissue (ILT) of common carp.

(A-G) Proximal ILT. (A) ZAP-70^{+} T-cells or NK-cells (brown). Highest numbers of positive cells were found in the basal pILT. The labelled cells clearly delimit the position of the basement membrane basally and the vascular cords holding the basal pILT-associated vessels. (B) WCL38^{+} putative mucosal T-cells (brown) appeared only in the intermediate compartment of the pILT. (C) IgT-1^{+} B-cells (red) in moderate numbers in the basal pILT, with far lower numbers in the intermediate and uppermost pILT and also in dILT (not shown). (D) PCNA^{+} cells (cells in proliferative phase) were present in high numbers in the basal pILT. (E) IgM^{+} cells (red) occurred in low numbers in all pILT compartments (white arrowheads). Also,

serum in blood vessels stained extensively (black arrowheads). (F) High numbers of epithelial cells were demonstrated by labelling for cytokeratin (brown). (G) Vascular cords (black arrowheads) traversing the cytokeratin-positive epithelium (brown) in the pILT in an oblique to parallel manner *(H-I)* Distal ILT (dILT). (H) $WCL38^{+}$ putative mucosal T-cells (brown) in the dILT along the trailing edge (Te). Positive cells were also seen in the leading edges (Le) epithelium. (I) Moderate numbers of IgM^{+} cells (brown) in the dILT. Note also extensive labelling of serum in the luminae of blood vessels. BC; branchial cleft, PC; pharyngeal cavity. Planes: (A-F); transversal, (G); sagittal, (H) and (I); dorsal. Scale bars: (A-H); 400 μm, (I); 200 μm.

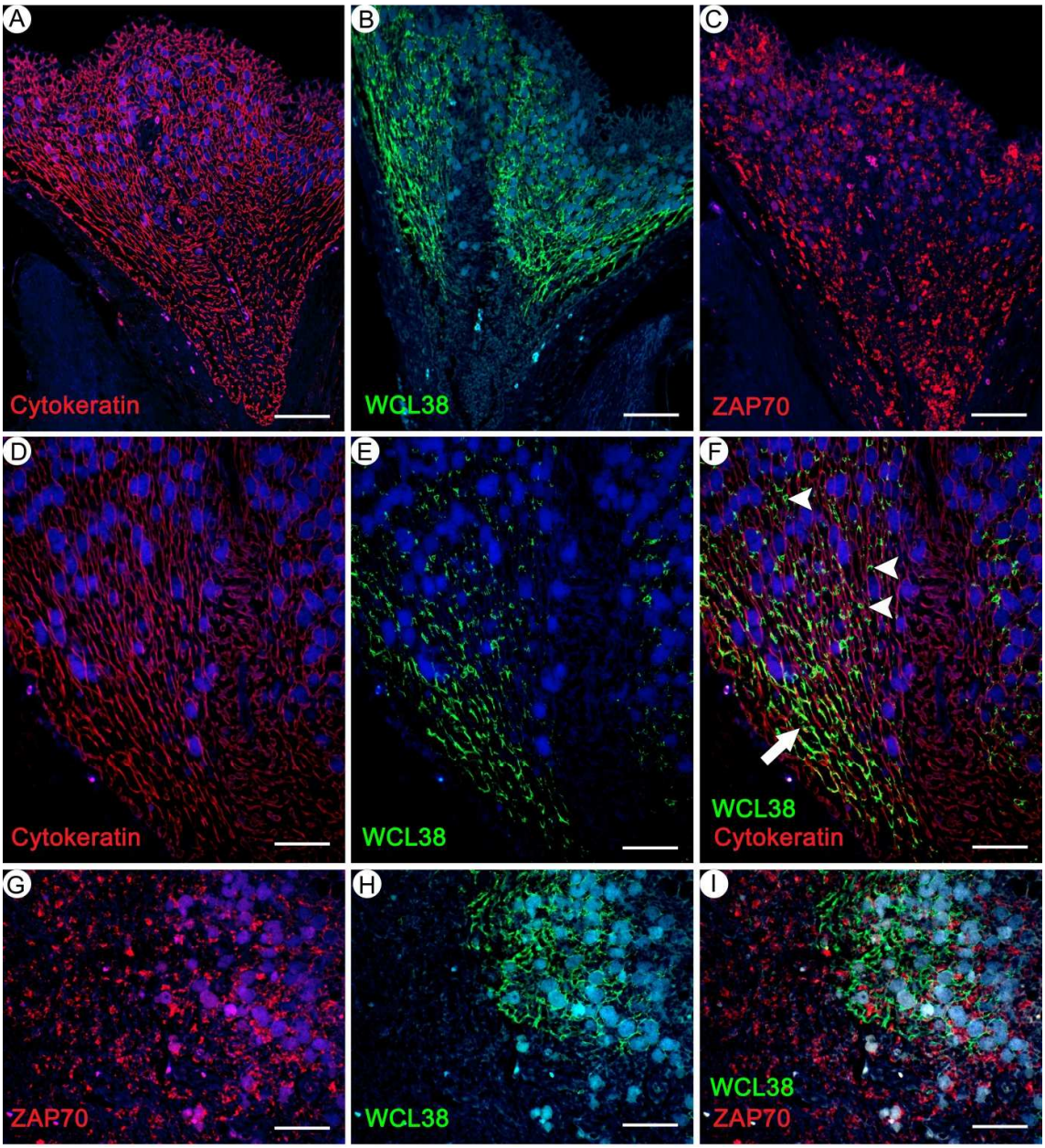

Figure 7: Immunofluorescence labelling of the gill proximal interbranchial lymphoid tissue (pILT) of common carp.

Eosinophilic granule cells (EGCs) with autofluorescent granules (blue) present in high numbers in the intermediate compartment (upper part of the image in A-F, right part in G-I). (A) Network of cytokeratin$^+$ cells (epithelial reticular cells, red) encompassing the entire ILT. (B) WCL38$^+$ putative mucosal T-cells (green) present in the intermediate compartment. (C) High numbers of ZAP-70$^+$ T-cells or NK-cells (red) in basal compartment, and moderate numbers in the uppermost and intermediate compartments. (F) Merged image of D (cytokeratin$^+$ cells, red) and E (WCL38$^+$ cells, green), indicating co-localization in reticular epithelial cells (arrow) but also single-labelled cells for either cytokeratin or WCL38 in the intermediate compartment. White arrowheads point to single labelled, WCL38$^+$ lymphocyte-

like cells. (I) Merged image of G (ZAP-70^{+} cells, red) and H (WCL38^{+} cells, green) at the transition between the basal and intermediate compartments, indicating low numbers of co-localization of these antibodies in lymphocyte-like cells of the intermediate compartment. All section in transversal plane. Scale bars: 100 µm.

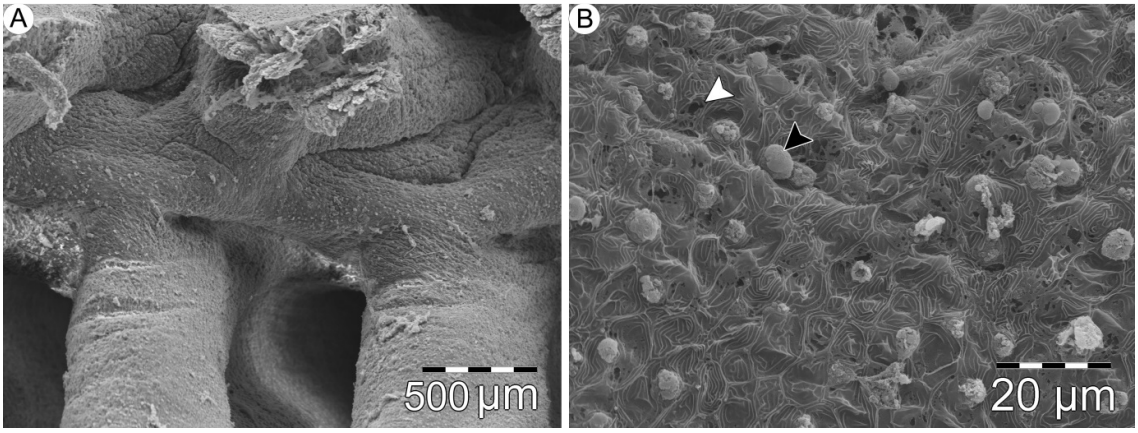

Figure 8: Surface-morphology of the gill proximal interbranchial lymphoid tissue (pILT) of common carp. No discernible difference in surface morphology was found in the region of the ILT tissue as compared with the other regions of multi-layered gill epithelium. (A) Disto-proximal projection of the distal ILT and pILT. Note the folded epithelium in the transition between pILT and dILT. (B) Higher magnification of the pILT epithelium. Protruding mucus from goblet cells (black arrowhead) surrounded by pavement cells with characteristic micro-ridges dominate the epithelial surface. Pits are probably associated with mitochondria-rich cells (white arrowhead).